UNIVERSITY OF MESSINA

Department of Chemical, Biological, Pharmaceutical

and Environmental Sciences

PhD course in Applied Biology and Experimental Medicine

XXXVIII Cycle (SSD BIO/19)

Curriculum: Experimental Medicine

PhD Coordinator: Prof. Emanuela Esposito

Herpes Simplex Virus Type 1 (HSV-1) infection of monocytic cells induces a strong release of chemokines in a Caspase-8-independent manner

PhD Candidate:

Maria Pia Tamburello

Tutor:

Prof.ssa Maria Teresa Sciortino

Co-Tutor:

Prof.ssa Rosamaria Pennisi

Academic Year 2024/2025

Table of contents

List of figures *6*

List of tables *8*

List of abbreviations *9*

Abstract *12*

Introduction *14*

Chapter I Herpes simplex type 1 (HSV-1) *14*

1.1. HSV-1 virion structure, genome organization, and life cycle **18**

1.2. Host immune responses to HSV-1 ..... **23**

1.3. Mechanisms of HSV-1 immune evasion **25**

1.4. Antiviral therapies against HSV-1 ..... **28**

Chapter II Caspase-8 in viral infection: from apoptotic to non-apoptotic functions *30*

2.1. Caspase-8 structure, activation, and cleavage **32**

2.1.1. Caspase-8 activity modulation by FLIP isoforms 34

2.1.2. Caspase-8 post-translational ubiquitination and phosphorylation 37

2.2. Caspase-8 as a central regulator of programmed cell death pathways **39**

2.2.1. Apoptosis pathways: extrinsic and intrinsic mechanisms 39

2.2.2. Necroptosis and its suppression by caspase-8 40

2.2.3. PANoptosis and pyroptosis 42

2.2.4. Caspase-8 as a molecular switch between autophagy and apoptosis 44

2.3. Caspase-8 pro-survival functions **46**

2.3.1. Caspase-8 and chemokine regulation 49

2.4. NF-κB pathway and its function during HSV-1 infection **51**

2.5. Chemokines in HSV-1 infection **55**

2.5.1. CC family 56

2.5.2. CXC family 57

2.5.3. Chemokine receptors 58

2.6. Aim of the study **59**

2.7. Materials and Methods **62**

Cell lines 62

Viruses 62

Bacteria 63

Plasmids 63

Primers 64

Generation of electrocompetent bacteria 65

Transformation of bacteria 66

Isolation of plasmid DNA and BAC DNA (Mini Prep) 66

Isolation of plasmid DNA and BAC DNA (Midi Prep) 67

Polymerase chain reaction (PCR) 67

Restriction enzyme digestion of DNA 67

Agarose gel electrophoresis 67
Purification of DNA fragments 68
RNA extraction, Reverse transcription 68
Quantitative polymerase chain reaction (qPCR) 68
DNA sequencing 69
En passant BAC mutagenesis 69
Transfection of plasmid DNA 70
Transfection of BAC DNA 71
Production of lentivirus 71
Transduction of cells 71
Generation of knockouts using the CRISPR/Cas9 system 72
Viral infections 73
Plaque assay 73
Cell lysis and immunoblotting 74
Antibodies and reagents 75
Live cell imaging 75
Quantification and statistical analysis 76

2.8. Results 77
2.8.1. HSV-1 replication in CASP8$^{+/+}$ and CASP8$^{-/-}$ THP-1 cells 77
2.8.2. Caspase-8 deficiency enhances chemokine expression during HSV-1 infection 83
2.8.3. Caspase-8 deficiency enhances NF-κB activation during HSV-1 infection 86
2.8.4. NF-κB pathway is required for chemokine induction during HSV-1 infection in THP-1 cells 88
2.8.5. HSV-1-induced chemokine expression requires active viral replication 90
2.8.6. Investigating RIPK1 regulation during HSV-1 infection in caspase-8-knockout cells .. 92
2.8.7. Investigating the role of caspase-8 in HSV-1 egress using a dual-fluorescent recombinant virus 95

2.9. Discussion 106

Chapter III Emerging HSV-1 Natural Therapies 109

3.1. Antiviral properties of olive leaf extracts and oleuropein 110

3.2. Aim of the study 110

3.3. Materials and Methods 112
Cell lines and viruses 112
Plant materials 112
Cell proliferation assay 113
Plaque assay 113
Viral infection 114
Cell lysis and immunoblotting 114
Antibodies 114
Viral DNA extraction and qPCR 114
RNA extraction and Reverse transcription 115
Quantitative polymerase chain reaction (qPCR) 115
Quantification and statistical analysis 116

3.4. Results 117
3.4.1. Antiviral activity of OESA and OESY 117
3.4.2. Antiviral activity of OESA and OESY compounds 119
3.4.3. Oleuropein suppresses viral replication by modulating PKR-dependent c-Fos and c-Jun activation 121

3.5. Discussion 123

Chapter IV Antiviral potential of food by-products *124*

4.1. Antiviral properties of almond blanched skin (BS) and blanch water (BW) **124**

4.2. Aim of the study **124**

4.3. Materials and Methods **125**

4.4. Results **126**

4.4.1. Antiviral Activity of blanched skin extracts (BSE) 126

4.5. Discussion **130**

Chapter V Study Limitations and Outlook *131*

5.1. Limitations of the study **131**

5.2. Future perspectives **132**

Conclusions *133*

References *135*

Acknowledgements *155*

List of figures

Figure 1. Acute and latent HSV-1 infection 16
Figure 2. HSV-1 virion structure 18
Figure 3. HSV-1 genome organization 20
Figure 4. HSV-1 life cycle 21
Figure 5. Schematic representation of procaspase-8 activation 34
Figure 6. Functional role of c-FLIP isoforms during death receptor-mediated apoptosis 36
Figure 7. Caspase-8 plays a central role in 44
Figure 8. Canonical and non-canonical NF-κB signaling pathways 52
Figure 9. Chemokine-mediated orchestration of innate and adaptive immune responses to tissue stress 56
Figure 10. En passant mutagenesis 70
Figure 11. Workflow for the generation of CRISPR/Cas9-mediated knockout cell lines 73
Figure 12. Characterization of CASP8-/- THP-1 cells 79
Figure 13. Evaluation of HSV-1 replication efficiency in CASP8+/+ and CASP8-/- THP- 81
Figure 14. Evaluation of HSV-1 replication efficiency in CASP8+/+ and CASP8-/- THP-1 cells at MOI 10. 82
Figure 15. qPCR analysis of chemokines gene expression in CASP8+/+ and CASP8-/- THP-1 cells upon HSV-1 infection 85
Figure 16. Analysis of NF-κB activation in CASP8+/+ and CASP8-/- THP-1 cells during HSV-1 infection 87
Figure 17. qPCR analysis of chemokines gene expression in HSV-1-infected THP-1 wild-type and DN IκBα cells 89
Figure 18. qPCR analysis of chemokines gene expression in HSV-1-infected THP-1 cells 91
Figure 19. RIPK1 expression upon HSV-1 infection in CASP8+/+ and CASP8-/- THP-1 cells at MOI 50 93
Figure 20. RIPK1 expression upon HSV-1 infection in CASP8+/+ and CASP8-/- HEp-2 cells at MOI 10 94
Figure 21. En passant mutagenesis of HSV-1-gH-mScarlet and HSV-1-VP26-mNeonGreen recombinants. 98
Figure 22. Live imaging of HEp-2 CASP8+/+ and CASP8-/- cells infection 100

Figure 23. En passant mutagenesis of HSV-1 gH-mScarlet VP26-mNeonGreen recombinant 102
Figure 24. HSV-1 recombinants characterization 104
Figure 25. Cytotoxic effects of OESA and OESY on HeLa cells 117
Figure 26. Evaluation of viral titers in HeLa cells after OESA and OESY treatment 118
Figure 27. Absolute quantification of viral DNA 118
Figure 28. Cytotoxicity assay of oleuropein 119
Figure 29. Antiviral activity of oleuropein 120
Figure 30. Activation of the innate antiviral response via phospho-PKR, phospho-c-Jun, and phospho-c-Fos in HSV-1-infected HeLa cells after oleuropein treatment 122
Figure 31. Cell viability assay of VERO cells treated with BSE from Fascionello and Tuono cultivars. 126
Figure 32. Antiviral effect of BSE on HSV-1 replication assessed by plaque reduction assay 128

List of tables

Table 1. BAC mutagenesis primers 64

Table 2. qPCR primers 64

Table 3. pSicoR primers 65

Table 4. Cytotoxicity (CC50), antiviral activity (EC50), and Selectivity index (SI) of blanched skin extracts (BSE) 127

List of abbreviations

ACV	Acyclovir
AIF	Apoptosis-inducing factor
ALPS	Autoimmune lymphoproliferative syndrome
Atg	Autophagy-related
Bcl10	B cell leukemia/lymphoma 10
BS	Blanched skin
BSE	Blanched skin extracts
BW	Blanch water
c-FLIP	Cellular FLICE-like inhibitory proteins
CASP8	Caspase-8
CASP8-/-	Caspase-8-knockout
CC50	Cytotoxicity
CMKLR1	Chemokine-like receptor 1
CMV	Cytomegalovirus
CPE	Cytopathic effect
CTLs	Cytotoxic T lymphocytes
DAMPs	Damage associated molecular pattern
DCs	Dendritic cells
DD	Death domain
DEDs	Death effector domains
DISC	Death-inducing signaling complex
DMEM	Dulbecco's Modified Eagle's High Glucose Medium
DN IκBα	Dominant-negative mutant of IκBα
dsDNA	Double-stranded DNA
dsRNA	Double-stranded RNA
E	Early
EC50	Effective concentration
Evs	Extracellular vesicles
FADD	Fas-associated death domain
GAG	Glycosaminoglycan
GAPDH	Glycerinaldehyd-3-phosphat-dehydrogenase
gD	Glycoprotein D
gH	Glycoprotein H
GPCRs	G protein-coupled receptors
GSDMD	Gasdermin D
H.p.i.	Hours post-infection
HHV-4	Epstein-Barr virus

HHV-8	Kaposi's sarcoma-associated herpesvirus
HSV-1	Herpes simplex virus type 1
HSV-2	Herpes simplex virus type 2
HSV-3	Varicella zoster virus
HveA	herpesvirus entry mediator A
HVEM	Herpesvirus entry mediator
IE	Immediate-early
IFN-α/β	Type I interferons
IFN-γ	Type II interferons
IFNRs	Interferon receptors
IKK	IκB kinase
IR	Internal repeats
IRAK1	Interleukin-1 receptor-associated kinase 1
ISGs	Interferon-stimulated genes
L	Late
LAT	Latency-associated transcript
LB	Luria Bertani
M-CSF	Macrophage colony-stimulating factor
MALT1	Mucosa-associated lymphoid tissue lymphoma translocation 1
MLKL	Mixed lineage kinase domain-like protein
MOI	Multiplicities of infection
MOMP	Mitochondrial outer membranes permeabilization
NF-κB	Nuclear factor kappa-light-chain-enhancer of activated B cells
NIK	NF-κB-inducing kinase
NK	Natural killer cells
NO	Nitric oxide
NPC	Nuclear pore complex
OAS	2′-5′ oligoadenylate synthetases
OESA	*Olea europaea* cultivated var. *sativa*
OESY	*Olea europaea* wild var. *sylvestris*
OEVs	Organelle-associated enveloped virions
oHSVs	Oncolytic HSVs
ori	Origin of DNA replication
PAA	Phosphonoacetic acid
PAI-2	Plasminogen activator inhibitor-2
PAK-2	Serine/threonine-protein kinase
PFA	Phosphonoformic acid
PFU	Plaque-forming units
PKD	Protein kinase D

PKR	Double-stranded RNA-activated protein kinase
PRR	Pattern recognition receptor
PRRs	Pattern recognition receptors
qPCR	Quantitative polymerase chain reaction
RHD	Rel homology domain
RHIM	RIP homotypic interaction motif
RLRs	RIG-I-like receptors
ROS	Reactive oxygen species
RPMI	Roswell Park Memorial Institute
RT	Room temperature
SI	Selectivity index
ssDNA	Single-stranded DNA
t.p.i.	Times post-infection
tBid	Truncated Bid
TCR	T cell receptors
TG	Trigeminal ganglia
TK	Thymidine kinase
TLRs	Toll-like receptors
UL	Unique long
US	Unique short
vCK	Viral chemokine
vCKR	Viral chemokine receptor
vDNA	Viral DNA
VHS	Virion host shutoff protein

Abstract

Herpes simplex virus type 1 (HSV-1) is a widespread human pathogen that can establish lifelong persistence after primary infection. Although antiviral drugs are available, their efficacy is often limited by the emergence of resistant strains, particularly in immunocompromised patients or in those undergoing prolonged treatment. The absence of effective vaccines and the growing problem of resistance underscore the need to better understand the molecular interplay between HSV-1 and host immunity, as well as to explore alternative antiviral strategies. During HSV-1 infection, while epithelial cells can counteract pro-apoptotic signals through the expression of viral proteins, immune cells such as monocytes and dendritic cells (DCs) remain more susceptible to virus-induced apoptosis. In monocytic cells, HSV-1 establishes a low-permissive infection, yet increasing evidence indicates that death-related proteins may exert non-apoptotic functions during infection. Among these, caspase-8, classically known as an initiator of extrinsic apoptosis, has emerged as a versatile regulator implicated in necroptosis, autophagy, inflammatory signaling, and viral replication.

This PhD project primarily investigated the role of caspase-8 in HSV-1 infection of monocytic cells, with a focus on viral immune evasion and modulation of host signaling pathways. Using CRISPR-Cas9-generated caspase-8-knockout THP-1 cells and wild-type or Us11/Us12-deleted HSV-1 strains, this work demonstrates that caspase-8 limits viral gene expression, restrains NF-κB activation, and tempers chemokine production, thereby contributing to the regulation of inflammatory responses. In addition, RIPK1 expression was found to be downregulated in caspase-8-deficient cells, further supporting its involvement in immune modulation. Here, “immunomodulation” refers to cell-intrinsic regulation of innate immune signaling in infected myeloid cells (captured by NF-κB activity, chemokine transcription, and RIPK1 expression) under the influence of viral immune-evasion factors (e.g., Us11) and caspase-8-dependent checkpoints.

The construction of recombinant HSV-1 viruses carrying fluorescent tags enabled preliminary insights into virion trafficking and maturation, suggesting a potential role of caspase-8 in late stages of the viral life cycle. Altogether, these findings

highlight caspase-8 as an important regulator of molecular pathways at the interface between HSV-1 and host immunity.

In addition to this central mechanistic investigation, the thesis includes complementary studies exploring the antiviral activity of selected plant-derived products. Hydroethanolic extracts from cultivated wild olive leaves exhibited antiviral activity, with oleuropein identified as a major bioactive compound associated with reduced HSV-1 gene expression and protein synthesis while activating PKR and AP-1 signaling. Similarly, almond by-products, such as blanching skin and blanching water, have been shown to exhibit antiviral properties. These exploratory studies broaden the scope of the thesis by examining alternative antiviral approaches, without extensive mechanistic dissection.

In conclusion, this work primarily advances the understanding of molecular signaling pathways during HSV-1 infection, particularly the role of caspase-8 in modulating viral replication and innate immune responses in monocytic cells, while secondarily highlighting plant-derived compounds as complementary sources of antiviral bioactivity. By combining mechanistic insights into caspase-8, NF-κB, and chemokine regulation with exploratory studies of natural bioactive molecules, this thesis contributes to a more comprehensive view of HSV-1-host interactions.

Introduction

Chapter I
Herpes simplex type 1 (HSV-1)

Herpes simplex virus type 1 (HSV-1) is a DNA virus that belongs to the *Alphaherpesvirinae* subfamily of the *Herpesviridae*, which also includes Herpes simplex virus type 2 (HSV-2), cytomegalovirus (CMV), varicella zoster virus (HSV-3), Epstein-Barr virus (HHV-4), HHV-6, HHV-7, and Kaposi's sarcoma-associated herpesvirus (HHV-8) (Lehman and Boehmer, 1999). With infection rates ranging from 45% to 98% among the world's population, including those in remote areas, HSV-1 is widespread globally. It is a significant public health concern and one of the most prevalent viral infections in humans (Fatahzadeh and Schwartz, 2007; Tyler, 2004).

Transmission typically occurs after mucosal contact with infected individuals, primarily through the exchange of salivary secretions. HSV-1 pathogenicity is linked to a wide range of clinical manifestations, including orofacial lesions referred to as “cold sores”, keratitis, conjunctivitis, and mucocutaneous infections (Boehmer and Nimonkar, 2003; Fatahzadeh and Schwartz, 2007; Tyler, 2004). While HSV-related diseases are generally non-fatal, in immunocompromised individuals, including transplant recipients, AIDS patients, and neonates, disseminated infections can result in blindness and encephalitis, causing significant morbidity and mortality (up to 70% if untreated) (Boehmer and Nimonkar, 2003; Tyler, 2004).

HSV-1 displays a distinct cellular tropism. Epithelial cells represent the primary sites of productive lytic replication, where the virus enters via glycoproteins such as gB, gC, and gD, engaging receptors including nectin-1 and herpesvirus entry mediator (HVEM) (Alandijany, 2019; Montgomery et al., 1996). In contrast, monocytes and other leukocytes are less permissive, producing two distinct populations: one productively infected and one resistant, reflecting the heterogeneity of susceptibility in monocytes/macrophages, dendritic cells, and T cells compared with epithelial cells (Bosnjak et al., 2005; Iannello et al., 2011; Kather et al., 2010; Mastino et al., 1997; Musarra-Pizzo et al., 2022). This

mechanism often results in restricted or abortive infection outcomes characterized by cytokines induction or apoptosis rather than robust viral replication (Melchjorsen et al., 2010, 2006; Musarra-Pizzo et al., 2022; Raftery et al., 1999). This duality enables HSV-1 to both ensure efficient spread through epithelial replication and modulate immune responses by targeting circulating immune cells (Alandijany, 2019).

Primary HSV-1 infection occurs in epithelial cells of the oral, nasal, or ocular mucosa. Productive replication within epithelial cells generates lesions evolving from vesicles to superficial erythematous ulcerations, which represent a typical cytopathic effect and lead to viral shedding at the site of infection for up to two weeks (Arvin et al., 2007). Following this initial replication, HSV-1 causes a lifelong infection due to its ability to infect sensory neurons that innervate the affected tissues of the skin, oral mucosa, and ocular mucosa. After invading nerve termini, virions are transported from the primary site of infection to neuronal axons, where latency is established (Nicoll et al., 2016; Zerboni et al., 2013).

During latency, the viral genome persists in the nuclei of sensory neurons, especially within the trigeminal ganglia (TG), as a circular episome of double-stranded DNA (Kramer and Enquist, 2013; Pomeranz et al., 2005; Steiner et al., 2007). Viral gene expression is silenced mainly during this phase, with the notable exception of the latency-associated transcript (LAT), a non-coding RNA that suppresses viral gene expression (Nicoll et al., 2016; Zerboni et al., 2013). Reactivation can occur spontaneously or in response to various stimuli, including stress or immune suppression. This process involves the renewed expression of lytic genes, the DNA replication, and the production of infectious virions (Arvin et al., 2007; Suzich and Cliffe, 2018).

Upon reactivation, viral progeny assemble within the nucleus, where gene expression, DNA replication, capsid assembly, and genome packaging occur (Ahmad and Wilson, 2020). Capsids then bud at the inner nuclear membrane and transit into the cytoplasm, where they acquire an envelope and exit the cell, completing the viral maturation process. From there, they are transported in an anterograde direction along axonal microtubules, often in association with cytoplasmic organelles as organelle-associated enveloped virions (OEVs), to reach

neuronal termini, the plasma membrane, or cell-cell junctions. This facilitates viral spread to neighboring uninfected epithelial tissues including ocular epithelia and oral mucosa, where new lytic cycles can be initiated (Ahmad and Wilson, 2020; Denes et al., 2018; Diwaker and Wilson, 2019; Knipe and Howley, 2013; Kramer and Enquist, 2013; Smith, 2012; Steiner et al., 2007; Valerio and Lin, 2019) (Figure 1).

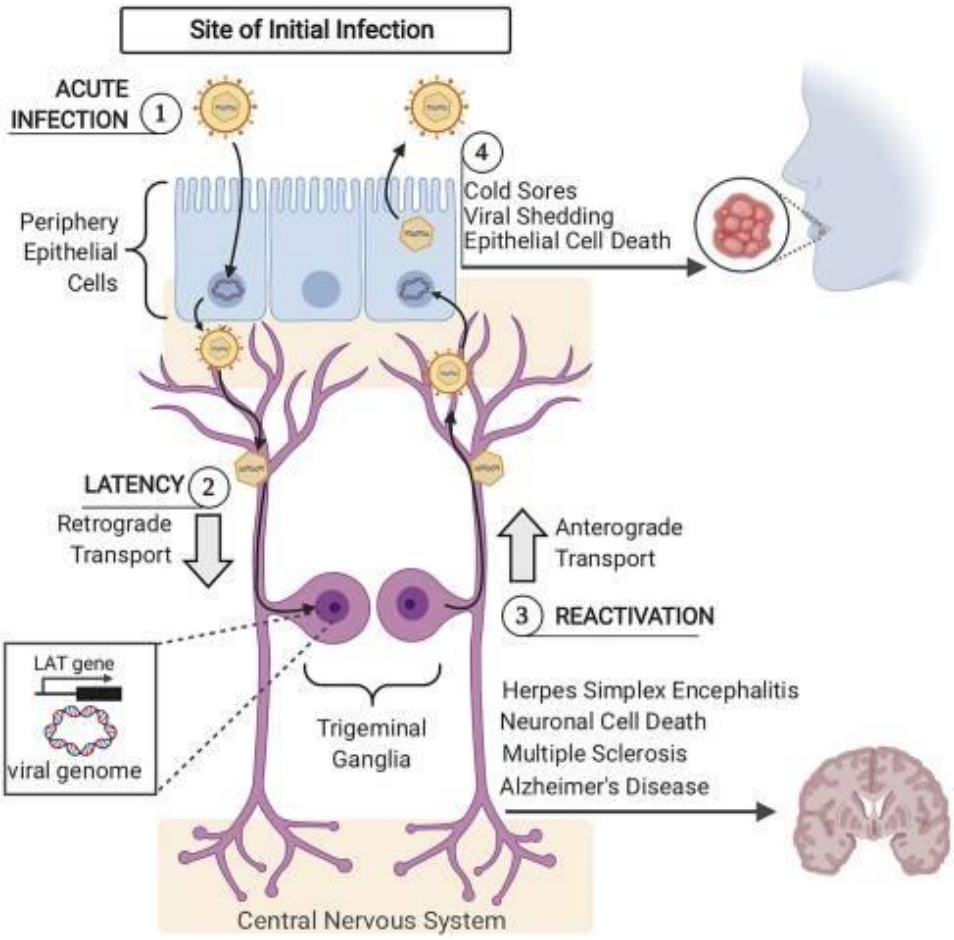

Figure 1. Acute and latent HSV-1 infection. (1) When viral envelopes fuse with plasma membranes, HSV-1 virions infiltrate epithelial cells and cause acute infection. The viral genome enters the nucleus of the epithelial cell via the viral nucleocapsid. Viral genome replication and gene expression in the nucleus result in the production of more infectious virions. Some newly produced virus particles infect adjacent sensory neurons. (2) Retrograde trafficking brings HSV-1 capsids to sensory ganglion neuronal cell bodies. The host cell silences viral genome transcription, except for the latency-associated transcript (LAT) gene, in the neuronal nucleus because viral DNA circularizes. Viral progeny in the central nervous system can cause herpes simplex encephalitis, neuronal cell loss, and, recently, Multiple Sclerosis and Alzheimer's Disease. (3) Viral nucleocapsids leave the neuronal nucleus and travel anterogradely to epithelial cells after reactivation. (4) Viral replication and progeny release damage epithelial cells and cause orofacial sores (Verzosa et al., 2021).

Clinically, HSV-1 is a persistent and incurable pathogen that remains within the host for the remainder of its life. Current therapeutic approaches for both primary and recurrent infections rely on nucleoside analogues such as acyclovir, valacyclovir, famciclovir, and ganciclovir (Sarisky et al., 2002; Whitley, 2006). However, since over 40% of patients experience recurrent infections that require repeated treatments, the emergence of drug-resistant HSV strains is becoming increasingly common (Piret and Boivin, 2011). Therefore, the study of new antiviral drugs poses a significant challenge in combating viral infections and preventing the development of drug resistance. From this perspective, natural products, such as crude extracts and bioactive molecules derived from plants, are recognized as promising sources of new antiviral compounds, thanks to their lower toxicity and alternative mechanisms of action compared to nucleoside analogues (Bhaskarachary et al., 2015)

1.1. HSV-1 virion structure, genome organization, and life cycle

The HSV-1 virion is a spherical particle, 150-225 nm in diameter, consisting of three main compartments: a lipid envelope embedded with viral glycoproteins, a proteinaceous tegument layer, and an icosahedral capsid enclosing the viral linear double-stranded DNA (dsDNA) genome (Newcomb et al., 1993) (Figure 2).

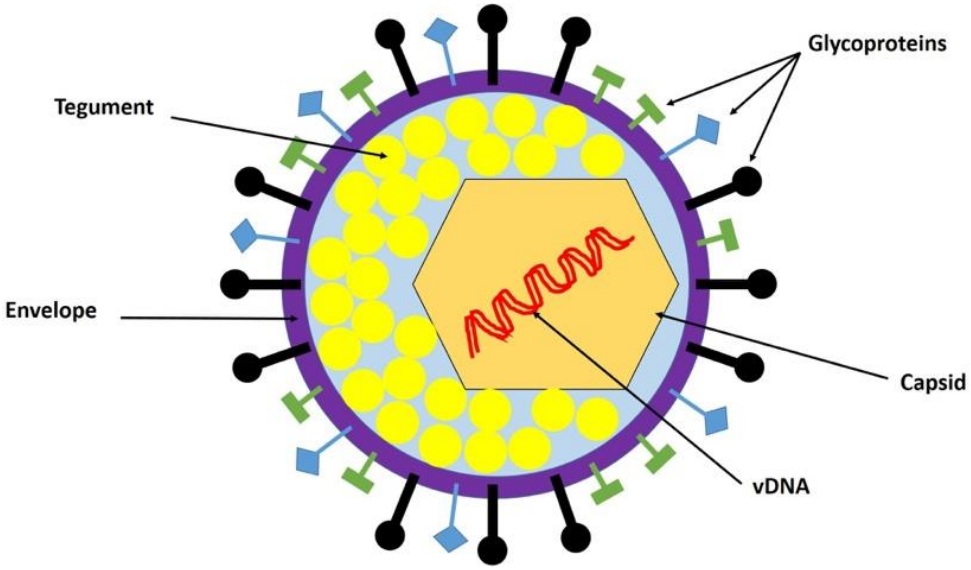

Figure 2. HSV-1 virion structure. The virion is composed of four main elements: the viral genome, the capsid, the tegument, and the envelope. The genome consists of a linear double-stranded DNA (dsDNA) packaged within the capsid. Surrounding the capsid lies the tegument, a protein-rich layer that bridges the capsid and the envelope. The outermost envelope is a lipid bilayer derived from the host cell membrane, in which viral glycoproteins are embedded as surface projections (Alandijany, 2019).

The viral envelope represents a lipid bilayer derived from the cellular membrane that encloses the tegument and contains several glycoproteins, which are major antigenic determinants involved in viral entry, intercellular spread, and immune evasion (Haarr and Skulstad, 1994). In particular, glycoprotein H (gH), encoded by the *UL22* gene, together with its partner gL, is critical for efficient folding, transport, and membrane fusion, playing a central role in viral infectivity, and cell-to-cell transmission (Gillet et al., 2007; Hutchinson et al., 1992; Omerović et al., 2005; Roop et al., 1993). The gH/gB complex is indispensable for nuclear egress,

as the simultaneous deletion of these proteins results in the accumulation of virions within the perinuclear space (Farnsworth et al., 2007).

The tegument, located between the capsid and the envelope, is an amorphous structure composed of at least 11 viral proteins (Haarr and Skulstad, 1994). Among these, VP16 (*UL48* gene product) is a multifunctional 65 kDa protein essential for productive infection. Although not directly required for DNA replication, HSV-1 recombinants lacking *UL48* display defective DNA packaging, altered replication, and an absence of infectious progeny (Weinheimer et al., 1992). VP16 functions as a transcriptional activator of immediate-early (IE) genes by recruiting cellular transcription factors and cooperating with Oct-1, thus initiating the viral gene expression cascade (LaBoissière and O'Hare, 2000). Additionally, VP16 interacts with other tegument and envelope proteins, including the virion host shutoff (VHS) protein, gB, gD, gH, UL47, and VP22, linking capsid-associated and envelope-associated proteins and thereby contributing to virion assembly and egress (Elliott et al., 1995; Fuchs et al., 2002; Smibert et al., 1994; Zhu and Courtney, 1994).

The capsid has an icosahedral architecture, ~125 nm in diameter, and consists of 162 capsomeres: 150 hexons and 12 pentons (Newcomb et al., 1993). Each hexon is composed of six copies of VP5, while eleven pentons contain five VP5 molecules. The twelfth penton is replaced by the UL6 portal complex, a cylindrical structure formed by 12 UL6 proteins that mediates DNA packaging (Newcomb et al., 2001). VP23 and VP19c, in a 2:1 ratio, connect triplet capsomeres, maintaining capsid integrity (Saad et al., 1999). Capsid maturation involves scaffold proteins VP22a and VP21 (Davison et al., 1992; Person et al., 1993), as well as the serine protease VP24, which is essential for DNA encapsidation (Cardone et al., 2012). VP26, a 12 kDa capsid protein encoded by *UL35*, is located on the hexon tips (McNabb and Courtney, 1992; Zhou et al., 1995). While dispensable for replication in vitro, VP26 is essential for producing infectious virions in sensory ganglia and accumulates in the nucleus through interactions with VP5 and VP22a (Chi and Wilson, 2000; Desai et al., 1998; Rixon et al., 1996; Taylor et al., 2002).

The HSV-1 genome consists of a linear dsDNA molecule of approximately 152-153 kbp, encoding about 75 open reading frames. It is divided into two regions, the unique long (UL, ~82%) and the unique short (US, ~18%), each flanked by inverted

repeats (a, b, c sequences), which enable the genome to form four isomeric conformation through recombination (Figure 3). After nuclear entry, the linear genome circularizes to create an "endless" structure, which is essential for replication (Boehmer and Nimonkar, 2003; Knipe and Howley, 2013; Lehman and Boehmer, 1999; Strang and Stow, 2005).

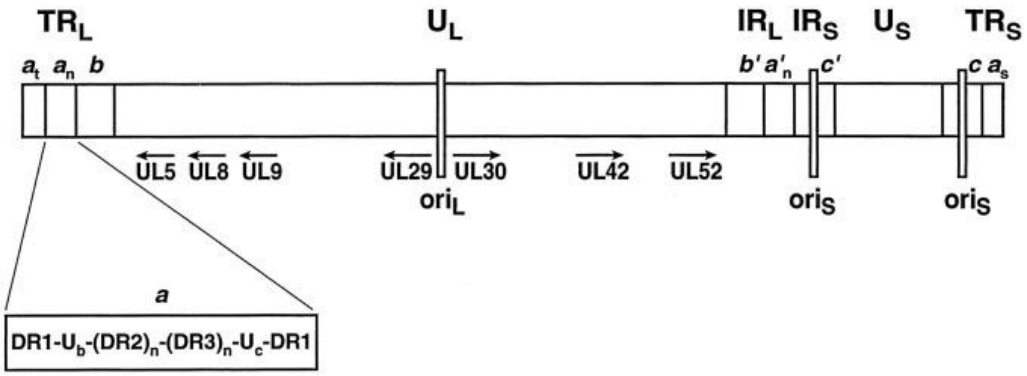

Figure 3. HSV-1 genome organization. The illustration shows the HSV-1 genome, highlighting the locations of the a, b, and c repeat regions within both the terminal repeats (TRL and TRS) and the internal repeats (IRL and IRS). The origins of DNA replication (oriL and oriS) are also indicated. Arrows mark the position and transcriptional orientation of the seven genes essential for viral DNA replication (Lehman and Boehmer, 1999).

HSV-1 replication is highly regulated and proceeds through a cascade of transcriptional events classified into immediate-early (IE, α), early (E, β), and late (L, γ) (Honess, 1975; Honess and Roizman, 1974) (Figure 4). HSV entry is a process that varies depending on the host cell type and occurs through direct fusion with the plasma membrane or by endocytosis. This step requires the participation of at least four envelope glycoproteins (gB, gC, gD, gH, and gL) that interact with specific cellular receptors (Gianni et al., 2010). Following entry, several tegument proteins remain attached to the nucleocapsid, facilitating its transport across the cytosol toward the nuclear pore complex (NPC). The microtubule network and the dynein motor complex support this trafficking. At the nuclear membrane, the capsid interacts with importin β (Ojala et al., 2000), enabling the viral DNA to be released via the UL6 portal protein into the nucleus, where transcription of viral genes proceeds in a regulated cascade (Newcomb et al., 2001).

All viral transcripts are synthesized by host RNA polymerase II and undergo 5' capping and 3' polyadenylation. VP16 triggers the transcription of IE genes, whose synthesis peaks at 2-4 hours post-infection (h.p.i.), including ICP0, ICP4, ICP22, ICP27, and ICP47, which then drive the transcription of early genes. IE proteins (i.e., ICP27) also act as suppressors of host transcription (Boehmer and Lehman, 1997; Campbell et al., 1984; Rice et al., 1989). Protein synthesis becomes detectable as early as 3 h.p.i., reaching its maximum between 5 and 7 h.p.i. Among the proteins expressed at this stage are key enzymes required for viral genome replication, including the origin-binding protein, DNA polymerase, the single-stranded DNA-binding protein, the helicase-primase complex, and several enzymes involved in DNA repair and nucleotide metabolism (Boehmer and Lehman, 1997; Knipe and Howley, 2013).

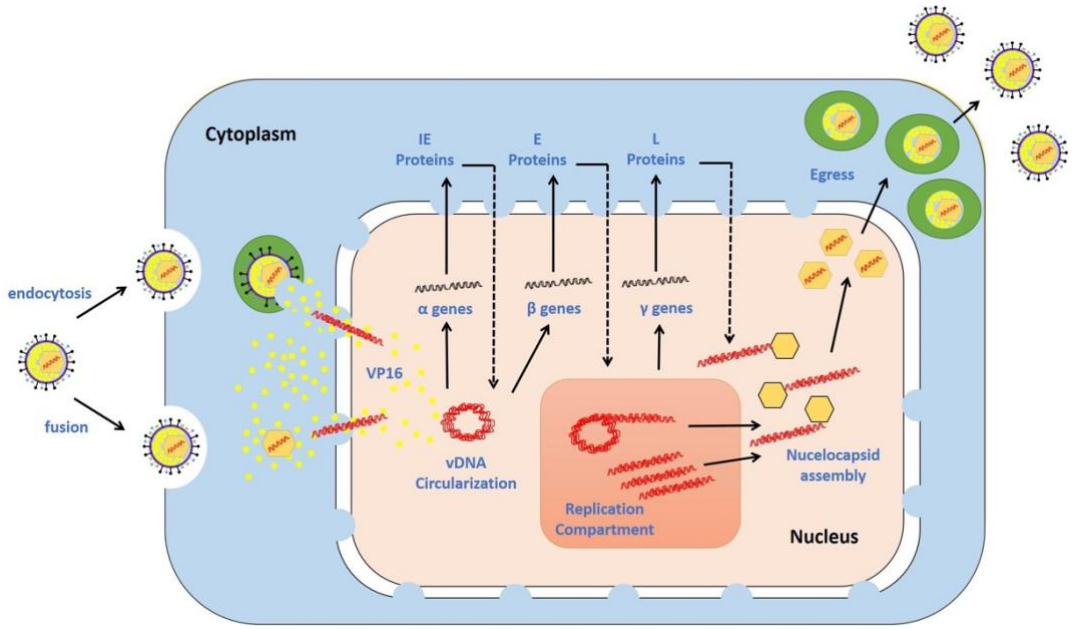

Figure 4. HSV-1 life cycle. Viral entry begins with the attachment of HSV-1 glycoproteins to specific cellular receptors, followed by entry through either the fusion of the viral envelope with the plasma membrane or via endocytosis. Once de-enveloped, the nucleocapsid is transported to the nuclear pore complexes, where the viral DNA (vDNA) is delivered into the nucleus. Gene expression occurs in a temporally regulated cascade comprising immediate-early (IE), early (E), and late (L) proteins. The virion-associated protein VP16 initiates IE gene transcription, while expression of E proteins depends on IE products and is essential for the onset of vDNA replication. HSV-1 DNA replication goes through a theta mechanism and subsequently transitions into rolling-circle replication. The production of L proteins is strictly dependent on prior vDNA synthesis and provides the structural components for virion assembly. Capsid formation occurs adjacent to replication compartments, enabling the packaging of vDNA into the capsid. The newly formed nucleocapsids bud through the nuclear membrane, traverse the cytoplasm, and fuse with the plasma membrane, acquiring tegument and envelope proteins. The release of mature progeny virions enables infection of neighboring cells, perpetuating the viral life cycle (Alandijany, 2019).

Viral DNA synthesis begins shortly after the onset of protein expression, typically between 3 and 15 h.p.i., with the bulk of replication occurring during the later phase of this interval (Boehmer and Lehman, 1997; Knipe and Howley, 2013). Viral DNA replication initiates at three origins: one oriL located within the UL region and two copies of oriS located within the inverted repeats (Lehman and Boehmer, 1999). Replication is initiated by the origin-binding protein UL9, which recognizes palindromic A+T-rich motifs and unwinds DNA in cooperation with ICP8 (He and Lehman, 2001; Olivo et al., 1988). UL9, containing ATP-binding and helicase motifs, binds origins as a homodimer and interacts with ICP8 to stabilize unwinding (Boehmer et al., 1993; Lee and Lehman, 1999). ICP8, encoded by *UL29*, is a binding protein that binds cooperatively to single-stranded DNA (ssDNA) with high affinity (Lee and Knipe, 1985; Makhov et al., 1996). Viral DNA polymerase, encoded by *UL30*, functions as a heterodimer with its processivity factor UL42. UL30 exhibits 3′→5′ exonuclease proofreading and RNase H activity, ensuring high-fidelity replication and Okazaki fragment processing (Crute and Lehman, 1989; Gallo et al., 1989; Gottlieb et al., 1990; Hernandez and Lehman, 1990; O'Donnell et al., 1987). DNA replication initiates through theta replication and then switches to a rolling-circle mechanism, generating concatemers that are subsequently cleaved and packaged into capsids (Boehmer and Lehman, 1997; Weller and Coen, 2012).

The final phase of the temporal cascade of HSV-1 gene expression is characterized by the synthesis of late proteins, which serve as structural components essential for virion assembly (Boehmer and Lehman, 1997; Knipe and Howley, 2013). Within the nucleus of infected cells, viral capsids accumulate and assemble, and then the viral DNA is packaged inside them through an energy-dependent process. Tegumentation occurs via Golgi-derived vesicles containing glycoproteins, which subsequently fuse with the plasma membrane to release mature virions (Homa and Brown, 1997).

1.2. Host immune responses to HSV-1

The host innate immune system plays a crucial role in the initial control of HSV-1 infection, limiting viral spread and shaping subsequent adaptive responses. Pattern recognition receptors (PRRs), such as Toll-like receptors (TLRs) and RIG-I-like receptors (RLRs), as well as cytosolic DNA sensors including cGAS-STING, detect viral nucleic acids and trigger signaling cascades that promote the secretion of type I interferons (IFN-α/β) and proinflammatory cytokines (Alandijany, 2019). These mediators activate interferon-stimulated genes (ISGs), which restrict viral replication and alert surrounding cells. The antiviral activity of type I and type II interferons (IFN-α/β and IFN-γ) is exerted primarily through the JAK/STAT pathway, leading to the induction of proteins such as double-stranded RNA-activated protein kinase (PKR) and 2′-5′ oligoadenylate synthetases (OAS), which act as effectors to suppress viral replication (Levy and García-Sastre, 2001). PKR, which presents an amino-terminal regulatory domain and a carboxy-terminal serine/threonine kinase domain, is activated by double-stranded RNA (dsRNA) generated during viral infection (Balachandran et al., 2000). Autophosphorylation of PKR leads to dimer formation and the phosphorylation of substrates, including eIF-2α and IκBα. The eIF-2α phosphorylated protein is inactive and blocks protein synthesis, thereby depriving the virus of its translational machinery. In contrast, the phosphorylation of IκBα promotes the activation of NF-κB (Bonnet et al., 2000; Gal-Ben-Ari et al., 2019). In addition, PKR can activate apoptotic responses by engaging the FADD/caspase-8 pathway, a process further potentiated by type I interferons, which sensitize infected cells to apoptosis through the activation of caspase-8 (Balachandran et al., 2000). PKR has also been implicated in the induction of autophagy, adding another layer of antiviral defense (Lussignol et al., 2013).

Apoptosis indeed represents an essential antiviral mechanism. It can be triggered through extrinsic signals, intrinsic stress, or a combination of both, culminating in the activation of initiator caspase-8, which subsequently activates caspase-3 and -7 to drive cellular breakdown. This process contributes to the elimination of infected cells and the degradation of viral components. HSV-1, however, modulates

apoptosis in a cell-type-dependent manner. While it can both trigger and inhibit apoptosis in epithelial cells during infection (Nguyen and Blaho, 2006), immune cells, such as NK cells, macrophages, and monocytes, are more prone to HSV-1-induced apoptosis (Raftery et al., 1999). Macrophages, dendritic cells, natural killer (NK) cells, and monocytes are also key players in the antiviral defense against HSV-1 (Alandijany, 2019; Levy and García-Sastre, 2001). Activated macrophages release cytokines such as TNF-α and type I interferons (Toews, 2009), which act directly against the virus and simultaneously stimulate NK cells to release IFN-γ, thereby amplifying antiviral effector functions. This reciprocal feedback enhances the production of nitric oxide (NO) and reactive oxygen species (ROS), establishing a hostile intracellular environment that restricts viral replication. Monocytes represent another critical component of the early antiviral response (Ellermann-Eriksen, 2005). They produce a wide range of proinflammatory mediators, including IL-1β, IL-6, TNF-α, and MCP-1, which not only shape the inflammatory milieu but also promote the recruitment of additional immune cells to the site of infection. Recruited monocytes can differentiate into macrophages or dendritic cells depending on local cues, thereby expanding the effector network at mucosal and peripheral sites of HSV-1 infection (Dash et al., 2024; Ellermann-Eriksen, 2005). Chemokines secreted by both resident and infiltrating immune cells serve as chemoattractants, coordinating leukocyte migration. During HSV-1 infection, chemokines such as CCL2, CCL3, CCL4, CCL5, CXCL9, and CXCL10 are induced in skin and mucosal tissues, where they recruit NK cells, T cells, and other effector populations, ultimately bridging innate and adaptive immunity. Importantly, in T cells, a phenomenon of “fratricide” has been described, whereby infected T cells upregulate death ligands that promote apoptosis in neighboring T cells (Raftery et al., 1999). Specifically, HSV-1 can productively infect activated cytotoxic T lymphocytes (CTLs) through the interaction of viral glycoprotein D (gD) with HVEM, a member of the TNF receptor family expressed on activated T cells (Montgomery et al., 1996; Whitbeck et al., 1997). Unlike in fibroblasts, where HSV-1 blocks antigen presentation by downregulating MHC class I, infected T cells maintain surface MHC class I expression, thus efficiently presenting viral peptides (Hill et al., 1994; York et al., 1994). This allows neighboring antiviral

CTLs to recognize viral antigens on infected T cells and to initiate apoptosis, turning infected T cells into decoy targets (Raftery et al., 1999).

The balance between apoptotic induction and suppression has profound implications for disease. For example, apoptotic cells are detectable in herpetic lesions of keratitis and encephalitis, suggesting that HSV-1-dependent regulation of cell death contributes not only to viral replication but also to tissue damage and pathology (DeBiasi et al., 2002; Miles et al., 2003). Moreover, sensitivity to HSV-1-induced apoptosis varies considerably among cell types: primary fibroblasts are relatively resistant, whereas transformed and tumor cells display heightened susceptibility, a phenomenon termed “viral oncoapoptosis”, which may have therapeutic potential in cancer treatment (Aubert and Blaho, 2003; Nguyen et al., 2005).

1.3. Mechanisms of HSV-1 immune evasion

During viral infection, host cells trigger a series of immune responses, beginning with the initiation of apoptotic signaling. Apoptosis is typically triggered between 0 and 3 h.p.i. before early and late viral gene expression occurs. However, the virus rapidly counteracts this process through the timely expression of anti-apoptotic proteins, preventing premature cell death and ensuring its own replication. Once immediate early and early proteins accumulate, apoptosis is efficiently blocked, establishing a “prevention window” that safeguards viral replication (Aubert and Blaho, 1999; Koyama and Adachi, 1997). HSV-1 expresses a wide range of gene products that interfere with host innate immune responses, including both interferon-mediated and apoptotic pathways. The ability of the virus to replicate and reactivate from latency depends on these virulence factors, which collectively ensure cell survival and viral persistence (You et al., 2017).

One primary strategy involves antagonism of the PKR pathway. The viral ICP34.5 protein antagonizes PKR by recruiting protein phosphatase 1α to dephosphorylate eIF-2α, thereby restoring protein synthesis (Chou et al., 1995; He et al., 1997). Similarly, the Us11 protein suppresses PKR activation by binding dsRNA and

associating with ribosomes, preventing PKR dimerization and activation. Its C-terminal proline-rich RNA-binding domain is sufficient to block PKR and sustain protein synthesis even in the absence of *ICP34.5* (Cassady and Gross, 2002; Peters et al., 2002; Poppers et al., 2000). Us11 also interacts with pattern recognition receptor (PRR)-mediated pathways, inhibiting the signaling of RIG-I and MDA5. It represses 2'-5' oligoadenylate synthetase (OAS) activity, interfering with FADD/caspase-8 signaling and autophagy (Balachandran et al., 2000; Sànchez and Mohr, 2007; Xing et al., 2012).

Us11 has been shown to play an additional role in modulating caspase-8. In monocytes and in epithelial cells, HSV-1 induces the accumulation of the caspase-8 p18 fragment through direct interaction of Us11 with caspase-8, bypassing the classical two-step cleavage pathway. The accumulation of p18 does not trigger apoptosis, distinguishing it from canonical caspase-8 activation; instead, it correlates with Atg3 cleavage, leading to the inhibition of autophagy and the promotion of viral replication (Musarra-Pizzo et al., 2022).

Besides, HSV-1 proteins interfere with IFN induction and signaling. ICP0 blocks interferon regulatory factor IRF3- and IRF7-mediated activation of interferon-stimulated genes (Eidson et al., 2002; Lin et al., 2004; Mossman et al., 2000). ICP27 prevents the phosphorylation, nuclear translocation, and transcriptional activity of STAT1, thereby blocking ISG activation downstream of type I IFN receptors (Johnson et al., 2008).

Multiple viral gene products also contribute to the inhibition of apoptosis. ICP6 (R1) inhibits Fas- and TNF-mediated apoptosis by interacting with caspase-8 and RIPK1, thereby preventing the formation of the death-inducing signaling complex (DISC) and the activation of caspase-8. It also blocks poly(I:C)-induced apoptosis by interfering with TRIF-RIP1-caspase-8 signaling and acts as a competitor to the RIP homotypic interaction motif (RHIM) domain, thereby disrupting RIP1-RIP3 interactions and inhibiting necrosome formation and necroptosis (Dufour et al., 2011a, 2011b; Guo et al., 2015). The serine/threonine kinase Us3 blocks apoptosis at a pre-mitochondrial stage. It phosphorylates pro-apoptotic Bcl-2 family members, including Bad and Bid, thereby preventing their activation, cytochrome c release, and caspase activation (Munger et al., 2001; Munger and Roizman, 2001).

Additionally, phosphorylation of Bid by Us3 prevents its cleavage by granzyme B, protecting infected cells from $CD8^+$ T cell-mediated killing (Cartier et al., 2003). Glycoproteins such as gD and gJ further inhibit Fas-mediated apoptosis, partly through modulation of the NF-κB pathway (Jerome et al., 1999; Medici et al., 2003).

In addition, the latency-associated transcript (LAT) plays a crucial role in neuronal survival. LAT inhibits caspase-8/9-dependent apoptosis and stabilizes phosphorylated AKT, blocking caspase-3-mediated apoptosis and promoting the maintenance of latency (Branco and Fraser, 2005; Carpenter et al., 2007; Henderson et al., 2002; You et al., 2017).

Altogether, these mechanisms illustrate the multifaceted strategies by which HSV-1 suppresses host cell death programs, ensuring efficient replication, long-term persistence, and reactivation potential (You et al., 2017).

1.4. Antiviral therapies against HSV-1

For decades, the clinical management of HSV-1 infections has relied on drugs that inhibit viral DNA synthesis. The compounds currently in use can be grouped into three major categories: acyclic guanosine analogues (e.g., Acyclovir, Ganciclovir, Famciclovir), acyclic nucleotide analogues (e.g., Cidofovir), and pyrophosphate analogues (e.g., Foscarnet) (Jiang et al., 2016; Reardon, 1989; Wagstaff and Bryson, 1994). Their activity is based on interfering with viral DNA polymerase, though they differ in activation and binding requirements. Acyclovir, the prototypical guanosine analogue, requires phosphorylation by the viral thymidine kinase (TK), which initiates a cascade of phosphorylation events by host kinases, ultimately yielding the active triphosphate form. This metabolite competes with deoxyguanosine triphosphate but, lacking a 3'-hydroxyl group, causes premature chain termination. Ganciclovir follows a similar pathway but modifies polymerase activity without strictly terminating DNA elongation (Reardon, 1989). Cidofovir, activated solely by host kinases, maintains efficacy against HSV strains defective in TK (Jiang et al., 2016; Safrin et al., 1999). Foscarnet (phosphonoformic acid, PFA), in contrast, bypasses the phosphorylation requirement entirely. By binding directly to the pyrophosphate-binding site of DNA polymerase, it prevents pyrophosphate cleavage during nucleotide incorporation, thereby halting viral DNA synthesis. Its independence from TK makes it particularly useful in infections sustained by TK-mutant HSV-1 isolates (Jiang et al., 2016; Wagstaff and Bryson, 1994).

Nevertheless, extensive clinical use of these drugs, especially Acyclovir (ACV) and its derivatives, has driven the emergence of resistant strains, a phenomenon particularly evident among immunocompromised patients. The molecular basis of resistance typically resides in mutations of *UL23*, which encodes TK, leading to reduced or absent kinase activity, or in *UL30*, which encodes the viral polymerase, altering substrate specificity. Resistance to ACV often extends to all TK-dependent analogues, leaving only TK-independent drugs such as Cidofovir or Foscarnet as effective options (Jiang et al., 2016; Morfin and Thouvenot, 2003). Due to these limitations, there is considerable interest in exploring novel therapeutic avenues.

One pharmacological approach under investigation is helicase-primase inhibition, which disrupts viral DNA replication at a stage independent of polymerase or TK function (Jiang et al., 2016).

Alongside these therapies, a growing amount of research has examined the antiviral potential of natural bioactive compounds. Extracts from plants, seeds, and essential oils are known not only for their antioxidant and immunomodulatory properties but also for direct antiviral effects (Bhaskarachary et al., 2015; Jiang et al., 2016). Among them, polyphenols stand out for their capacity to disrupt virus-cell interactions. For instance, phenolic compounds have been shown to block HSV-1 glycoprotein binding to glycosaminoglycan (GAG) receptors on the host surface (El-Toumy et al., 2018). Flavonoids, such as quercetin, illustrate this potential clearly: they inhibit infection by HSV-1, including acyclovir-resistant strains. Mechanistically, quercetin prevents viral entry at early stages and downregulates NF-κB signaling, which is crucial for viral gene expression (Hung et al., 2015). Curcumin, another well-studied polyphenol, inhibits HSV-1 differently. It diminishes IE gene expression by acting on the VP16-dependent recruitment of RNA polymerase II to viral promoters, thereby slowing the lytic cycle (Kutluay et al., 2008).

Chapter II

Caspase-8 in viral infection: from apoptotic to non-apoptotic functions

The previous chapter has outlined the structural, immunological, and therapeutic aspects of HSV-1 infection. A recurrent theme, emerging from these sections, is the virus's ability to finely manipulate host cell fate decisions and inflammatory signaling to ensure persistence and replication. HSV-1 targets host factors that regulate programmed cell death and innate immune signaling, which are central to balancing antiviral defense and viral fitness. In this context, caspase-8 has emerged as a critical molecular hub at the crossroads of apoptosis, inflammatory cell death, and pro-survival signaling pathways during viral infection.

Caspase-8 is a central decision-maker at the interface between host defense and virus-host interaction, integrating signals from death receptors, pattern-recognition receptors, and stress pathways to determine whether to select between apoptosis (which can limit pathogen spread) and inflammatory cell deaths, such as necroptosis and pyroptosis. Many viruses, including herpesviruses, have evolved strategies to modulate caspase-8's catalytic and scaffold functions, favoring replication, tuning NF-κB-dependent transcription, and restraining excessive inflammation that would otherwise curb viral fitness. In HSV-1 infection, caspase-8 also intersects with autophagy control and RIPK1-dependent checkpoints, shaping outcomes in epithelial and myeloid cells (Fritsch et al., 2019; Guo et al., 2015; Han et al., 2021; Newton et al., 2019). Apoptosis is a physiological mechanism to remove unwanted, damaged, or infected cells, and caspase-8 is its key initiator in the extrinsic pathway (Tummers and Green, 2017). HSV-1 is adept at modulating apoptosis to promote its replication via multiple virulence factors; among them, the tegument protein Us11 protects cells from heat- and staurosporine-induced apoptosis and counteracts host autophagy. In monocytic THP-1 cells, HSV-1 induces an early wave of autophagy that likely facilitates viral internalization. In contrast, late in infection, autophagy is inhibited or stabilized to support efficient replication, highlighting a temporal rewiring of degradative

pathways that converges on caspase-8-regulated checkpoints (Javouhey et al., 2008; Lussignol et al., 2013; Siracusano et al., 2016). Building on this framework, prior work on immune versus non-immune cells suggests that leukocytes (lymphocytes, monocytes/macrophages, and dendritic cells) typically sustain low-productive HSV-1 infections with apoptosis as a prominent cytopathic effect, whereas epithelial cells support robust replication; however, the molecular logic that restricts HSV-1 in immune cells remains incompletely defined. Given caspase-8's dual roles in apoptosis and non-apoptotic signaling (e.g., necroptosis control, autophagy crosstalk), dissecting how HSV-1 virulence factors reprogram caspase-8 in these distinct cellular contexts is essential to explain differential permissivity and inflammatory outcomes (Fritsch et al., 2019; Newton et al., 2019). Canonically, caspase-8 undergoes a two-step autoproteolytic processing in which the first cleavage between p18 and p10 yields p43/p41 and p12, followed by processing to the active p18/p10 heterotetramer (Kallenberger et al., 2014). An alternative route, described upon CD95 stimulation, involves an initial cleavage between the prodomain and p18, generating p26/p24 and p30 before the release of p18/p10 (Hoffmann et al., 2009). In THP-1 and epithelial models, Us11 can directly promote a non-canonical caspase-8 cleavage that bypasses the first step and produces p18, without engaging downstream apoptotic execution, implicating Us11-p18 interplay in rewiring caspase-8 outputs away from apoptosis (Musarra-Pizzo et al., 2022). Functionally, the absence of caspase-8 reduces HSV-1 protein/DNA accumulation (Musarra-Pizzo et al., 2022) and infectious yield and perturbs late replication steps linked to envelopment and egress (consistent with altered Rab5 and LAMP-1 distribution) (Raza et al., 2018; Torres et al., 2008), supporting a model in which caspase-8, beyond apoptosis initiation, contributes to membrane trafficking events that enable virion maturation and release. Together with the broader literature on non-apoptotic roles of caspase-8 (cell adhesion/migration, monocyte differentiation, lymphocyte activation, NF-κB signaling) (Fianco et al., 2018; Shalini et al., 2015), caspase-8 is positioned as a context-dependent proviral factor whose activity state and cleavage pattern tilt the balance between antiviral restriction and efficient HSV-1 replication (Marino-Merlo et al., 2023; Musarra-Pizzo et al., 2022).

2.1. Caspase-8 structure, activation, and cleavage

Caspase-8 is a member of the cysteine-dependent aspartate-specific protease family, synthesized as an inactive zymogen and localized in the cytosol. All caspases share a conserved catalytic domain in which a cysteine side chain mediates peptide bond hydrolysis specifically after aspartate residues in protein substrates. This property is unusual among proteases, and underpins their role as signal transducers rather than nonspecific degradative enzymes (Fuentes-Prior and Salvesen, 2004; Pop and Salvesen, 2009; Thornberry, 1998).

Within the apoptotic subgroup, caspases are classified into initiator (or apical) caspases (caspase-8, caspase-9, and caspase-10) that trigger the cascade, and effector caspases (caspase-3, caspase-6, and caspase-7) that thereby trigger the apoptotic program (Pop and Salvesen, 2009; Thornberry, 1998; Zhang et al., 2024). Initiators are further divided between those acting in the extrinsic apoptotic pathway (caspase-8, caspase-10) and those in the intrinsic pathway (caspase-9) (Pop and Salvesen, 2009). Unlike effectors, which exist as inactive dimers that become activated upon interdomain cleavage, initiators are inert monomers that require dimerization at signaling platforms such as the death-inducing signaling complex (DISC) (Chang, 2003; Fuentes-Prior and Salvesen, 2004).

The *CASP8* gene undergoes extensive alternative splicing, resulting in the production of eight isoforms (a-h). Of these, only caspase-8/a (55 kDa) and caspase-8/b (54 kDa) are consistently expressed across different cell types at detectable levels. These two isoforms differ by only 15 amino acids in the linker region between the prodomain and the catalytic domain, and both are recruited to the DISC upon receptor stimulation with similar kinetics (Scaffidi et al., 1997). Additional isoforms, such as caspase-8/c and caspase-8/d, have been proposed to modulate apoptotic sensitivity, either by dampening or enhancing caspase-8 activity; however, their physiological relevance remains uncertain due to their low expression (Scaffidi et al., 1997). At the structural level, procaspase-8 consists of a long N-terminal prodomain and a C-terminal catalytic domain. The prodomain contains tandem death effector domains (DED1 and DED2), which mediate interaction with FADD and allow recruitment to the DISC. The catalytic domain is organized into a large subunit (~20 kDa, p20/p18) carrying the catalytic cysteine

and histidine residues, and a small subunit (~10-12 kDa, p12/p10) that contributes to the substrate-binding pocket (Fuentes-Prior and Salvesen, 2004; Kallenberger et al., 2014; Zhang et al., 2024). Activation occurs when procaspase-8 molecules are recruited to the DISC, leading to dimerization, a proximity-induced mechanism that converts the zymogen into an active enzyme (Chang, 2003; Fuentes-Prior and Salvesen, 2004). Once dimerized, caspase-8 undergoes autoproteolytic cleavage at conserved aspartate residues. Cleavage within the enzymatic domain (Asp374, Asp348) separates the large and small subunits, producing intermediates such as p43/p41 and p10. In contrast, cleavage at the junction between the prodomain and the catalytic domain (Asp220, Asp216) yields fragments p26/p24 and p30. Subsequent processing results in the release of mature p18 and p10 subunits, which assemble into a heterotetramer ($p18_2$-$p10_2$) that dissociates from the DISC and functions in the cytosol (Kallenberger et al., 2014) (Figure. 5). Interestingly, cleavage occurs via both intradimeric and interdimeric mechanisms: prodomain cleavage sites are processed within the same dimer, whereas interactions between separate DISC-associated dimers facilitate cleavage in the enzymatic domain. This results in a temporal regulation in which sustained membrane-bound p43 activity is followed by transient cytosolic p18/p10 activity, functioning as a molecular “timer” for apoptotic signaling (Kallenberger et al., 2014).

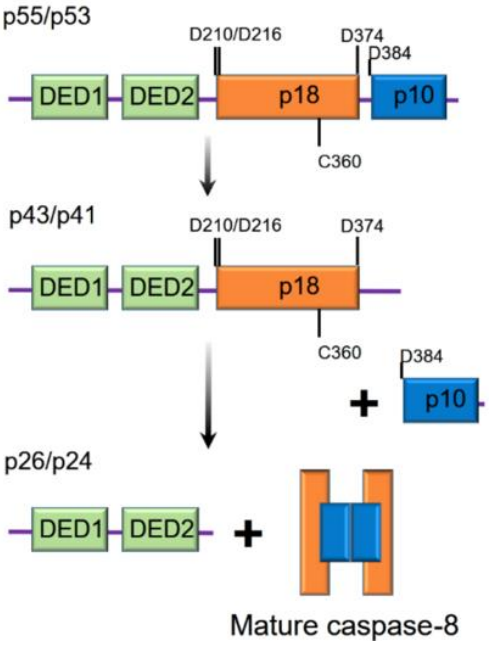

Figure 5. Schematic representation of procaspase-8 activation. Procaspase-8 (p55/p53) is an inactive precursor composed of two death effector domains (DEDs), a large subunit (p18), and a small subunit (p10). Its maturation depends on sequential autoproteolytic processing at conserved aspartic residues. Cleavage between the large and small subunits at Asp374 (D374) and Asp348 (D348) produces the intermediates p43/p41 and p10. Additional cleavage between the prodomain and the catalytic domain occurs at Asp220 (D220) and Asp216 (D216), resulting in the generation of the fragments p26/p24 and p30. Further processing of either p43/41 or p30 results in the formation of the mature p18 and p10 subunits, which assemble into a heterotetramer comprising two large and two small subunits (Han et al., 2021).

Collectively, this multi-step maturation process highlights caspase-8 as a finely tuned molecular switch. Depending on its processing state and interaction partners, caspase-8 can either initiate apoptosis, or participate in alternative signaling outcomes such as cell survival and inflammation (Newton et al., 2019; Pop and Salvesen, 2009; Zhang et al., 2024).

2.1.1. Caspase-8 activity modulation by FLIP isoforms

Cellular FLICE-like inhibitory proteins (c-FLIP) represent central modulators of caspase-8 activation at the death-inducing signaling complex (DISC). They are structurally related to caspase-8, sharing the two N-terminal death effector domains (DEDs), but lack proteolytic activity due to amino acid substitutions in the catalytic domain (Tsuchiya et al., 2015). The human CASP8 and FADD-like apoptosis

regulator (*CFLAR* gene), located on chromosome 2q33-34 adjacent to *CASP8* and *CASP10*, encodes multiple isoforms through alternative splicing, primarily c-FLIP$_L$ (55 kDa), c-FLIP$_S$ (27 kDa), and c-FLIP$_R$ (25 kDa) (Irmler et al., 1997; Tsuchiya et al., 2015). The functional outcome of c-FLIP recruitment to the DISC depends on the isoform and its relative abundance. c-FLIP$_S$ and c-FLIP$_L$, which lack the catalytic domain, act as dominant-negative inhibitors by competing with procaspase-8 for binding to FADD and blocking its activation (Krueger et al., 2001; Tsuchiya et al., 2015). While c-FLIP$_L$ forms heterodimers with procaspase-8, at low concentrations, it can facilitate the initial processing of procaspase-8, generating catalytically competent, though incompletely cleaved, caspase-8 intermediates (Chang, 2002; Micheau et al., 2002; Tsuchiya et al., 2015). These DISC-tethered heterodimers cleave specific proximal substrates such as RIPK1 or c-FLIP itself but fail to release fully processed caspase-8 into the cytosol, thereby attenuating apoptosis while sustaining non-apoptotic signaling. Cleavage of c-FLIP$_L$ generates truncated forms such as p43-FLIP and p22-FLIP, which further modulate DISC dynamics (Tsuchiya et al., 2015). The heterodimeric caspase-8-c-FLIP$_L$ complex has been shown to exhibit substrate specificity comparable to caspase-8 homodimers, although subtle differences may favor distinct signaling outcomes (Micheau et al., 2002). Mathematical modeling and quantitative studies confirmed that the balance between procaspase-8 and c-FLIP isoforms is a decisive factor in determining whether DISC signaling results in apoptosis, survival, or alternative death pathways (Kallenberger et al., 2014; Tsuchiya et al., 2015) (Figure 6).

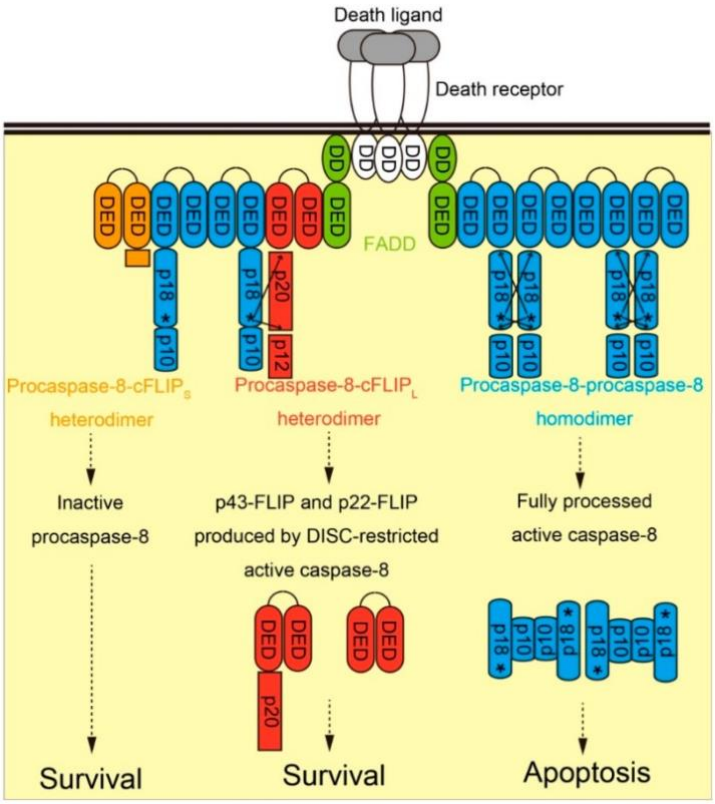

Figure 6. Functional role of c-FLIP isoforms during death receptor-mediated apoptosis. Upon ligand binding, death receptors trimerize and recruit the adaptor FADD via DD-DD interaction. Through DED-DED interactions, procaspase-8 (blue) and c-FLIP isoforms (c-FLIP$_L$, red; c-FLIP$_S$, orange) are assembled at the DISC. The functional outcome depends on the isoform and its abundance. Procaspase-8 homodimers undergo complete processing, resulting in the generation of active caspase-8, which activates effector caspases and induces apoptosis. c-FLIP$_S$ acts as a dominant-negative inhibitor by competing with procaspase-8 for FADD binding, thereby blocking caspase-8 activation and preventing apoptosis. In contrast, c-FLIP$_L$ forms heterodimers with procaspase-8, promoting partial processing of procaspase-8 and producing catalytically active but incompletely cleaved intermediates (p43-FLIP and p22-FLIP) that further modulate DISC dynamics, thereby attenuating apoptosis and leading to cellular survival (Tsuchiya et al., 2015).

Notably, c-FLIP isoforms also regulate caspase-8 within death receptor-independent complexes, such as the ripoptosome, thereby influencing the switch between apoptosis and necroptosis. In this context, the presence of c-FLIP$_L$ promotes limited caspase-8 activity, sufficient to cleave RIPK1 and dismantle the complex, thereby favoring survival. In contrast, c-FLIP$_S$ incorporation fails to activate caspase-8 and instead drives necroptosis via the RIPK1-RIPK3-MLKL axis (Feoktistova et al., 2011; Tsuchiya et al., 2015). c-FLIP functions as a fine regulator of caspase-8, with isoform-specific and concentration-dependent effects. This dual capacity, to both suppress and enable caspase-8 activity, explains its pivotal role in

regulating apoptosis, necroptosis, and non-apoptotic caspase-8 functions, ensuring proper control of cell fate decisions (Tsuchiya et al., 2015).

2.1.2. Caspase-8 post-translational ubiquitination and phosphorylation

Ubiquitination events strongly influence the regulation of caspase-8 downstream of death receptors. Upon stimulation of TNFR family receptors, caspase-8, recruited to the DISC, can undergo polyubiquitination at distinct sites, resulting in divergent functional outcomes (Jin et al., 2009). Jin et al., 2009 demonstrated that ubiquitination of caspase-8 at its small catalytic subunit (p10) is mediated by a CUL3-based E3 ligase. This modification allows the ubiquitin-binding protein p62/sequestosome-1 to cluster polyubiquitinated caspase-8, thereby promoting its proteolytic maturation into catalytically active heterotetramers. In contrast, TRAF2-dependent ubiquitination of caspase-8 at its large catalytic subunit (p18) facilitates proteasomal degradation after autoproteolytic release into the cytoplasm, thereby reducing the apoptotic response (Gonzalvez et al., 2012). These apparently opposing mechanisms demonstrate that ubiquitination functions as a dual regulatory switch, promoting caspase-8 activation in a DISC-restricted context (via the CUL3/p62 axis) or limiting its pro-apoptotic potential through cytosolic degradation (via the TRAF2 axis) (Gonzalvez et al., 2012; Jin et al., 2009). Beyond the DISC, ubiquitin-related modifications also modulate caspase-8 function in alternative complexes such as the ripoptosome, influencing the switch between apoptosis and necroptosis (Feoktistova et al., 2011; Tenev et al., 2011). Indeed, caspase-8, together with FADD and c-FLIP, restrains RIPK1/RIPK3-driven necroptosis during embryogenesis, highlighting that the roles of ubiquitination and scaffolding converge to maintain homeostasis (Fritsch et al., 2019; Mocarski et al., 2015).

Phosphorylation adds a further regulatory layer to caspase-8 activity, modulating both apoptotic and non-apoptotic signaling. Cursi et al., 2006 first reported that Src kinases phosphorylate Tyr380 in the intersubunit linker of caspase-8, thereby preventing processing into the fully active enzyme and blocking Fas/CD95-induced apoptosis. Tyr380 phosphorylation also enables binding of the Src Homology 2

(SH2) domain containing p85α subunit, incorporating caspase-8 into multiprotein complexes that regulate cytoskeletal remodeling, adhesion, and migration (Keller et al., 2018). In cancer, this modification has been associated with pro-tumorigenic roles. For instance, Finlay and Vuori, 2007 demonstrated that caspase-8 supports cell adhesion via Src and Erk signaling independently of its proteolytic activity, while Fianco et al., 2016 showed that aberrant Tyr380 phosphorylation promotes anoikis resistance and tumor progression. Other residues further expand the regulatory complexity of caspase-8. Alvarado-Kristensson et al., 2004 identified phosphorylation on Ser364 (human neutrophils), mediated by the serine/threonine mitogen-activated protein kinase p38-MAPK, which delays apoptosis during inflammation. Additionally, phosphorylation of Ser387 by cyclin-dependent kinase B1 (Cdk1) suppresses Fas/CD95-induced apoptosis in mitotic cells (Matthess et al., 2010). Importantly, phosphorylation is not only inhibitory: it can reprogram caspase-8 towards non-apoptotic scaffolding roles. Han et al., 2021 described that caspase-8 regulates inflammasome responses, IL-1β production, and NF-κB activation, while Henry and Martin, 2017 showed that in response to TRAIL, caspase-8 forms a "FADDosoma" complex with FADD and RIPK1 that triggers NF-κB activation and cytokines expression independently of catalytic activity. These non-apoptotic outcomes are tightly linked to post-translational regulation.

2.2. Caspase-8 as a central regulator of programmed cell death pathways

Caspase-8 has emerged as a pivotal molecular switch orchestrating the balance between different forms of programmed cell death, including apoptosis, necroptosis, pyroptosis, and autophagy. By integrating upstream signals from death receptors, pattern-recognition receptors, and intracellular stress pathways, caspase-8 determines whether a cell undergoes immunologically silent apoptosis or inflammatory types of death. Its catalytic activity and scaffold functions are both required to prevent aberrant inflammation and ensure organismal homeostasis (Fritsch et al., 2019; Han et al., 2021; Mocarski et al., 2015; Newton et al., 2019; Weinlich et al., 2017). Genetic inactivation of caspase-8 causes embryonic lethality due to uncontrolled necroptosis and intestinal inflammation, underscoring its essential role as a checkpoint in cell fate decisions (Fritsch et al., 2019; Kaiser et al., 2011).

2.2.1. Apoptosis pathways: extrinsic and intrinsic mechanisms

Apoptosis represents a tightly regulated form of cell death crucial for development, tissue homeostasis, and host defense against pathogens. By eliminating infected or damaged cells in an immunologically silent manner, apoptosis restricts pathogen replication and prevents inflammation. Morphologically, apoptosis is characterized by plasma membrane blebbing, chromatin condensation, nuclear fragmentation, and the packaging of cellular content into apoptotic bodies that are rapidly cleared by phagocytes without triggering inflammation (Häcker, 2000).

Two main pathways converge to activate executioner caspases, orchestrating apoptosis: the extrinsic and intrinsic pathways. The extrinsic pathway is triggered by extracellular ligands such as Fas ligand (CD95L), TRAIL, or TNF-α binding to their respective death receptors (DRs) (FAS/CD95, TRAIL-RI/DR4, TRAIL-RII/DR5, and TNFR1). Receptor trimerization recruits the adaptor protein Fas-associated death domain (FADD) via death domain (DD) interactions, which in turn

binds procaspase-8 through DED-DED interactions. This assembly results in the formation of the DISC, where proximity-induced dimerization and autoproteolytic processing convert procaspase-8 into its active form (Locksley et al., 2001; Shen et al., 2018; Zhang et al., 2024).

Intracellular stress, including DNA damage, cytotoxic stress, or the withdrawal of growth factors, triggers the activation of the intrinsic pathway. Members of the BCL-2 family tightly control this pathway as pro-apoptotic proteins (BAX, BAK, and BH3-only proteins). Caspase-8 provides a critical link between extrinsic and intrinsic apoptosis by cleaving the BH3-only protein Bid. Truncated Bid (tBid) translocates to the mitochondria. It promotes BAX/BAK oligomerization, thereby amplifying apoptotic signaling through the mitochondrial outer membranes permeabilization (MOMP) and release of mitochondrial pro-apoptotic factors into the cytosol: cytochrome c, second mitochondria-derived activator of caspase Smac/DIABLO, and apoptosis-inducing factor (AIF) (Wang and Tjandra, 2013; Zhang et al., 2024; Zou et al., 2003). Cytochrome c forms a complex with Apaf-1 and procaspase-9, known as the apoptosome, which serves as a platform for the activation of caspase-9. Activated caspase-9 subsequently cleaves and activates caspase-3 and -7, orchestrating the execution phase of apoptosis (Delbridge et al., 2016; Zhang et al., 2024) (Figure 7).

2.2.2. Necroptosis and its suppression by caspase-8

The engagement of death receptors triggers a complex signaling cascade that can culminate in apoptosis, necroptosis, or cell survival, depending on the specific molecular context. At the molecular level, the sequence of events begins with TNFR1 activation by TNF, leading to the assembly of the TNFR1 signaling complex (Complex I), which is composed of TRADD, RIPK1, TRAF2, cIAP1/2, and the linear ubiquitin chain assembly complex (LUBAC). Ubiquitination of RIPK1 and NEMO within this platform activates TAK1- and IKK-dependent NF-κB signaling, driving expression of pro-survival genes and cytokines such as TNF and IL-6 (Iwai et al., 2014; Micheau and Tschopp, 2003; Sedger and McDermott,

2014) (Figure 7). When ubiquitination or phosphorylation of RIPK1 is impaired, RIPK1 dissociates from Complex I and interacts with FADD and procaspase-8, forming Complex IIa, also known as the ripoptosome. Through RHIM-mediated interactions, this complex recruits RIPK3, establishing a hub that determines whether the outcome will be apoptosis or necroptosis (Feng et al., 2007; Feoktistova et al., 2011). Other studies have shown that caspase-8 activity within the ripoptosome not only controls the decision between apoptosis and necroptosis but also influences inflammatory signaling. Amaral and Bortoluci, 2020; Han et al., 2021 demonstrated that caspase-8, in cooperation with FADD, can regulate inflammasome activation and IL-1β maturation, underscoring its role as a broader regulator of inflammation beyond cell death. Similarly, Keller et al., 2018 highlighted that the balance between caspase-8 and c-FLIP at the ripoptosome is decisive, showing that minimal caspase-8 activity at the DISC or ripoptosome is sufficient to prevent necroptosis while avoiding complete apoptotic execution, indicating that caspase-8 acts in a graded rather than binary manner (Schilling et al., 2014). Conversely, excess c-FLIP$_S$ or pharmacological inhibition of caspase-8 (e.g., zVAD-fmk) or downregulation of FADD prevents caspase-8 activity, favoring the formation of the necroptosome (Complex IIb). Within this complex, RIPK1 and RIPK3 undergo reciprocal phosphorylation, leading to RIPK3 oligomerization and recruitment of the mixed lineage kinase domain-like (MLKL) protein, which is phosphorylated and activated (Sun et al., 2012) and then translocated to the plasma membrane, where it forms disruptive pores, culminating in necroptotic cell death accompanied by the release of host-derived factors and damage associated molecular pattern (DAMPs) and inflammatory mediators (Cai et al., 2014). Post-translational modifications, such as phosphorylation and ubiquitination, also fine-tune caspase-8's function, with reports indicating that these modifications modulate both apoptotic suppression and non-apoptotic roles, including migration and NF-κB signaling (Keller et al., 2018).

Necroptosis is a caspase-independent but genetically programmed form of cell death that plays a crucial role in infection, cancer, neurodegeneration, and inflammatory disorders. Morphologically, necroptosis is characterized by cell swelling, loss of plasma membrane integrity, and release of pro-inflammatory

intracellular contents. It can be triggered by ligands of TNFRs, Toll-like receptors (TLRs), or interferon receptors (IFNRs), all of which converge on the RHIM-dependent assembly of RIPK1-RIPK3 complexes (Cao and Mu, 2021). Caspase-8 serves as the physiological suppressor of this pathway. By cleaving RIPK1 and RIPK3, active caspase-8 prevents necrosome formation and thus blocks necroptosis (Fritsch et al., 2019; Mocarski et al., 2015). Inhibition of caspase-8 by pathogens, mammalian inhibitors, or chemical caspase inhibitors (e.g., zVAD-fmk) promotes necroptosis downstream of DR or TLR stimulation (Newton et al., 2019; Sun et al., 2012). Genetic evidence highlights the pivotal role of caspase-8 in regulating necroptosis. Mice lacking caspase-8, FADD, or CFLAR (c-FLIP) genes die during embryogenesis due to uncontrolled RIPK3/MLKL-driven necroptosis and associated inflammation (Kaiser et al., 2011; Mocarski et al., 2015). Remarkably, this lethal phenotype is completely rescued in double-knockout mice lacking both caspase-8 and RIPK3 or MLKL, as well as in *Fadd*$^{-/-}$ *Ripk1*$^{-/-}$ mice, which are viable and healthy (Fritsch et al., 2019; Kaiser et al., 2011). These findings clearly demonstrate that the caspase-8-FADD-c-FLIP complex is indispensable for maintaining the balance between apoptosis and necroptosis, functioning as a checkpoint to prevent excessive inflammatory cell death (Fritsch et al., 2019; Newton et al., 2019).

2.2.3. PANoptosis and pyroptosis

Beyond its well-characterized roles in apoptosis and necroptosis, caspase-8 also interfaces with pyroptotic and inflammatory pathways, positioning itself as a central coordinator of multiple death programs. Pyroptosis is an inflammatory form of programmed cell death mediated by inflammasomes, which activate caspase-1 and caspase-11/4/5 to cleave gasdermin D (GSDMD), thereby forming plasma membrane pores that allow the release of pro-inflammatory cytokines such as IL-1β and IL-18 (Figure 7). Caspase-8, while not a canonical pyroptotic protease, has been shown to regulate inflammasome activity and intersect with this pathway in several contexts (Han et al., 2021; Jiang et al., 2021). One key mechanism is the

direct modulation of the NLRP3 inflammasome. In the absence of caspase-8, dendritic cells exposed to lipopolysaccharide (LPS) exhibit hyperactivation of the NLRP3 inflammasome, resulting in excessive IL-1β secretion. This effect depends on RIPK1, RIPK3, and MLKL, suggesting that caspase-8 restrains inflammasome activation by limiting the necroptotic machinery (Kang et al., 2013). In addition, caspase-8 can act in parallel with caspase-1 to process pro-IL-1β and pro-IL-18, contributing to cytokines maturation even when canonical inflammasome caspases are absent or insufficient (Han et al., 2021). Han et al., 2021 demonstrated that caspase-8 cleavage activity can substitute for caspase-1 in specific settings, highlighting its non-redundant role in inflammatory cytokines production. Furthermore, through interactions with FADD and RIPK1, caspase-8 can also regulate gasdermin-mediated pore formation, thereby linking death receptor signaling to pyroptotic outcomes. The integration of apoptosis, necroptosis, and pyroptosis into a unified cell death program has led to the definition of PANoptosis. This concept reflects the existence of higher-order protein complexes, termed PANoptosome, in which caspase-8 collaborates with RIPK1, RIPK3, FADD, and apoptosis-associated speck-like protein containing CARD (ASC) aggregation, as well as inflammasome components, to orchestrate multiple death modalities simultaneously (Jiang et al., 2021). In this context, caspase-8 functions as both a protease and a scaffold: its catalytic activity ensures cleavage of apoptotic and necroptotic substrates, while its structural role facilitates the recruitment of inflammasome components and gasdermins. Importantly, catalytically inactive caspase-8 mutants (e.g., C362S) cause embryonic lethality in mice, accompanied by uncontrolled necroptosis and pyroptosis, further underlining its central role in preventing inflammatory pathology (Fritsch et al., 2019; Jiang et al., 2021; Newton et al., 2019). Together, these findings establish caspase-8 as a master regulator of PANoptosis. By coordinating apoptotic, necroptotic, and pyroptotic pathways, caspase-8 safeguards tissue homeostasis and immune balance. Its dysregulation, whether by genetic deficiency, pathogen inhibition, or excessive inflammasome activation, results in hyperinflammation and tissue damage (Han et al., 2021; Jiang et al., 2021; Weinlich et al., 2017).

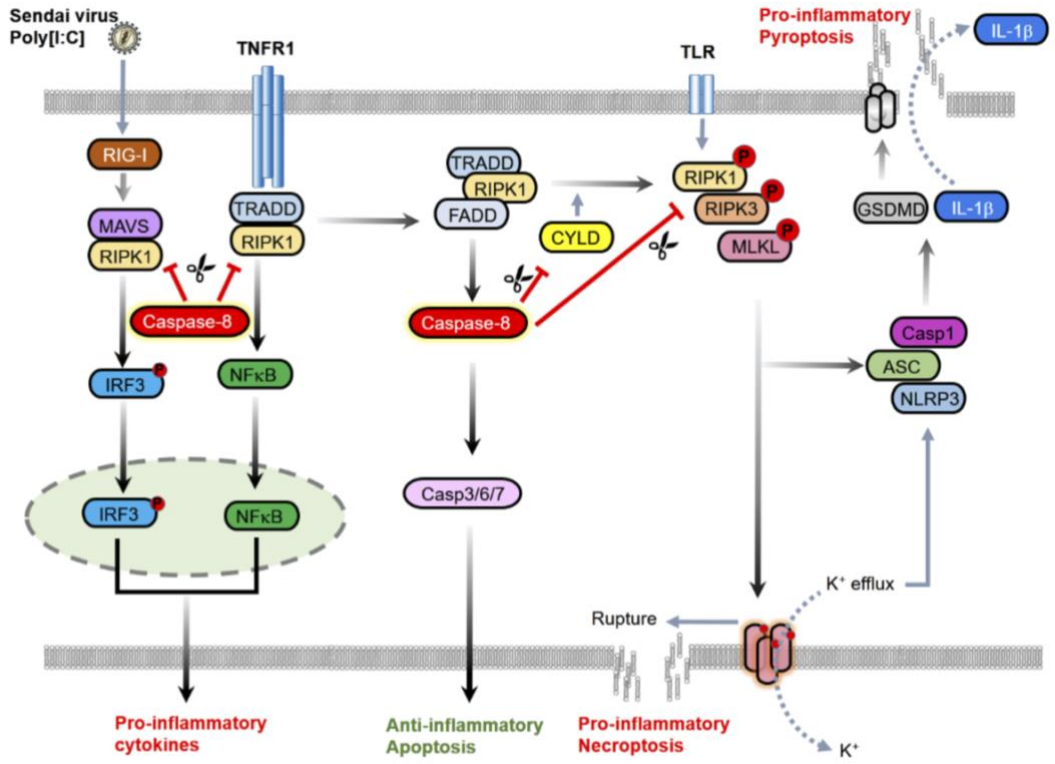

Figure 7. Caspase-8 plays a central role in controlling inflammation by promoting apoptosis, suppressing necroptosis, and restraining proinflammatory signaling pathways. Following activation of death receptors such as TNFR1, caspase-8 is recruited into a complex with FADD, RIPK1, and the TNFR1-associated death domain protein (TRADD), where it becomes activated. Once active, caspase-8 initiates apoptotic cell death by processing effector caspases, including caspase-3, -6, and -7. In parallel, caspase-8 prevents necroptosis (proinflammatory form of cell death) by cleaving and inactivating pro-necroptotic mediators such as RIPK1, RIPK3, and CYLD. Furthermore, caspase-8 is necessary to block Toll-like receptor (TLR)-driven, MLKL-dependent inflammasome activation. Its cleavage of RIPK1 also contributes to dampening the production of proinflammatory cytokines mediated by NF-κB or IRF3 in response to TNF or Sendai virus. In schematic representations, blue arrows denote activation events, red blunt-ended arrows indicate inhibition, and blue dotted arrows represent molecular release (Han et al., 2021).

2.2.4. Caspase-8 as a molecular switch between autophagy and apoptosis

Autophagy is a conserved catabolic pathway that maintains cellular homeostasis by degrading cytoplasmic material through lysosomal activity. It is orchestrated by autophagy-related (Atg) proteins, among which Beclin-1 provides a central scaffold for autophagosome formation by binding cofactors, while p62/sequestosome-1 functions as an adaptor that delivers ubiquitinated proteins to autophagosomes (Furuya et al., 2005; Huang et al., 2013; Tanida, 2011). Under basal conditions,

autophagy promotes survival; however, accumulating evidence has revealed an intricate reciprocal regulation between autophagy and apoptosis, with caspase-8 acting as a molecular switch that determines cell fate (Yu et al., 2004). Caspase-8 exerts this role through multiple mechanisms. Active caspase-8 can cleave autophagy proteins, establishing a negative feedback loop that suppresses excessive autophagy and reinforces apoptosis. For instance, caspase-8 directly cleaves Atg3, thereby impairing autophagosome formation (Oral et al., 2012), and Beclin-1, which reduces its pro-autophagic functions and enhances apoptotic signaling (Wirawan et al., 2010). Conversely, autophagosomes themselves have been shown to serve as platforms for intracellular DISC assembly, which is necessary for procaspase-8 cleavage and activation (Young et al., 2012). The adaptor protein p62 is critical in this process, as it facilitates the recruitment of caspase-8 to autophagosomal membranes. When autophagy is inhibited, p62 accumulates, thereby promoting caspase-8-dependent apoptosis (Huang et al., 2013). On the other hand, autophagic degradation of caspase-8 has been reported to restrain apoptosis, indicating a bidirectional regulatory loop between the two pathways (Hou et al., 2010). This crosstalk is also evident in specialized contexts such as T cell proliferation. During clonal expansion, caspase-8 is recruited to FADD-Atg5-Atg12 complexes, where it prevents hyperactive autophagy and thereby limits RIPK1-dependent necroptosis, ensuring controlled T cell survival and expansion (Bell et al., 2008). Similarly, in the context of viral infection, caspase-8 cleavage of Beclin-1 supports efficient HSV-1 egress by preventing virion entrapment in autophagic vesicles, underscoring its role in fine-tuning the balance between autophagy and apoptosis during host-pathogen interactions (Marino-Merlo et al., 2023; Wirawan et al., 2010).

2.3. Caspase-8 pro-survival functions

Although caspase-8 is classically known as an initiator caspase driving apoptosis, a large body of evidence demonstrates that it also exerts crucial pro-survival functions. While its canonical role is to initiate apoptosis, caspase-8 also performs a wide array of pro-survival functions, including the promotion of embryonic development, regulation of cell adhesion and migration, facilitation of monocyte differentiation, and support of T and B cell proliferation. It also contributes to NF-κB activation and tumorigenesis, depending on cellular context (Fianco et al., 2018; Kang et al., 2004; Shalini et al., 2015; Sordet et al., 2002). These functions are mediated through both its enzymatic activity and non-catalytic scaffolding properties, highlighting caspase-8 as a versatile regulator of cell fate and immune homeostasis (Fritsch et al., 2019; Han et al., 2021; Mocarski et al., 2015).

Genetic studies have demonstrated the essential role of caspase-8 in embryogenesis, as knockout mice die in utero around day 10.5 with severe cardiac malformations and defective yolk sac vascularization (Sakamaki et al., 2002; Varfolomeev et al., 1998; Yeh et al., 1998). Partial knockout experiments, where only the DED domain was expressed, indicated that neural and cardiac defects arise secondarily from impaired yolk sac angiogenesis (Sakamaki et al., 2002), a finding confirmed by endothelial-specific deletion of caspase-8 using Cre/loxP technology, which resulted in circulatory failure and embryonic lethality (Kang et al., 2004). This embryonic lethality is not rescued by ablation of downstream apoptotic caspases. Still, it is completely prevented by the simultaneous deletion of *RIPK3* or *MLKL*, key effectors of necroptosis, indicating that the primary role of caspase-8 in development is to suppress necroptotic cell death (Fritsch et al., 2019; Kaiser et al., 2011; Mocarski et al., 2015). Interestingly, human caspase-8 deficiency is not universally lethal. Patients with inherited caspase-8 deficiency present with immune defects but survive postnatally, likely because caspase-10, a paralog absent in mice, can partially compensate for the deficiency. This highlights both conserved and species-specific roles of caspase-8 in development (Chun et al., 2002).

The role of caspase-8 in cancer is complex, as it functions at the crossroads of apoptosis induction and cell survival. The loss or silencing of *CASP8* has been

described in several malignancies, including neuroblastoma and small-cell lung carcinoma, often correlating with resistance to apoptosis and a poor prognosis (Fulda et al., 2001; Hopkins-Donaldson et al., 2003; Teitz et al., 2000). Phosphorylation at Tyr380 by Src kinases suppresses apoptosis and enhances tumorigenic traits, including migration, adhesion, and anoikis resistance in glioblastoma cell lines (Cursi et al., 2006; Fianco et al., 2018, 2016). High caspase-8 expression correlates with a poor prognosis in glioblastoma, sustaining NF-κB activation, cytokines secretion, and neo-angiogenesis in the tumor microenvironment (Fianco et al., 2017; Henry and Martin, 2017; Rébé et al., 2006). Thus, caspase-8 can function both as a tumor suppressor, when its apoptotic activity is intact, and as a tumor promoter, when rewired towards non-apoptotic pathways (Stupack, 2013). In addition, dominant-negative isoforms, such as caspase-8L (long), generated by alternative splicing, lack the protease domain but retain DEDs. These isoforms are recruited to the DISC, where they competitively inhibit wild-type caspase-8, preventing apoptotic signaling (Himeji et al., 2002; Mohr et al., 2005). Furthermore, caspase-8 has been linked to therapeutic resistance. In glioblastoma and colorectal cancer models, caspase-8 expression sustains NF-κB and MAPK signaling, conferring resistance to chemotherapy and promoting survival under stress (Fianco et al., 2018, 2017; Kim et al., 2003).

Caspase-8 activity is essential for monocyte-to-macrophage differentiation. Circulating monocytes, produced daily, either infiltrate tissues to differentiate into macrophages or dendritic cells or undergo Fas-dependent apoptosis when in excess (Sordet et al., 2002). Studies using primary human monocytes have demonstrated that inhibition of caspase-8 activity or its genetic silencing blocks macrophage differentiation, instead triggering RIPK1/RIPK3-dependent necroptosis (Cathelin et al., 2006; Kang et al., 2013). Evidence from human monocytes stimulated with macrophage colony-stimulating factor (M-CSF) revealed limited caspase-8 activation that did not trigger apoptosis but was required for macrophage maturation. Inhibition of caspase-8 by z-VAD-fmk abrogated macrophage differentiation (Sordet et al., 2002). During this process, caspase-8 cleaves substrates involved in cytoskeletal reorganization, adhesion, and transcription, including the plasminogen activator inhibitor-2 (PAI-2), the serine/threonine-

protein kinase PAK-2, α-tubulin, and vinculin-α (Cathelin et al., 2006; Solier et al., 2017). M-CSF stimulation drives the formation of a molecular platform comprising FADD, RIPK1, FLIP, and procaspase-8, which resembles, but is distinct from, the canonical DISC (Jacquel et al., 2009; Rébé et al., 2006). Here, caspase-8 selectively cleaves RIPK1, preventing sustained NF-κB activation and favoring differentiation over inflammation (Rébé et al., 2006). Importantly, typical apoptotic substrates such as PARP and lamin B remain uncleaved, indicating a selective use of caspase-8 proteolysis in differentiation rather than apoptosis (Cathelin et al., 2006). Autophagy also participates in this process. M-CSF induces autophagy, and key proteins involved in autophagy, such as ATG5 and p62, colocalize with caspase-8/FADD/FLIP/RIPK1 complexes, linking autophagy to caspase-8 activation during differentiation (Jacquel et al., 2012a, 2012b; Obba et al., 2015).

Caspase-8 also plays a pivotal role in adaptive immunity, particularly in regulating T cell activation and expansion (Bell et al., 2008). Apoptosis ensures the homeostatic balance of lymphocyte populations, preventing autoimmunity. Mutations in Fas, FasL, or caspase-8 cause pleiotropic defects in lymphocyte activation, leading to combined immunodeficiency in humans (Chun et al., 2002; Fisher et al., 1995; Wu et al., 1996). Homozygous *CASP8* deficiency results in defective apoptosis during the thymic selection of autoreactive T cells, leading to an autoimmune lymphoproliferative syndrome (ALPS), characterized by lymphadenopathy, splenomegaly, and autoimmunity (Chun et al., 2002). Unlike ALPS linked to Fas or caspase-10 mutations, caspase-8 deficiency is uniquely associated with impaired activation of T, B, and NK cells, recurrent HSV infections, and defective responses to immunization (Chun et al., 2002; Rager-Zisman et al., 1987). Mice with T cell-specific deletion of caspase-8 display profound immunodeficiency due to impaired proliferation and survival of activated T cells (Salmena et al., 2003). At the mechanistic level, T cell receptors (TCR) engagement induces caspase-8 activation, promoting T cell proliferation and IL-2 production. Inhibition with caspase blockers, such as z-VAD-fmk or z-IETD-fmk, reduces proliferation and cytokines release (Alam et al., 1999; Kennedy et al., 1999). Deficiency of FADD or FLIP yields similar phenotypes, confirming that this DISC-like machinery supports T cell activation rather than apoptosis (Walsh et al., 1998;

Yeh et al., 2000). Additionally, caspase-8 N-terminal DEDs mediate NF-κB activation downstream of TNFRs independently of enzymatic activity (Chaudhary et al., 2000; Hu et al., 2000). Caspase-8 forms complexes with the T cell signaling molecules, B cell leukemia/lymphoma 10 (Bcl10) and the paracaspase mucosa-associated lymphoid tissue lymphoma translocation 1 (MALT1), recruiting the IκB kinase (IKK) to the TCR signaling platform to induce NF-κB activation (Su et al., 2005). TRAF6 also interacts with caspase-8, facilitating its translocation to lipid rafts where NF-κB substrates are cleaved (Bidère et al., 2006).
Collectively, these findings establish caspase-8 as a master regulator of T cell activation, integrating apoptotic suppression, NF-κB signaling, autophagy control, and cell cycle regulation.

2.3.1. Caspase-8 and chemokine regulation

One important non-apoptotic role of caspase-8 is its ability to act as a scaffold protein. In response to death receptor engagement, caspase-8 forms complexes with FADD and RIPK1, termed FADDosoma, which activate NF-κB and drive the transcription of pro-inflammatory mediators, including chemokines. This function does not require proteolytic activity, highlighting the dual nature of caspase-8 in signaling outcomes (Henry and Martin, 2017). Consistently, Newton et al., 2019 reported that catalytically inactive caspase-8 mutants can still promote NF-κB activation, suggesting that scaffold functions are sufficient to trigger pro-inflammatory signaling in some contexts. Feltham et al., 2017 demonstrated that deletion of caspase-8 in dendritic cells leads to heightened inflammatory cytokine and chemokine responses, in part dependent on RIPK1 and MyD88, thereby indicating that caspase-8 actively modulates TLR-driven transcriptional programs. Tummers and Green, 2017 similarly highlighted that ligation of CD95, TRAILR, or TLR4 can induce NF-κB-dependent pro-inflammatory gene expression in a caspase-8-dependent manner. Moreover, Hu et al., 2000 showed that procaspase-8 itself contributes to NF-κB activation, while its active form can cleave signaling intermediates such as RIP and NF-κB-inducing kinase (NIK). Caspase-8 also

contributes to inflammasome regulation (Kang et al., 2013) Han and collaborators showed that caspase-8 can either limit or promote inflammasome-dependent IL-1β maturation depending on cellular context, thereby indirectly influencing downstream chemokine induction (Han et al., 2021).

In caspase-8-knockout dendritic cells, NLRP3 inflammasomes are hyperactivated, leading to increased IL-1β production and exacerbated inflammatory responses (Kang et al., 2013). Similarly, Han et al., 2021 and Orning and Lien, 2021 highlighted that caspase-8 can substitute for caspase-1 under certain conditions to drive inflammasome-dependent cytokines production, reinforcing its role at the interface of cell death and inflammatory signaling. In the context of PANoptosis, Jiang et al., 2021 and Newton et al., 2019 reported that caspase-8 loss or catalytic inactivation leads to uncontrolled necroptosis and pyroptosis, resulting in excessive IL-1β and chemokine production, which can drive pathological inflammation. Mechanistic studies further connect caspase-8 activity to antiviral responses. For example, Wang et al., 2022, p. 2 and Yu et al., 2024 showed that caspase-8 cleavage of RIPK1 and other regulators can restrain excessive NF-κB and IRF3 activation. By integrating death receptor signaling, TLR pathways, inflammasome activity, and transcriptional programs such as NF-κB and IRF3, caspase-8 indirectly ensures that chemokine production is appropriately balanced between host defense and the prevention of immunopathology (Feltham et al., 2017; Han et al., 2021; Henry and Martin, 2017; Newton et al., 2019; Orning and Lien, 2021; Zhang et al., 2024).

2.4. NF-κB pathway and its function during HSV-1 infection

The nuclear factor kappa-light-chain-enhancer of activated B cells (NF-κB) is one of the most conserved and versatile transcription factor families in mammalian cells, coordinating responses to infections, inflammation, stress, and tissue injury (Figure 8). The family includes five members (RelA (p65), RelB, c-Rel, NF-κB1 (p50), and NF-κB2 (p52)) which can form various homo- or heterodimers, and all share a Rel homology domain (RHD) that mediates DNA binding, dimerization, and interaction with inhibitory IκB proteins (Hayden and Ghosh, 2011; Zhang et al., 2017). Under basal conditions, NF-κB dimers are retained in the cytoplasm through association with IκBs (IκBα, IκBβ, IκBε, among others). Upon stimulation by a wide variety of triggers, including cytokines, microbial products, growth factors, and cellular stress, these IκBs are phosphorylated by the IKK complex (composed of IKKα, IKKβ, and the regulatory subunit NEMO), leading to their ubiquitination and degradation by the proteasome. This event liberates NF-κB dimers, enabling their nuclear translocation and subsequent activation of target genes (Bonizzi and Karin, 2004; Hayden and Ghosh, 2011). There are two major NF-κB activation routes: the canonical pathway and the non-canonical pathway. The canonical pathway is typically triggered by pro-inflammatory cytokines (e.g., TNF-α, IL-1β), TLR ligands, or antigen receptors, leading to the rapid phosphorylation and degradation of IκBα through IKKβ/NEMO-dependent mechanisms. This allows nuclear translocation of p50/RelA or p50/c-Rel dimers. In contrast, the non-canonical pathway is activated by certain TNFR superfamily members (e.g., CD40, BAFFR, LTβR) and involves NF-κB-inducing kinase (NIK) and IKKα homodimers. These mediate the phosphorylation and processing of p100 into p52, which then forms heterodimers with RelB and enters the nucleus to drive gene transcription linked to lymphoid organogenesis and adaptive immunity (Hayden and Ghosh, 2011; Zhang et al., 2017). NF-κB activity is finely regulated through multiple mechanisms, including post-translational modifications (such as phosphorylation and ubiquitination) and autoregulatory feedback loops. One example is the NF-κB-induced transcription of IκBα, which re-sequesters active dimers in the cytoplasm, ensuring timely signal resolution (Hayden and Ghosh, 2011). The relevance of this pathway is underscored by its involvement in

numerous diseases and disorders. Dysregulation of NF-κB has been implicated in autoimmune disorders, chronic inflammation, immunodeficiencies, and various forms of cancer. Loss-of-function mutations in core components (e.g., IKKβ, NEMO, and RelB) can lead to severe immunological defects such as ectodermal dysplasia or combined immunodeficiency (Bonizzi and Karin, 2004; Zhang et al., 2017).

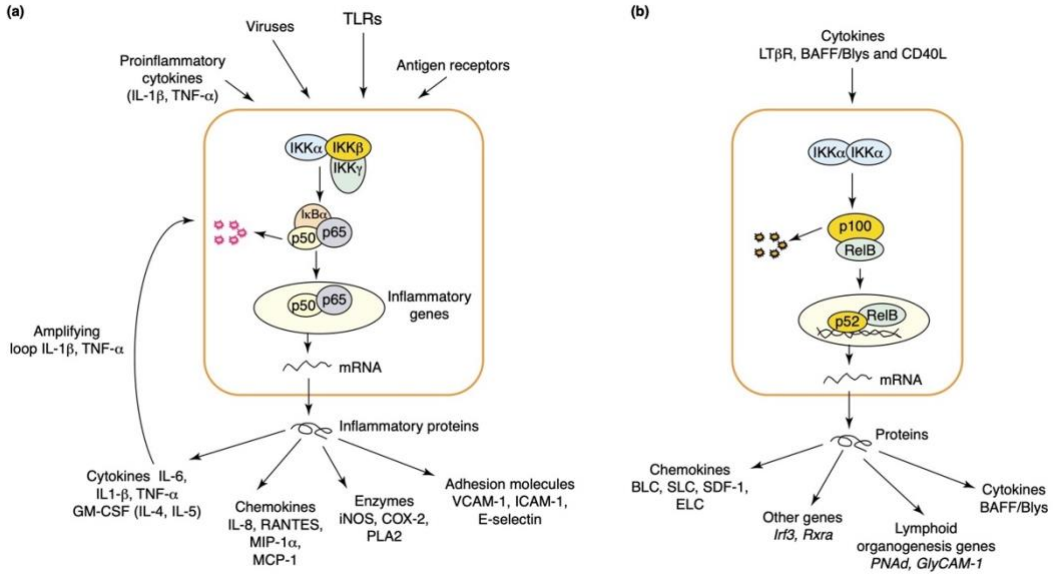

Figure 8. Canonical and non-canonical NF-κB signaling pathways. (a) Various inflammatory stimuli, including proinflammatory cytokines such as IL-1β and TNF-α, trigger the canonical NF-κB pathway. Upon activation, this pathway leads to the coordinated transcription of numerous genes involved in inflammation and innate immunity. Notably, IL-1β and TNF-α are both upstream activators and downstream targets of NF-κB, establishing a self-amplifying positive feedback loop. (b) The non-canonical NF-κB pathway is activated by specific signals, including the lymphotoxin-β receptor (LTβR), B-cell activating factor (BAFF), and CD40 ligand (CD40L). It is dependent on NF-κB-inducing kinase (NIK) and IKKα homodimers. This pathway culminates in the nuclear translocation of p52/RelB heterodimers and is primarily involved in regulating genes required for the development and maintenance of secondary lymphoid tissues. Abbreviations**:** BAFF, B-cell-activating factor; BLC, B-lymphocyte chemoattractant; CD40L, CD40 ligand; COX-2, cyclooxygenase-2; ELC, Epstein-Barr virus-induced ligand chemokine; GM-CSF, granulocyte-macrophage colony-stimulating factor; ICAM-1, intercellular adhesion molecule-1; IKK, IκB kinase; IL-1β, interleukin-1β; iNOS, inducible nitric oxide synthase; LT, lymphotoxin; MCP-1, monocyte chemoattractant protein-1; MIP-1α, macrophage inflammatory protein-1α; NIK, NF-κB-inducing kinase; PLA2, phospholipase A2; SDF-1, stromal cell-derived factor-1α; SLC, secondary lymphoid tissue chemokine; TLRs, Toll-like receptors; TNF-α, tumor necrosis factor-α; VCAM-1, vascular cell adhesion molecule-1 (Bonizzi and Karin, 2004).

In the context of viral infection, NF-κB functions as a central hub in innate immunity, promoting the transcription of pro-inflammatory cytokines, chemokines, and interferon-stimulated genes. However, it can also be subverted by viruses to

promote their own replication and persistence (Hayden and Ghosh, 2011). A hallmark of HSV-1 infection is its ability to activate the NF-κB pathway in host cells, particularly in monocytes and other myeloid cells. In these cell types, a biphasic activation of NF-κB has been described: an early wave triggered independently of viral gene expression, and a second wave dependent on de novo synthesis of viral proteins (Marino-Merlo et al., 2016; Santoro et al., 2003). The first phase of NF-κB activation is initiated by viral glycoprotein D (gD), which interacts with herpesvirus entry mediator A (HveA), a member of the TNF receptor family expressed on monocytes. This interaction is sufficient to induce NF-κB activation, even in the absence of viral replication, as demonstrated using UV-inactivated HSV-1 or mutated gD protein (Santoro et al., 2003; Sciortino et al., 2007). These observations are consistent with earlier findings showing that other herpesviruses also activate host signaling through envelope-receptor interactions (Smith and Helenius, 2004). In U937 and THP-1 cells, NF-κB activation could be induced by soluble gD and was abolished by monoclonal antibodies that block the gD-HveA interaction. Furthermore, cells lacking HveA expression, such as HEp-2, did not respond to gD or UV-inactivated HSV-1, confirming the receptor-specific nature of this replication-independent pathway (Sciortino et al., 2007). The second phase of NF-κB activation occurs 3-4 hours post-infection and is dependent on the expression of viral genes (Santoro et al., 2003). In THP-1 cells infected with HSV-1EGFP, p65 phosphorylation was detected only in cells expressing the viral fluorescent protein, indicating that active viral replication is required to sustain NF-κB signaling (Venuti et al., 2019). Functionally, NF-κB activation in monocytic cells serves a protective role. Inhibition of the pathway via a dominant-negative form of IκBα enhances viral replication and late protein expression in U937 cells, suggesting that NF-κB activation imposes a block on HSV-1 progression (Marino-Merlo et al., 2016). Additionally, NF-κB helps prevent HSV-1-induced apoptosis by limiting lysosomal membrane permeabilization and subsequent caspase-3 activation. Importantly, apoptosis and productive infection rarely co-occurred in the same cell, suggesting a protective bifurcation of cell fate regulated by NF-κB (Galluzzi et al., 2008; Marino-Merlo et al., 2016). NF-κB also regulates miRNA expression during HSV-1 infection. Specifically, miR-146a is upregulated in an

NF-κB-dependent manner in THP-1 cells, targeting interleukin-1 receptor-associated kinase 1 (IRAK1) and forming a feedback loop that modulates inflammatory signaling (Venuti et al., 2019). Altogether, these findings highlight a dual role for NF-κB in monocytic cells infected with HSV-1: it restricts viral replication and supports cell survival, while simultaneously initiating a tightly controlled inflammatory response. This contrasts with its function in epithelial cells, where HSV-1 exploits NF-κB to promote replication and delay apoptosis (Marino-Merlo et al., 2016).

2.5. Chemokines in HSV-1 infection

Chemokines are a subclass of cytokines that play a crucial role in the trafficking of immune cells. They orchestrate leukocyte migration through interactions with transmembrane G protein-coupled receptors (GPCRs), contributing to tissue homeostasis and inflammation (Matsushima et al., 2011). Chemokines are classified into four major families, CC, CXC, CX3C, and XC, based on the arrangement of conserved cysteine residues. CC chemokines attract monocytes, dendritic cells (DCs), NK cells, and T lymphocytes, while CXC chemokines mainly recruit neutrophils (Palomino and Marti, 2015). In the context of HSV-1 infection, chemokines orchestrate the recruitment of innate and adaptive immune cells to infected tissues. However, their activity may also contribute to immunopathology (Azher et al., 2017; Carr and Tomanek, 2006) (Figure 9).

HSV-1 modulates the chemokine environment to favor its replication and persistence. During primary infection, the virus triggers a strong inflammatory response characterized by the upregulation of several chemokines (Pontejo et al., 2018), including CXCL10, CXCL9, CCL2, CCL3, and CCL5, which are implicated in both protective immunity and tissue damage (Azher et al., 2017; Carr and Tomanek, 2006; Smith et al., 2022). Experimental models of HSV keratitis and encephalitis demonstrate that chemokines are involved in neutrophil recruitment, Th1 polarization, and the trafficking of cytotoxic T cells (Azher et al., 2017; Smith et al., 2022). However, HSV-1 also subverts chemokine signaling through multiple viral proteins (both viral chemokines (vCK) and viral chemokine receptors (vCKR)) that either mimic, neutralize, or degrade host chemokines (Pontejo et al., 2018). This subversion blunts immune clearance, facilitating viral latency and reactivation (Martinez-Martin et al., 2015).

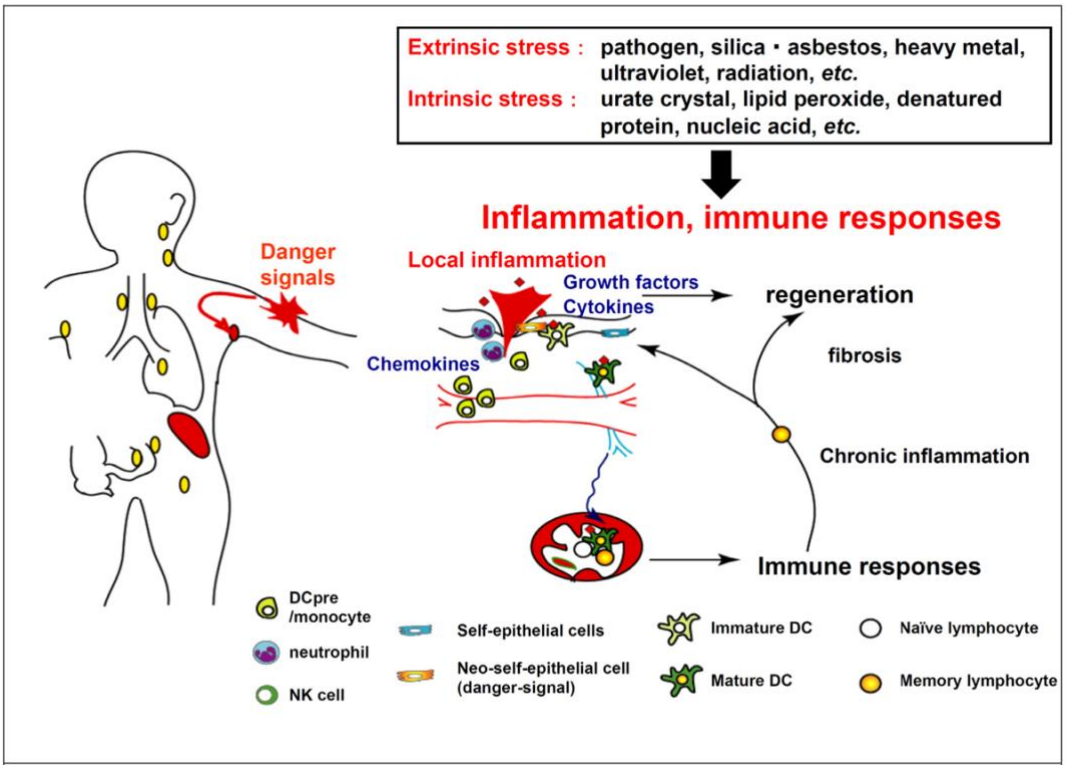

Figure 9. Chemokine-mediated orchestration of innate and adaptive immune responses to tissue stress. Extrinsic and intrinsic stresses induce localized inflammation, resulting in the release of cytokines, chemokines, and growth factors by injured epithelial cells. Chemokines attract neutrophils, monocytes, and dendritic cell precursors to inflamed tissue, thereby establishing the primary line of host defense (innate immunity). Immature dendritic cells penetrate the tissue, acquire antigens, mature, and move to draining lymph nodes through afferent lymphatics. There, they stimulate antigen-specific naïve and memory T cells, which subsequently migrate back to the site of inflammation to facilitate the secondary defense mechanism (adaptive immunity) (Matsushima et al., 2011).

2.5.1. CC family

The CC family is important in HSV-1 immunity, with CCL2 (MCP-1), CCL3 (MIP-1α), CCL4 (MIP-1β), and CCL5 (RANTES) playing significant roles. These chemokines primarily recruit, through receptors such as CCR2 and CCR5, monocytes, macrophages, DCs, and activated T cells to infected sites, supporting both innate and adaptive responses (Azher et al., 2017; Palomino and Marti, 2015). CCL2 is upregulated in HSV-1-infected tissues, thereby promoting the infiltration of monocytes and macrophages. Although this response supports viral clearance, it may also amplify inflammatory damage (Lai et al., 2017; Wang et al., 2024). In cancer models using oncolytic HSVs engineered to express CCL2, this chemokine

enhanced the infiltration of CD4+ and CD8+ T cells and increased the secretion of IL-1, IL-6, and TNF-α (Wang et al., 2024). CCL3 and CCL4 are also elevated during HSV infection, contributing to the recruitment of neutrophils and CD4+ T cells. These chemokines are associated with the development of HSV-induced corneal immunopathology. Mice lacking CCL3 exhibit increased corneal disease, suggesting a protective role (Azher et al., 2017; Smith et al., 2022). Infected macrophages and epithelial cells express CCL5 (RANTES), which mediates the recruitment of T cells and NK cells (Melchjorsen et al., 2002). However, *Alphaherpesviruses* can encode chemokine-binding proteins that can neutralize CCL5 and interfere with its signaling, highlighting its relevance in host-virus interactions (Pontejo et al., 2018).

2.5.2. CXC family

Among the CXC chemokines, CXCL10 (IP-10) and CXCL9 (MIG) play crucial roles in HSV-1 immune responses. These chemokines are induced by type I and II interferons and act through the CXCR3 receptor, which is expressed on activated T cells, NK cells, and dendritic cells (Elemam et al., 2022; McKimmie and Michlmayr, 2014). Their expression is upregulated in multiple tissues during HSV infection, including the brain, cornea, and retina, where they support the recruitment of effector T cells to sites of viral replication (Carr et al., 2003; Thapa et al., 2008). Neutralization of CXCL10 in murine models leads to impaired CD4+ and CD8+ T cell infiltration, increased viral load, and enhanced retinal damage, supporting a protective role for this chemokine (Carr et al., 2003). Similarly, mice deficient in CXCL10 or its receptor CXCR3 show increased susceptibility to HSV infection of the genital tract and brain, further underscoring its role in antiviral immunity (McKimmie and Michlmayr, 2014; Thapa et al., 2008). However, excessive or prolonged CXCL10 expression in the CNS may contribute to inflammation-associated damage (McKimmie and Michlmayr, 2014). In addition to CXCL10 and CXCL9, CXCL4 (PF4) has been studied in the context of cytokine-armed oncolytic HSVs (oHSVs). Engineered oHSVs expressing CXCL4 have been shown to

enhance dendritic cell activation and T cell responses in tumor models, although direct evidence of its role during wild-type HSV-1 infection is lacking (Wang et al., 2024).

2.5.3. Chemokine receptors

Chemokine function depends on its interaction with specific receptors expressed on the surface of immune cells. CXCR3 is the shared receptor for CXCL9, CXCL10, and CXCL11. It is highly expressed on Th1 cells, NK cells, and activated CD8+ T cells and plays a central role in directing their migration to inflamed tissues. In HSV infection, CXCR3-mediated recruitment of T cells is essential for viral control in the CNS and genital mucosa (McKimmie and Michlmayr, 2014; Thapa et al., 2008). CCR5, which binds CCL3, CCL4, and CCL5, is involved in the recruitment of monocytes, macrophages, and T cells during infection. Its role has been well documented in the context of HSV-induced corneal inflammation and viral clearance (Carr and Tomanek, 2006). CMKLR1 (Chemokine-like receptor 1), the receptor for chemerin, is expressed by monocyte-derived dendritic cells, macrophages, and NK cells. CMKLR1 is involved in the resolution of inflammation and the regulation of innate responses. Its expression on mucosal immune cells suggests a potential role in viral infections at epithelial surfaces (Yoshimura and Oppenheim, 2011).

2.6. Aim of the study

During viral infection, host cells initiate programmed cell death mechanisms, primarily apoptosis, to limit viral replication and dissemination. HSV-1, however, has evolved complex strategies to subvert these responses and ensure its own survival. In epithelial cells, HSV-1 induces pro-apoptotic signals upon entry, which are subsequently counteracted by the expression of specific viral proteins (Dufour et al., 2011a; Musarra-Pizzo et al., 2022). Unlike epithelial cells, immune cells such as monocytes and dendritic cells are more prone to HSV-1-induced apoptosis (Bosnjak et al., 2005; Kather et al., 2010; Mastino et al., 1997). In THP-1 monocytic cells, HSV-1 establishes a low-permissive infection often associated with cell death. However, recent evidence suggests that death-related proteins may be repurposed for non-apoptotic functions. Among these, caspase-8, traditionally recognized as an initiator of extrinsic apoptosis, has been implicated in alternative processes, including necroptosis, autophagy, and immune signaling. Recent studies have reported that the HSV-1 late protein Us11 promotes non-canonical activation of caspase-8. Specifically, Us11 binds to procaspase-8 and induces its cleavage into the p18 subunit, without triggering downstream apoptotic events, such as caspase-3 or PARP activation, a phenomenon observed in both THP-1 and HEp-2 cells. Infection with the Us11/Us12-deleted mutant virus (R3630) confirmed that p18 accumulation is Us11-dependent, and that its absence correlates with reduced cleavage and preserved apoptotic susceptibility (Musarra-Pizzo et al., 2022). These findings support a model in which caspase-8 may play a non-apoptotic role in viral immune evasion and replication.

Moreover, HSV-1 infection has been shown to activate the NF-κB pathway in monocytoid cells with a biphasic kinetic profile: an early wave triggered by viral receptor interaction (e.g., gD-HVEM) and a later wave dependent on viral gene expression. Notably, phosphorylation of the NF-κB p65 subunit was restricted to cells actively expressing viral genes, suggesting a correlation between productive infection and inflammatory signaling (Venuti et al., 2019). Furthermore, during HSV-1 replication, caspase-8 has been implicated in the inhibition of autophagy through cleavage of Atg3 (Musarra-Pizzo et al., 2022), supporting the idea that in

HSV-1-infected immune cells, caspase-8 may contribute to inflammatory rather than apoptotic responses.

On this basis, the first aim of this study was to investigate the role of caspase-8 in the inflammatory response during HSV-1 infection in monocytic cells. This was achieved by generating a caspase-8 knockout model in THP-1 monocytic cells using CRISPR-Cas9 technology. Specifically, the first objective was to determine whether caspase-8 regulates the expression of inflammatory chemokines in response to HSV-1 infection, potentially through the NF-κB pathway. Since chemokine transcription is known to increase during HSV-1 infection, we quantified chemokine mRNA levels in wild-type ($CASP8^{+/+}$) and caspase-8-knockout ($CASP8^{-/-}$) THP-1 cells infected with either HSV-1 wild-type or R3630 virus. This approach aimed to clarify the potential role of caspase-8 in regulating chemokines and its interaction with inflammatory signaling pathways.

Subsequently, we aimed to elucidate the interplay between caspase-8 and RIPK1 during HSV-1 infection. Given that caspase-8 and RIPK1 form a signaling scaffold that tunes NF-κB activation and cell-death checkpoints (Fritsch et al., 2019; Newton et al., 2019), we asked whether caspase-8 supports RIPK1 induction in infected cells and whether this depends on viral immune-evasion genes. To this end, we compared RIPK1 mRNA and protein levels in $CASP8^{+/+}$ and $CASP8^{-/-}$ THP-1 and HEp-2 cells infected with HSV-1 wild-type or the Us11/Us12-deleted mutant R3630, and related RIPK1 abundance to viral transcripts/proteins and chemokine expression, as well as to NF-κB readouts. Moreover, previous data suggested a role for caspase-8 in viral egress. In permissive $CASP8^{-/-}$ HEp-2 cells, Musarra-Pizzo e collaborators have observed impaired release of HSV-1 particles, delayed accumulation of viral proteins such as ICP8 and UL42, and reduced viral DNA load, indicating that caspase-8 may facilitate viral replication and egress through non-apoptotic mechanisms.

Therefore, the third aim of this study was to investigate the involvement of caspase-8 in HSV-1 maturation and spread. To achieve this, recombinant HSV-1 viruses expressing two fluorescent tags (one (mNeonGreen) linked to the capsidic VP26, and the other (mScarlet) to the envelope glycoprotein gH) were constructed. The fluorescent virus enabled the visualization and analysis of viral particle trafficking

and release in CASP8$^{+/+}$ and CASP8$^{-/-}$ HEp-2 cells. The construction of these fluorescent HSV-1 recombinants provided preliminary insights into virion trafficking and maturation, highlighting a potential role for caspase-8 in viral egress.

2.7. Materials and Methods

Cell lines

VERO (African green monkey kidney), HEK-293T (human embryonic kidney cells transformed with SV40 T-antigen), HEp-2 (human HeLa contaminant carcinoma), and THP-1 (human acute monocytic leukemia) cells were obtained from ATCC (https://www.atcc.org/). VERO cells were maintained in Dulbecco's Modified Eagle's High Glucose Medium (DMEM) (Euroclone) supplemented with 6% fetal bovine serum (FBS) (Euroclone). HEK-293T cells were maintained in DMEM supplemented with 10 % FBS. HEp-2 cells were cultured in Roswell Park Memorial Institute (RPMI)-1640 medium (Euroclone) supplemented with 10 % FBS. $CASP8^{+/+}$ and $CASP8^{-/-}$ THP-1 cells were cultured in RPMI-1640 medium supplemented with 10 % FBS, 4.5 g/L D-glucose (Sigma-Aldrich), 1 mM sodium pyruvate (Sigma-Aldrich), and 10 mM Hepes buffer (Sigma-Aldrich). DN IκBα THP-1 cells, stably transfected with a dominant negative mutant IκBα, were cultured in RPMI-1640 medium supplemented with 10 % FBS, 4.5 g/L D-glucose (Sigma-Aldrich), 1 mM sodium pyruvate (Sigma-Aldrich), and 10 mM Hepes buffer (Sigma-Aldrich), and maintained under selection with 400 µg/mL of Geneticin (Gibco). All culture media were supplemented with a mixture of 100 U/mL penicillin and 100 µg/mL streptomycin (Lonza, Belgium). All cell lines were incubated at 37 °C and 5 % CO_2.

Viruses

The wild-type herpes simplex virus type 1 (HSV-1) and the recombinant R3630 were kindly provided by Professor Dr. Bernard Roizman (University of Chicago). HSV-1 (F) is the prototype HSV-1 strain F, whereas the recombinant R3630 virus lacks the *Us11* and *Us12* genes. Viral stocks were propagated and then titrated in VERO cells.

Other viruses employed in this study are pYEbac102Y, from Yasushi Kawaguchi, kindly provided by Martin Messerle, a BAC-derived clone of HSV-1 strain F that harbors a chloramphenicol resistance gene; HSV-1 gH-mScarlet (produced in this study), a BAC-derived clone of HSV-1 strain F expressing the red fluorescent (mScarlet)-tagged gH protein; HSV-1 VP26-mNeonGreen (produced in this study),

a BAC-derived clone of HSV-1 strain F expressing a green fluorescent protein (mNeonGreen)-tagged VP26 protein; and HSV-1 gH-mScarlet-VP26-mNeonGreen (produced in this study), a BAC-derived clone of HSV-1 strain F expressing both the red fluorescent (mScarlet)-tagged gH protein and the green fluorescent protein (mNeonGreen)-tagged VP26 protein.

For experimental infection, HSV-1, R3630, HSV-1 gH-mScarlet, HSV-1 VP26-mNeonGreen, and HSV-1 gH-mScarlet-VP26-mNeonGreen, diluted in medium or medium alone (mock-infected), were adsorbed onto cells for 1 hour at 37 °C in 5 % CO_2 with gentle shaking, at different multiplicities of infection (MOI). The inoculum was then removed and replaced with fresh medium. Cells were maintained at 37 °C in 5% CO_2 and harvested at the indicated times post-infection (t.p.i.) to perform experiments.

Bacteria

E. coli DH10B strain (Life Technologies) was grown in Luria Bertani (LB) broth in the presence of selection at 37 °C overnight.

E. coli GS1783 strain, a derivative of EL250, but with an l-arabinose inducible I-sceI expression cassette, was grown in Luria Bertani (LB) broth in the presence of chloramphenicol 1:2500 at 30 °C overnight.

Plasmids

pcDNA-mScarlet and pcDNA-mNeonGreen are plasmids constructed by Gibson assembly and obtained from pEPkan-S, a template plasmid for *En passant* mutagenesis, containing the I-Sce-aphA1 cassette and kanR with the insertion of mScarlet and mNeonGreen sequences.

pSico-CRISPR/Cas9 is a vector containing fusion gRNA-tracrRNA, encoding for *S. pyogenes* Cas9 enzyme, *amp*, and *puro* resistance. pMD2.G is a packaging vector, a lentiviral *gag*, *pol, rev* encoding vector, with an *amp* resistance. pCMVR8.91 is an envelope vector, encoding the VSV-G protein, with an *amp* resistance. The pSico-CRISPR/Cas9 and the two helper plasmids, pMD2.G and pCMVR8.91, were kindly provided by Robert Jan Lebbink.

Primers

Table 1.

BAC mutagenesis primers		
Name	**Sequence (5'-3')**	**Application**
Seq UL35 FWD	CTATTTGGTGGGTGGTTGGTG	To sequence verify UL35
Seq UL35 REV	ACGACATTAAACGCAAGGCT	
mNeon UL35 HR FWD	GACACCCCCATATCGCTTCCCGACCTCCG GTCCCGATGGCCGTCCCGCAAGTGAGCAA GGGCGAGGA	To insert mNeon in UL35 of HSV-1 BAC
mNeon UL35 HR REV	ATGCCAAGCGCCCGGACGCTATCGGTGGT AACGGTGCTGGGGCGGTGAAACTTGTACA GCTCGTCCATGC	
mScarlet UL22 HR FWD	ACGGGCCCCGTGGGTTAGGGACGGGGTCC CCCATGGGGAATGGTTTATGGGTGAGCAA GGGCGAGGC	To insert mScarlet in UL22 of HSV-1 BAC
mScarlet UL22 HR REV	CAGTCGTGGACCTGACCCCACGCAACGCC CAAAATAATAACCCCCACGAACTTGTACA GCTCGTCCATGCC	
Seq UL22 FWD	GGCCCAGGGCTCGCAGCCAA	To sequence verify UL22
Seq UL22 REV	TTATTCGCGTCTCCAAAAAA	
Seq UL22 internal primer REV	GGCACCCTGATCTACAAGGT	

Table 2.

qPCR primers		
Name	**Sequence (5'-3')**	**Application**
ICP0 FWD	TCTGCATCCCGTGCATGAAAAC	To PCR amplify ICP0
ICP0 REV	CTGATTGCCCGTCCAGATAAAG	
UL42 FWD	CTCCCTCCTGAGCGTGTTTC	To PCR amplify UL42
UL42 REV	CACAAAGCTCGTCAGTTCGC	
Us11 FWD	GGCTTCAGATGGCTTCGAG	To PCR amplify Us11

Us11 REV	GGGCGACCCAGATGTTTAC	
NF-KB FWD	TAAAGCCCCCAATGCATCCAAC	To PCR amplify NF-KB
NF-KB REV	CCAAATCCTTCCCAGACTCCAC	
VHS FWD	ACATAACTGCGGTGCTCTTC	To PCR amplify VHS
VHS REV	CCGAAATTCTAACCCAACAG	
GAPDH FWD	ACATCATCCCTGCCTCTAC	To PCR amplify GAPDH
GAPDH REV	CTGCTTCACCACCTTCTTG	
CCL2 FWD	ATCAATGCCCCAGTCACCTG	To PCR amplify CCL2
CCL2 REV	TCTCCTTGGCCACAATGGTC	
CCL4 FWD	GCTTCCTCGCAACTTTGTGG	To PCR amplify CCL4
CCL4 REV	TCACTGGGATCAGCACAGAC	
CCL13 FWD	AGCCAGATGCACTCAACGTC	To PCR amplify CCL13
CCL13 REV	TCTCCTTGCCCAGTTTGGTT	
CXCL10 FWD	GCCATTCTGATTTGCTGCCT	To PCR amplify CXCL10
CXCL10 REV	ATGCTGATGCAGGTACAGCG	
CXCL11 FWD	ACTTGGGTACATTATGGAGGCT	To PCR amplify CXCL11
CXCL11 REV	TGTCTTTGCATAGGCCCTGG	

Table 3.

Name	**Sequence (5'-3')**	**Application**
SEQ pSicoR	TGCAGGGGAAAGAATAGTAGAC	To sequence verify gRNA cloning

Generation of electrocompetent bacteria

A single colony of *E. coli* DH10B and GS1783 was inoculated into 10 mL of pre-warmed LB medium and cultured overnight at 37 °C and 30 °C, respectively, with continuous shaking. The following day, 5 mL of the bacteria pre-culture was added to 200 mL of LB medium and incubated at 37 °C (DH10B) and 30 °C (GS1783, with 15 μg/mL chloramphenicol) with continuous shaking. Once the OD600 reached 0.5-0.6, the DH10B strain cultures were immediately cooled on ice for 20 minutes. Meanwhile, the cultures of the GS1783 strain were incubated at 42 °C for 15 minutes to induce recombinase expression, and then cooled down, as was the DH10B strain. Bacteria were further pelleted by centrifugation at 5,000 × g for 10 minutes at 4 °C. The pellet was then washed twice with 100 mL of ice-cold sterile water and resuspended in 10 mL of 10% (v/v) ice-cold glycerol and pelleted again.

Lastly, the bacterial pellet was dissolved in 1 mL of 10% (v/v) ice-cold glycerol, immediately aliquoted, and stored at -80 °C.

Transformation of bacteria

Electrocompetent bacteria were transformed by electroporation. 50 µL of frozen bacteria were thawed on ice and mixed with either 150 ng of purified PCR-amplified DNA fragment (*E. coli* GS1783), 1-10 ng of plasmids, or 4 µL of ligation product (*E. coli* DH10B). After 10-15 minutes of incubation on ice, the mixture was transferred into pre-chilled 2 mm electroporation cuvettes and pulsed using the Gene Pulser XCell (Bio-Rad) with the settings of 2,500 V, 25 µF, and 200 Ω. Immediately after electroporation, 900 µL of warm LB medium was added to the bacteria, which were then transferred into a microcentrifuge tube. Bacteria were then incubated for 1 hour at 30 °C (*E. coli* GS1783) or 37 °C (*E. coli* DH10B). Next, the bacteria were pelleted by centrifugation at 500 × g for 5 minutes. The bacterial pellet was resuspended and plated on LB agar plates containing the corresponding antibiotics, and then incubated overnight at the appropriate temperature in a bacterial incubator.

Isolation of plasmid DNA and BAC DNA (Mini Prep)

Single-clone bacteria containing plasmid or BAC of interest were inoculated in 5 mL of LB medium supplemented with the required antibiotics and incubated overnight under proper conditions. Plasmid DNA was extracted from *E. coli* DH10B bacteria using the Mi-Plasmid MiniPrep Kit according to the manufacturer's protocol. BAC DNA was extracted from *E. coli* GS1783 as follows: 10 mL of the overnight culture was centrifuged at 11,000 × g for 1 minute at 4 °C, and the pellet was resuspended in 400 µL of ice-cold S1 buffer. 400 µL of ice-cold S2 buffer was then added to the mixture and gently mixed by inversion three times. After 4 minutes of incubation at RT, 400 µL of ice-cold S3 buffer was added, and the tubes were gently inverted five times. The samples were incubated on ice for 7 minutes and then centrifuged at 11,000 × g for 20 minutes at 4 °C. The clear supernatant was transferred into a new tube and mixed with 0.8X the volume of isopropanol by inverting the tube three times. The tube was centrifuged at 11,000

× g for 30 minutes at 4 °C. The pellet was then washed with 500 µL of 70 % (v/v) ethanol and centrifuged again at 11,000 × g for 5 minutes at 4 °C. The DNA pellet was dried and then dissolved in 25 µL of 10 mM Tris-HCl (pH 8.0). To facilitate the resuspension of the DNA pellet, the tubes were incubated at 37 °C with continuous shaking for 1 hour.

Isolation of plasmid DNA and BAC DNA (Midi Prep)

Bacteria were incubated in 200 mL of LB medium supplemented with the required antibiotics overnight at the appropriate temperature. The DNA was extracted using the NucleoBond Midi Xtra Kit according to the manufacturer's protocol. The high-copy protocol was used for plasmid DNA extraction, while the low-copy protocol was used for the extraction of BAC DNA. The plasmid DNA pellet was dissolved using 200-400 µL of Tris-HCl buffer (pH 8.0), while BAC DNA was dissolved using 50-150 µL of Tris-HCl buffer (pH 8.0).

Polymerase chain reaction (PCR)

PCR was performed by using DreamTaq (Thermo Fisher Scientific) or Q5 (NEB) High-Fidelity DNA polymerases according to the manufacturer's protocol. DreamTaq polymerase was used for colony PCR. Q5 polymerase was used for sequencing purposes.

Restriction enzyme digestion of DNA

DNA restriction digestion was performed using FastDigest restriction enzymes (Thermo Fisher Scientific) according to the manufacturer's protocol. 1 µg of plasmid DNA was used for analytical plasmid restriction, and 2 µg of plasmid DNA were used for cloning procedures. Plasmid DNA was digested at 37 °C for 20 minutes using the reaction setup according to the manufacturer's instructions. For analytical BAC restriction, 1-3 µg of BAC DNA were digested at 37 °C for 1 hour.

Agarose gel electrophoresis

PCR products and plasmid fragments were analyzed on 1 % (w/v) TAE agarose gels and run at 120 V for 30-60 minutes. BAC DNA fragments were analyzed on

0.6 % (w/v) TBE agarose gels and run at 50 V overnight, followed by 100 V for 4 hours. All gels contained 0.5 μg/mL of ethidium bromide. The O'GeneRuler (Thermo Fisher Scientific) was used as a DNA size ladder. DNA bands were visualised with GelDoc XR+ (Bio-Rad) and analysed with Image Lab software.

Purification of DNA fragments

DNA bands of interest were excised from TAE agarose gels, and the DNA fragments were then purified from the agarose gel using a NucleoSpin Gel and PCR cleanup kit according to the manufacturer's protocol. Purified DNA was quantified by a NanoDrop-1000 (Peqlab) photometer. DNA was stored at 4 °C for short-term use and at -20 °C for long-term storage.

RNA extraction, Reverse transcription

Total RNA was extracted using TRIzol® (Life Technologies), according to the manufacturer's instructions, and DNase-treated before cDNA transcription as follows: 1 μg of RNA was incubated at 37 °C for 2 hours with 5 μL of 10X DNase I Buffer, 2 μL of Recombinant RNase-free DNase I (10U) (2270A TaKaRa), and RNase inhibitor (20U) (N251A Promega). The concentration of extracted RNA was determined using the Qubit™ RNA HS Assay (Invitrogen). Total RNA (0.5 μg) was reverse transcribed using avian myeloblastosis virus reverse transcriptase (Promega, Madison, WI) under the following conditions: denaturation at 70 °C for 10 min, followed by 42 °C for 45 min, 52 °C for 45 min, and 95 °C for 5 min.

Quantitative polymerase chain reaction (qPCR)

The cDNAs were used for quantitative real-time PCR using the QuantiNova SYBR Green PCR Kit (Qiagen) and specific primers (10 μM each). Quantitative polymerase chain reaction (qPCR) was performed in the Qiagen QIAquant 96 2plex PCR Thermal Cycler machine. The thermal profile consists of a 2-minute incubation at 95 °C, followed by 40 cycles of 5 seconds of denaturation at 95 °C and 10 seconds of annealing/extension at 60 °C. The cDNA copy numbers were quantified using the ΔΔCt method and normalised to the GAPDH housekeeping

gene. The analytic primers for RT-PCR are reported in Table 2. Each quantitative real-time PCR experiment includes a minus-reverse transcriptase control.

DNA sequencing

PCR products and plasmid DNA were sequenced by SEQLAB (Sequence Laboratories, Göttingen, Germany). HSV-1 genome sequences were determined using Illumina sequencing and Nanopore sequencing at the Next-Generation Sequencing facility of the Leibniz-Institut für Virologie (LIV, Hamburg, Germany).

***En passant* BAC mutagenesis**

Mutation of BACs using *en passant* was performed as previously described by Tischer et al., 2010, and as illustrated by De Oliveira et al., 2008. Shortly, a linear DNA fragment containing the I-SceI-aphAI-cassette and a duplicate of the region of interest with the desired mutation was generated by PCR using the pEP-Kan-S plasmid as a template. Alternatively, a plasmid shuttle was used. After purification, 150 ng of the PCR product was used to transform GS1783, which carries the HSV-1 F strain BAC. Transformed bacteria were then spread on LB agar plates containing chloramphenicol and or kanamycin and incubated overnight at 30 ºC. The resulting bacterial clones were checked using enzyme restriction digestion, analytical PCR, colony PCR, and sequencing. Positive clones were then used for the second recombination procedure. Second recombination requires the expression of recombinases, such as I-SceI, which is induced by the addition of 2 % (w/v) L-arabinose and incubation at 42 °C (Figure 10). Recombinant bacteria were then plated on LB agar containing 1 % L-arabinose and chloramphenicol. The resulting bacterial clones were also checked for loss of kanamycin resistance using enzyme restriction digestion, analytical PCR, and sequencing. Positive clones were grown out in 200 mL liquid culture for BAC Midi Prep.

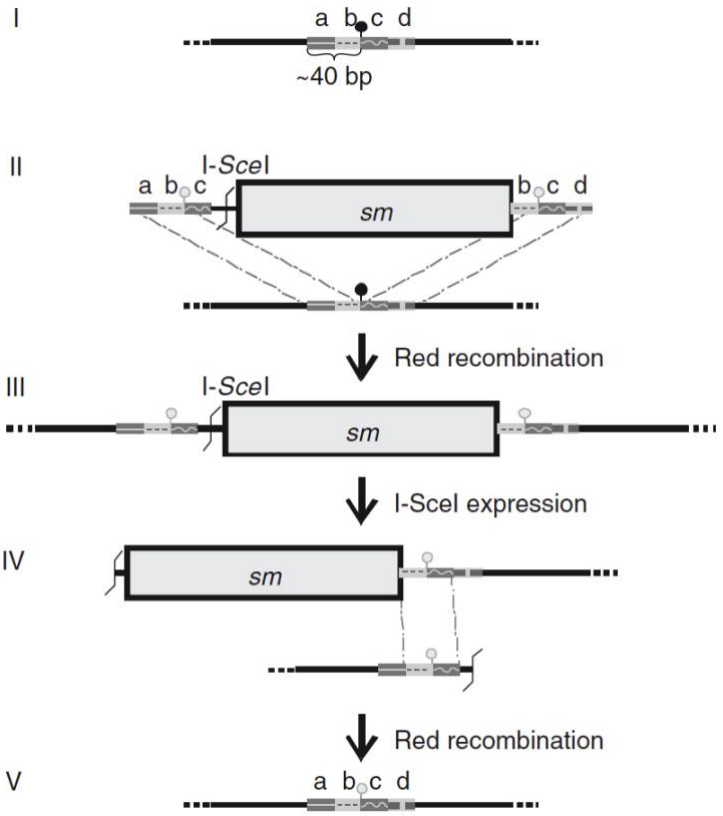

Figure 10. ***En passant*** **mutagenesis.** Generation of point mutations. I - target sequence; II - PCR product of a marker cassette recombines with target sequences; III - co-integrate; IV - in vivo I-SceI cleavage results in a new substrate for second Red recombination between duplicated sequences; V - final mutant sequences; a-d - identical sequences of approx. 20 bp each, also represented by bars with identical shape and shading; sm-positive selection marker (e.g., kanamycin resistance gene aphAI); - I-SceI restriction site; - sequence to be modified; - modified sequence (may also be insertions that can be fitted into primers such as small epitope tags) (Tischer et al., 2010).

Transfection of plasmid DNA

Plasmid DNA was transfected into HEK-293T cells using polyethylenimine (PEI). 4 x 10^6 293T cells were seeded in a 10 cm^2 dish and transfected using 8 µg of plasmid DNA. The plasmid and PEI (32 µL, considering a ratio with the DNA of 1:4) were first resuspended in separate tubes in 100 µL of DMEM without supplements. After 5 minutes of incubation, they were mixed by vortexing, incubated for 15 minutes at RT, and delivered to the cells. The medium was changed 6-8 hours post-transfection. The supernatant was collected at 48 and 72 hours post-transfection for further use.

Transfection of BAC DNA

HSV-1 BAC DNA was transfected into eukaryotic cells to reconstitute the virus. The HSV-1 reconstitution was performed in VERO cells. 1 x 10^5 cells were seeded in a 6-well plate, and after overnight incubation, they were transfected using 3 µg of DNA and 10 µL of Polyfectamine. The DNA and the polyfectamine were resuspended separately in 100 µL DMEM without supplements. After 5 minutes of incubation at RT, they were mixed by using a pipette and incubated for 15 minutes at RT. Afterwards, 500 µL of complete media was added to the mix, and the DNA with the transfection reagent was delivered to the cells. When the cells reached 90% confluence, they were transferred into a 15 cm² dish, and the reconstitution of HSV-1 was monitored and documented by fluorescence microscopy.

Production of lentivirus

Briefly, 293T cells were seeded at a density of 4 × 10^6 cells per 100 mm dish one day before transfection. On the second day, 4 µg pSicoR-CRISPR-PuroR was mixed with 3 µg of the packaging plasmid pCMVdR8.91 and 1 µg of the envelope plasmid pMD2.G in 1 mL of DMEM medium without serum and antibiotics for lentivirus production. After vortexing, 32 µl of PEI was added to the DNA solution. The mixture was incubated for 15 minutes at room temperature (RT) after thoroughly mixing. Then, it was loaded onto the cells drop by drop. The medium was changed after 6-8 hours of transfection. After 48 and 72 hours of transfection, supernatants containing the virus were harvested and sterilized using a 0.45 µm filter. They were either directly used to infect target cells for transduction or stored at -80 °C for later use.

Transduction of cells

To transduce cells in suspension, THP-1 cells were diluted to 5 x 10^5 cells in 1 mL of medium and mixed with 500 µL of the filtered supernatant containing lentivirus into a 2 mL Eppendorf tube. Polybrene was added to the mixture at a final concentration of 8 µg/mL and incubated for 6 hours at 37 °C. The mixture was then centrifuged at 250 × g for 7 minutes at RT, and the cell pellet was resuspended in 3

mL of complete growth medium. Cells were transferred into a 6-well plate and incubated for 48 hours at 37 °C. The transduced cells were finally selected using 1.5 µg/mL of puromycin, applied every third day, until complete selection was achieved.

Generation of knockouts using the CRISPR/Cas9 system

The lentiviral CRISPR/Cas9 vector pSicoR-CRISPR-PuroR was used to generate CASP8 knockout THP-1 clones, essentially as described by van Diemen et al., 2016. The gRNAs that target genes of interest were designed using the online tool E-CRISP (http://www.e-crisp.org/E-CRISP/designcrispr.html).

Three guide RNAs were synthesized and cloned individually in the lentiviral vector (performed by Jiajia Tang, Leibniz-Institut für Virologie (LIV, Hamburg, Germany)), and verified by sequencing:

g1, 5'-ACC GGAACTTCAGACACCAGGCA-3';

g2, 5'-ACC GCGGAATGTAGTCCAGGCTC-3';

g3, 5'-ACC GATGGAGAAGAGGGTCATCC-3'

Lentiviruses were generated using standard second-generation packaging vectors in HEK-293T cells. Wild-type THP-1 cells were transduced with CASP8-targeting or empty lentiviral CRISPR/Cas9 vectors in the presence of polybrene. The cells were selected with 1 µg/mL puromycin. Polyclonal cultures were subcultured to obtain single-cell clones (Figure 11), and caspase-8 protein expression was evaluated for each clone by immunoblot analysis.

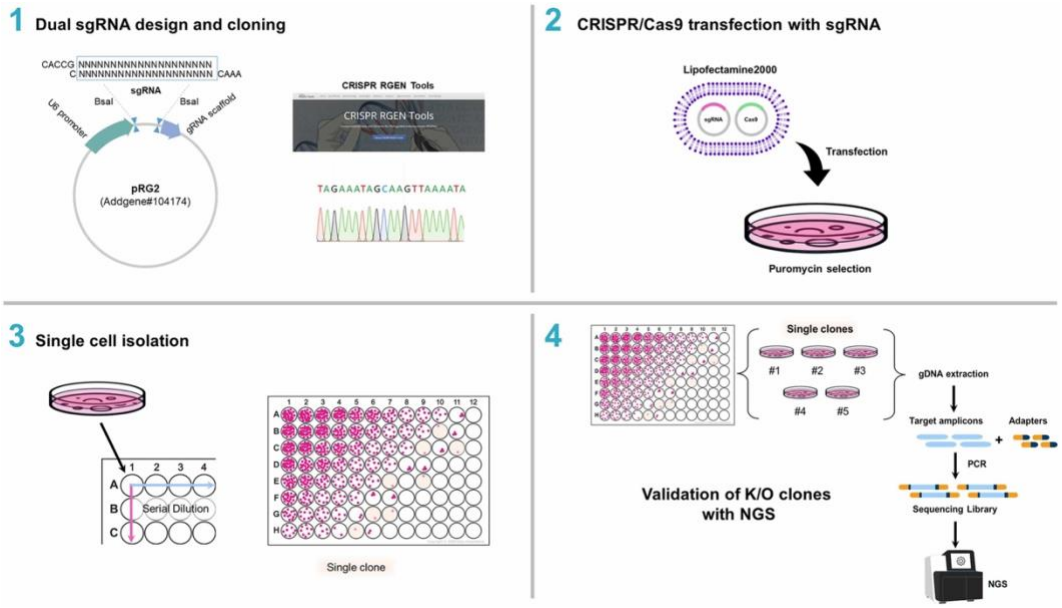

Figure 11. Workflow for the generation of CRISPR/Cas9-mediated knockout cell lines. The procedure includes: (1) design and cloning of dual sgRNAs targeting the gene of interest; (2) transfection of cells with sgRNAs; (3) isolation of single-cell clones; and (4) validation of gene knockout by next-generation sequencing (NGS) (Hong et al., 2024).

Viral infections

Cells were seeded in appropriate culture flasks and maintained under standard conditions. Cells were infected with the HSV-1 virus at a multiplicity of infection (MOI) based on the plaque-forming units (PFU) per milliliter (mL) of the virus stock. Infection was allowed to proceed for 1 hour at 37 °C. After the infection period, the viral inoculum was carefully removed, and the cells were washed with growth medium to eliminate residual unbound viruses. Fresh growth medium was then added to the cells. The samples were incubated for an additional time post-infection and then collected and processed for subsequent analyses, depending on the objectives of each experimental condition (e.g., plaque reduction assay, gene expression analysis, or protein quantification).

Plaque assay

Plaque assay was carried out in VERO cells. Supernatants were subjected to three freeze-thaw cycles. After overnight incubation, cells were infected with serial dilutions of log10 (10^{-4} to 10^{-7}) in DMEM containing 1% FBS. Each dilution was

done in triplicate. The infection was conducted for 1 hour at 37 °C on a shaker; afterwards, the viral inoculum was removed and replaced with culture medium containing 0.8% methylcellulose, which was added to each well to prevent the formation of a secondary plaque. After 72 h.p.i., the methylcellulose was removed from the wells, and the plaques were visualized by crystal violet staining and counted under an inverted light microscope.

Cell lysis and immunoblotting

For protein analysis of the whole cell lysates, cell pellets were collected at the indicated time after infection, washed in 1X phosphate-buffered saline (PBS), and lysed in 1X SDS sample buffer. The cleared extracts were sonicated and then boiled at 95 °C for 5 minutes.

Proteins were separated according to their molecular weight into a polyacrylamide gel formed by two different phases: stacking gel (loading gel) containing 5 % of acrylamide and resolving gel (separation gel) containing various percentages of SDS-polyacrylamide. Then, the proteins were transferred to a nitrocellulose membrane by wet transfer, which was performed by applying 100 V for 60 minutes or 35 mA overnight. Afterwards, the transfer efficiency was quickly evaluated using a Ponceau S staining solution. Then the membranes were blocked using 5 % (w/v) non-fat milk powder in TBS-T buffer for 60 minutes at RT on a shaking platform. Membranes with specific primary antibodies were incubated overnight at 4 °C on a shaking platform. The following day, the membranes were washed three times for 5 minutes each with TBS-T buffer and incubated with secondary antibodies coupled with Horseradish peroxidase (HRP) for 1 hour at RT on a shaking platform. Primary and secondary antibodies were diluted in 5 % (w/v) BSA and non-fat milk powder in TBS-T buffer, respectively. Afterwards, the membranes were washed three times for 5 minutes each in TBS-T buffer and incubated with LiteUP WB Chemiluminescent Substrate (Euroclone) for 5 minutes in the dark. The chemiluminescent signal was detected and imaged using X-ray films or Fusion Capture Advance FX7 16.15 (Peqlab) device or ChemiDoc Touch Imaging System (Bio-Rad). Quantitative densitometry analysis of immunoblot band intensities was

performed using ImageJ Software or Bio-Rad Image Lab 6 Software. Target protein levels were normalized to those of the housekeeping gene.

Antibodies and reagents

Primary antibodies used included anti-GAPDH (sc-32233), anti-HSV-1 UL42 (sc-53333), RIPK1 (sc-133102), anti-HSV-1 gD (sc-21719) were purchased from Santa Cruz Biotechnology; anti-βactin (ab8226) from Abcam; monoclonal anti-ICP0 was kindly provided by Professor Bernard Roizman; anti-phospho-NF-κB p65 (Ser536) (#3033) from Cell Signaling Technology; anti-Caspase-8 (human) monoclonal antibody (12F5; ALX-804-242) directed against the p55 unit was purchased from Enzo Life Sciences. HRP-conjugated goat anti-mouse and anti-rabbit IgG secondary antibodies were obtained from Merck Millipore.

Phosphonoacetic acid (PAA), from Sigma-Aldrich, was used as an inhibitor of DNA synthesis in HSV-infected cells and was dissolved in the medium at a concentration of 300 µg/mL during and after HSV-1 adsorption (Honess and Watson, 1976).

Live cell imaging

1 x10^6 HEp-2 cells were cultured in a µ-Dish 35 mm Quad (ibidi) and imaged with a Spinning Disk Nikon TI2 (Yokogawa W2 and Andor iXON 888 cameras) equipped with a controlled environment incubator (37 °C, 5% CO_2, constant humidity) and with the Perfect Focus System for continuous maintenance of focus, using a Plan Apo TIRF 100x (oil immersion) objective. Time-lapse experiments were performed overnight, and images were collected with acquisitions of at least 3 focal planes every 15 minutes, using an exposure time of 500 ms, with illumination light shuttered between acquisitions. ZGamma, brightness, and contrast were adjusted on displayed images (identically for compared image sets) using NIS-Elements software.

Image manipulation

All of the microscopy data was handled with FIJI (Fiji Is Just IMAGEJ). All images from the same experiment were acquired using the same microscope.

Quantification and statistical analysis

Data are expressed as the mean ± SD of three independent experiments. For data analysis, the Graphpad Prism 9 Software (GraphPad Software, San Diego, CA, USA) was used. Student's t-test and One-way ANOVA were used for statistical analysis to compare different conditions. The asterisks (*, **, and ***) indicate the significance of *p-values* less than 0.05, 0.01, and 0.001, respectively. For qPCR analysis, means ± standard deviations were calculated from two biological replicates and three technical replicates.

2.8. Results

2.8.1. HSV-1 replication in CASP8$^{+/+}$ and CASP8$^{-/-}$ THP-1 cells

To investigate the role of caspase-8 deficiency during HSV-1-infected monocytic cells, we generated Caspase8-knockout (CASP8$^{-/-}$) THP-1 cells using CRISPR-Cas9. Briefly, THP-1 cells were transduced with lentiviral CRISPR/Cas9 vectors encoding sgRNAs targeting *CASP8*, followed by puromycin selection and isolation of single-cell clones, as described in Materials and Methods. Gene disruption was verified by sequencing and confirmed by immunoblotting for caspase-8 protein expression (Figure 12a). Previous studies have demonstrated that Us11 can directly interact with procaspase-8, promoting its cleavage into the p18 subunit through a non-canonical mechanism that bypasses the initial autoproteolytic steps and does not trigger apoptosis. This cleavage has been observed in both THP-1 and epithelial cells and is thought to be involved in a pro-viral functions (Musarra-Pizzo et al., 2022). Therefore, to assess whether the absence of Us11 affects viral protein expression in CASP8$^{-/-}$ THP-1 cells, and to determine whether this modulation affects viral replication dynamics, we included in our experimental design the recombinant R3630 virus, which lacks both *Us11* and *Us12*.

Therefore, the impact of caspase-8 deficiency on both HSV-1 and the recombinant R3630 replication was evaluated by infecting both wild-type (CASP8$^{+/+}$) and CASP8$^{-/-}$ THP-1 cells. Representative viral proteins and gene expression were assessed 24 h.p.i. (Figure 12b, c, d, e). Immunoblotting for the immediate-early protein ICP0 and the envelope glycoprotein gD revealed increased accumulation of both viral proteins in CASP8$^{-/-}$ THP-1 cells compared to wild-type THP-1 cells. Densitometric analysis normalized to GAPDH confirmed a significant increase in ICP0 and gD expression in CASP8$^{-/-}$ THP-1 cells (Figure 12c, 12d). Additionally, we assessed the accumulation of the representative viral gene *VHS* in CASP8$^{-/-}$ THP-1 cells compared to wild-type cells during HSV-1 replication using qPCR. Significantly higher levels of *VHS* transcripts were observed in CASP8$^{-/-}$ THP-1 cells at 24 h.p.i. compared to CASP8$^{+/+}$ cells (Fig. 12e VII, VIII). The increase in *VHS* transcripts in caspase-8-deficient cells indicated that caspase-8 activity could

restrict viral gene expression or replication. This restriction may limit the progression of efficient viral replication. Moreover, at 24 h.p.i., a reduction in *VHS* transcripts was observed in both CASP8$^{+/+}$ and CASP$^{-/-}$ THP-1 cells infected with the R3630 mutant compared to wild-type HSV-1 (Fig. 12e IV, VIII). The significant differences detected between HSV-1 and R3630 infections support the conclusion that deletion of Us11/Us12 alters viral gene expression dynamics and/or replication kinetics in this cellular system.

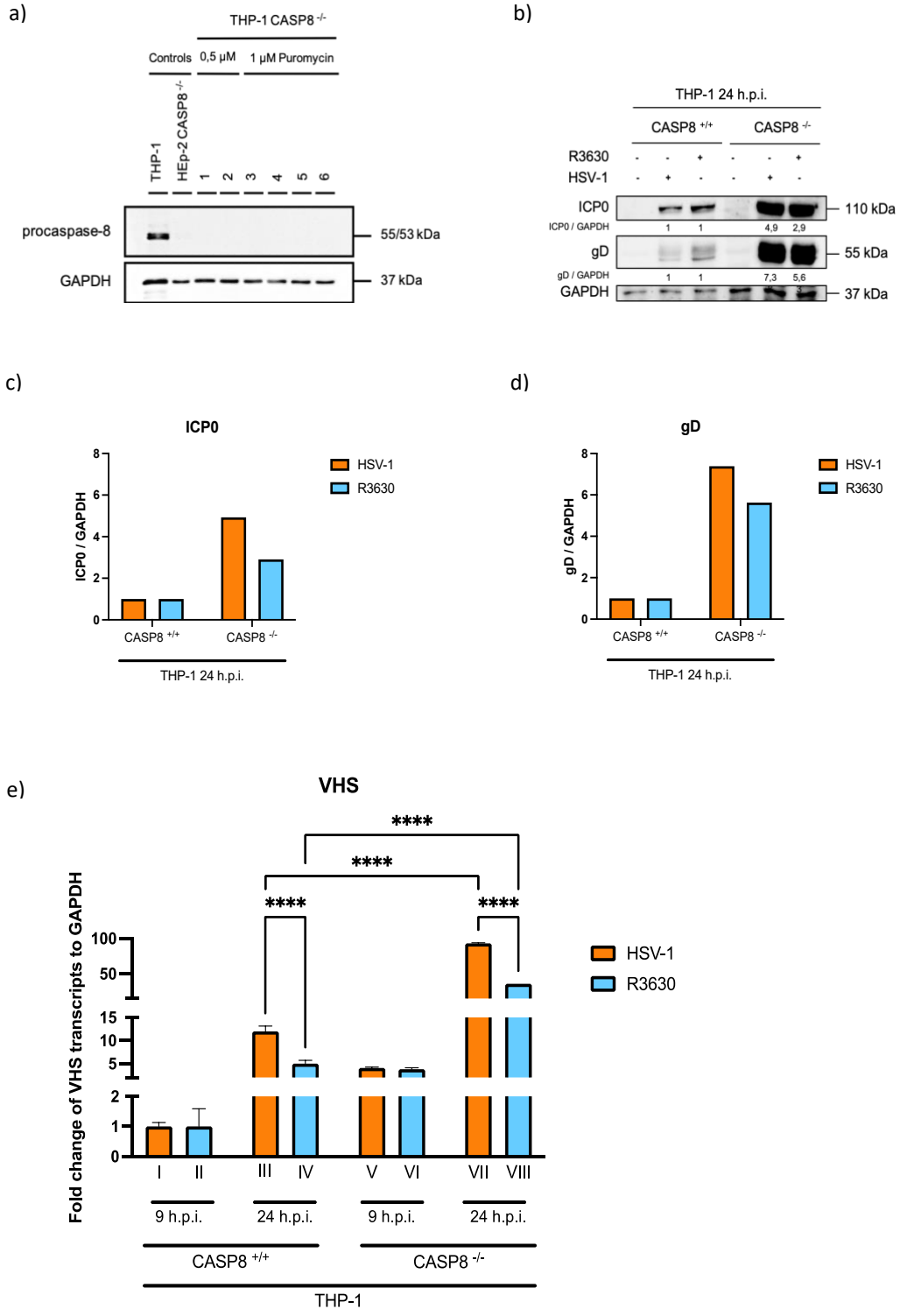

Figure 12. Characterization of CASP8$^{-/-}$ THP-1 cells. (a) Immunoblot analyses of lysate of CASP8$^{+/+}$ THP-1 cells and CASP$^{-/-}$ THP-1 cells for the accumulation of the knocked-out gene. GAPDH was used as a loading control. (b) Western blot analysis of viral proteins in CASP8$^{+/+}$ and CASP8$^{-/-}$ THP-1 cells infected or not with HSV-1 and R3630 (ΔUs11/Us12) viruses at MOI 50 and

collected at 24 h.p.i. (c) (d) The graphs represent the relative fold change of ICP0 (α) and gD (γ) bands' intensity over the GAPDH band intensity. The membranes were probed with antibodies directed against the viral proteins ICP0 and gD. Quantitative densitometry analysis of immunoblot band intensities was performed using ImageLab Bio-Rad software, and the results are expressed as the fold change over the housekeeping gene. (e) qPCR time-course analysis of VHS viral gene in $CASP8^{+/+}$ and $CASP8^{-/-}$ THP-1 cells infected or not with HSV-1 and R3630 (ΔUs11/Us12) viruses at MOI 50 and collected at 9 and 24 h.p.i. Asterisks (*, **, ***, ****) indicate the significance of *p-values* less than 0.05, 0.01, 0.001, and 0,0001, respectively.

To investigate the impact of caspase-8 deficiency on the production of new viral particles, wild-type and $CASP8^{-/-}$ THP-1 cells were infected with either HSV-1 or the mutant strain R3630 at MOI of 50. Cells were incubated for 9, 24, and 48 h.p.i., and cytopathic effects were monitored by inverted light microscopy. At the same time points (9, 24, and 48 h.p.i.), samples were collected for viral titration by plaque assay on VERO cells. At MOI 50, cytopathic effect (CPE) was evident by 24 h.p.i. and became more pronounced by 48 h.p.i. in both $CASP8^{+/+}$ and $CASP8^{-/-}$ THP-1 cells, with no substantial differences in CPE patterns between the two cell lines (Figure 13a).

Quantification of viral particles at 9, 24, and 48 h.p.i. revealed a modest but statistically significant difference in total virus production between $CASP8^{+/+}$ and $CASP8^{-/-}$ THP-1 cells, with the knockout cells displaying approximately a half-log increase in viral titers, irrespective of the viral strain used (Figure 13b).

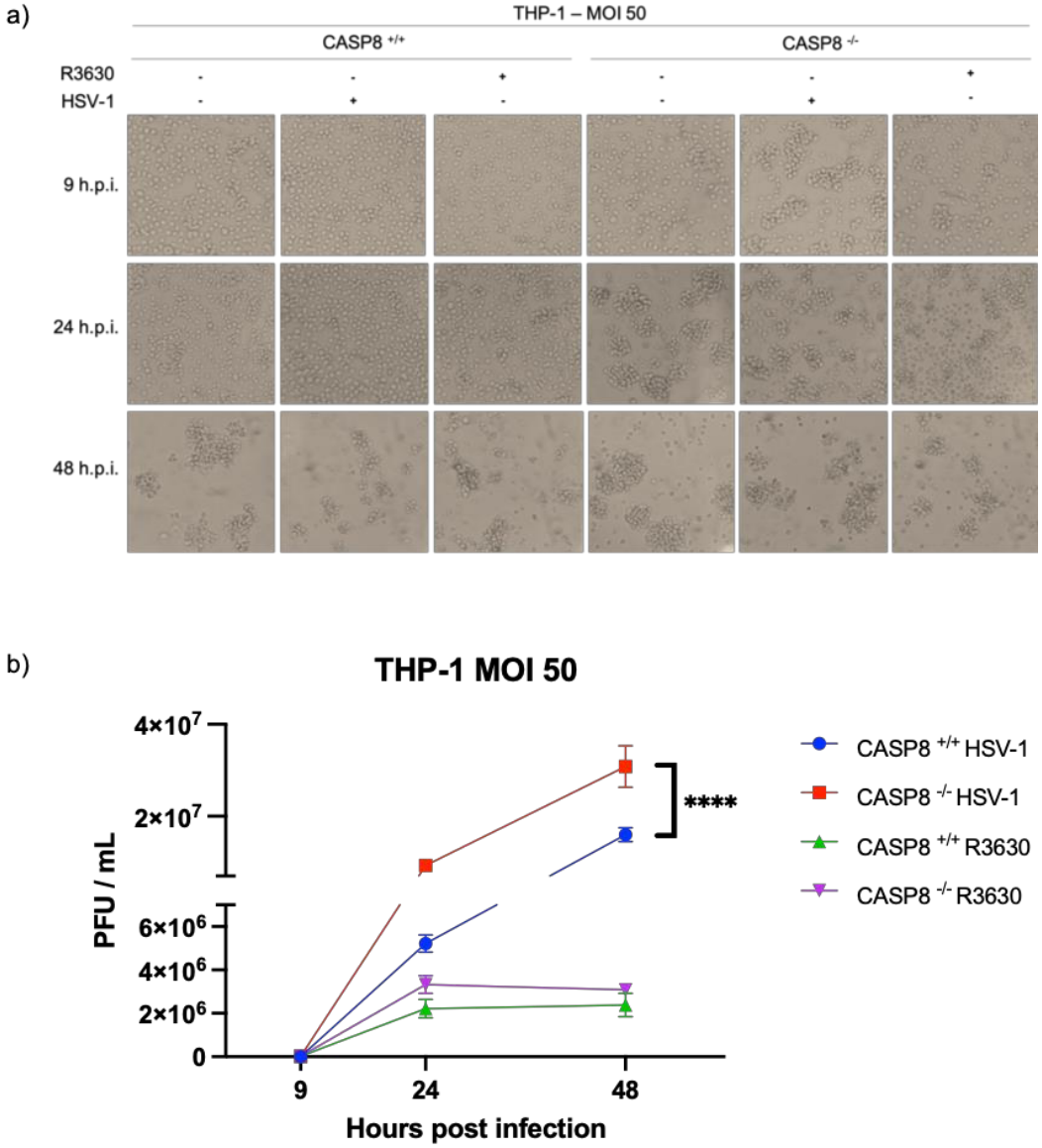

Figure 13. Evaluation of HSV-1 replication efficiency in CASP8$^{+/+}$ and CASP8$^{-/-}$ THP-1 cells at MOI 50. Comparison of HSV-1 replication efficiency in CASP8$^{+/+}$ and CASP8$^{-/-}$ THP-1 cells infected or not with HSV-1 and R3630 (ΔUs11/Us12) viruses at MOI 50 and harvested at different times p.i. (a) The cytopathic effect was observed under an inverted light microscope (magnification × 20) at 9, 24, and 48 h.p.i. (b) Samples were harvested at 9, 24, and 48 h.p.i., and viral yield was assessed by titration of total viral particles. Data are expressed as mean (± SD) of triplicates.

Since infection at MOI of 50 revealed a small but statistically significant difference (half a logarithmic unit) in viral titers between CASP8$^{+/+}$ and CASP8$^{-/-}$ THP-1 cells, we next sought to assess whether caspase-8 deficiency might exert a more pronounced effect under conditions of lower viral input. Therefore, we repeated the experiment at MOI of 10 to allow a more gradual progression of infection, thereby

facilitating the detection of subtle differences in viral spread and HSV-1-induced cytopathic effects that may be less evident at high MOI.

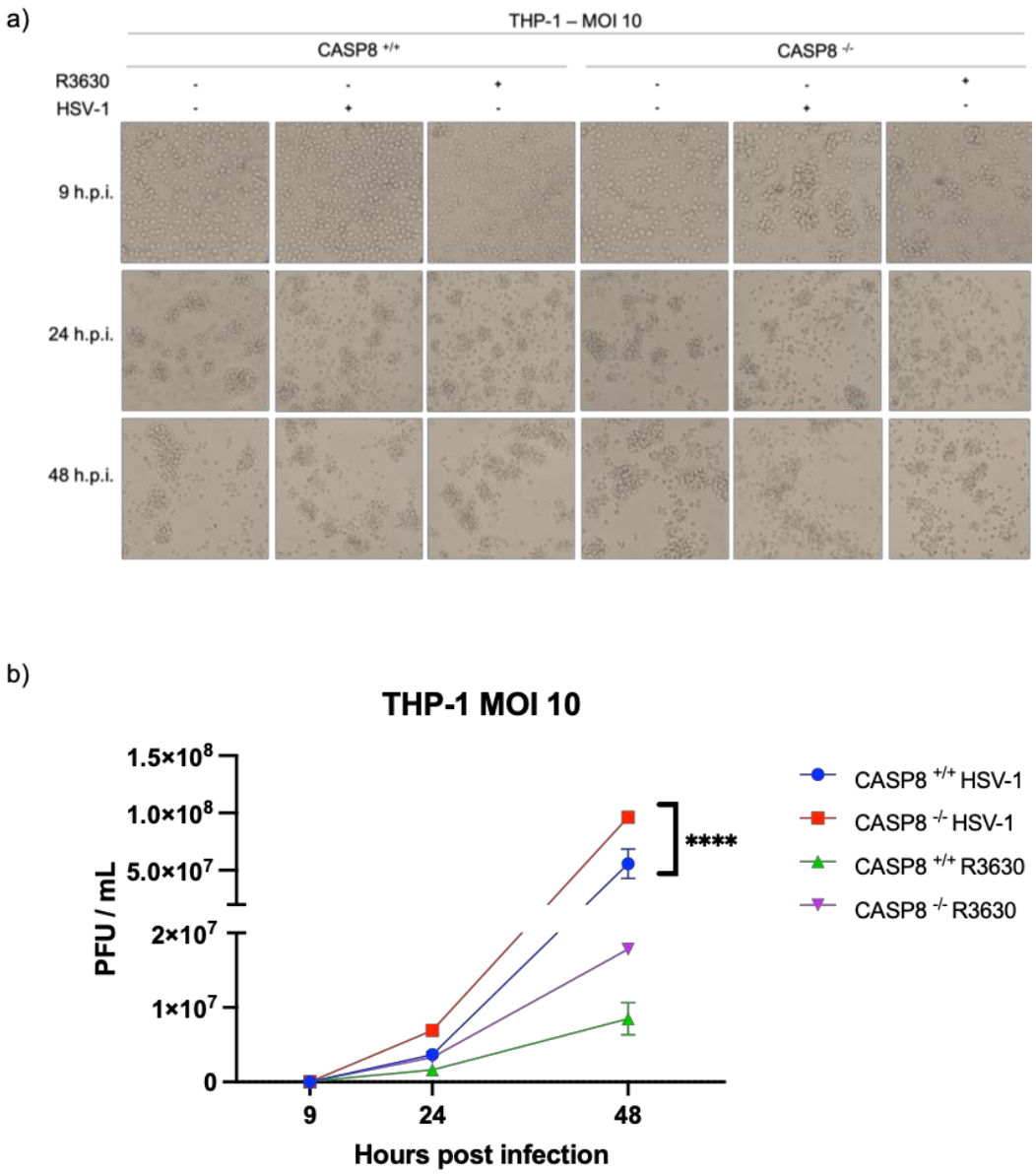

Figure 14. Evaluation of HSV-1 replication efficiency in CASP8$^{+/+}$ and CASP8$^{-/-}$ THP-1 cells at MOI 10. Comparison of HSV-1 replication efficiency in CASP8$^{+/+}$ and CASP8$^{-/-}$ THP-1 cells infected or not with HSV-1 and R3630 (ΔUs11/Us12) viruses at MOI 10 and harvested at different times p.i. (a) The cytopathic effect was observed under an inverted light microscope (magnification × 20) at 9, 24, and 48 h.p.i. (b) Samples were harvested at 9, 24, and 48 h.p.i., and viral yield was assessed by titration of total viral particles. Data are expressed as mean (± SD) of triplicates.

Wild-type and CASP8$^{-/-}$ THP-1 cells were infected with HSV-1 or the mutant strain R3630 at MOI of 10. Cytopathic effects were monitored up to 48 h.p.i., and viral titers were determined at 9, 24, and 48 h.p.i. by plaque assay on VERO cells, as described in the Materials and Methods section.

Similarly to what was observed at a MOI of 50, infection at MOI 10 resulted in a reproducible difference in viral titers between CASP8$^{+/+}$ and CASP8$^{-/-}$ cells, with the knockout cells showing approximately a half-log increase in viral production. Although this difference was statistically significant, it was not substantial in magnitude, indicating that caspase-8 deficiency exerts only a limited effect on the overall production of infectious viral particles under these conditions (Figure 14a and b).

Together, these results demonstrate that while the absence of caspase-8 does not markedly influence viral particle production, it promotes the intracellular accumulation of viral proteins and transcripts during HSV-1 infection, supporting a potential role for caspase-8 in the intrinsic antiviral defense of monocytic THP-1 cells by modulating viral gene expression.

2.8.2. Caspase-8 deficiency enhances chemokine expression during HSV-1 infection

It is well established that HSV-1 infection leads to the activation of caspase-8 in various cell types without necessarily triggering apoptosis. However, a previous analysis in THP-1 cells indicated that in both wild-type HSV-1 and R3630-infected cells, the cleavage of caspase-3 and PARP, a downstream effector of caspase-8, occurred at a later point post-infection. This finding confirms the activation of the apoptotic pathway in a portion of the infected cell population (Musarra-Pizzo et al., 2022). However, this still allows productive viral replication.

Since there is no clear role for caspase-8, a protein involved in cell death, during HSV-1 infection in THP-1 cells, we next investigated whether caspase-8 influences the inflammatory response during HSV-1 infection. We focused on changes in chemokine expression, which are small signaling proteins that attract immune cells.

Chemokines are critical mediators of leukocyte recruitment and tissue inflammation during viral infections. HSV-1 has been shown to trigger a robust chemokine response through the activation of pattern recognition receptors and downstream signaling pathways such as NF-κB and IRF3 (Alandijany, 2019; Melchjorsen et al., 2006). Specifically, upregulation of RANTES/CCL5 has been observed in the murine macrophage-like cell line J774A.1 (Melchjorsen et al., 2002), as well as in human monocyte-derived macrophages and dendritic cells (Melchjorsen et al., 2006). Moreover, increased expression of CXCL10, CCL2, and CCL3 has been reported in human primary macrophages (Melchjorsen et al., 2010, 2006), suggesting an important role for these chemokines in the antiviral response to HSV-1 infection.

Caspase-8 has been shown to regulate inflammatory signaling beyond its canonical role in cell death, acting both enzymatically and as a scaffolding protein that promotes cytokines production and inflammatory gene transcription through the recruitment of RIPK1 and activation of NF-κB, as well as through its interplay with RIPK3 signaling pathways (Fritsch et al., 2019; Henry and Martin, 2017; Pang and Vince, 2023; Simpson et al., 2021; Su et al., 2005). On this basis, we hypothesized that chemokine expression might be altered in the absence of caspase-8. To address this question, we measured the mRNA levels of five representative chemokines (CCL2, CCL4, CCL13, CXCL10, and CXCL11) by qPCR in CASP8+/+ and CASP8-/- THP-1 cells. Cells were infected at MOI of 50 with either HSV-1 or R3630. Samples were harvested at 9 and 24 h.p.i. (Figure 15a-e)

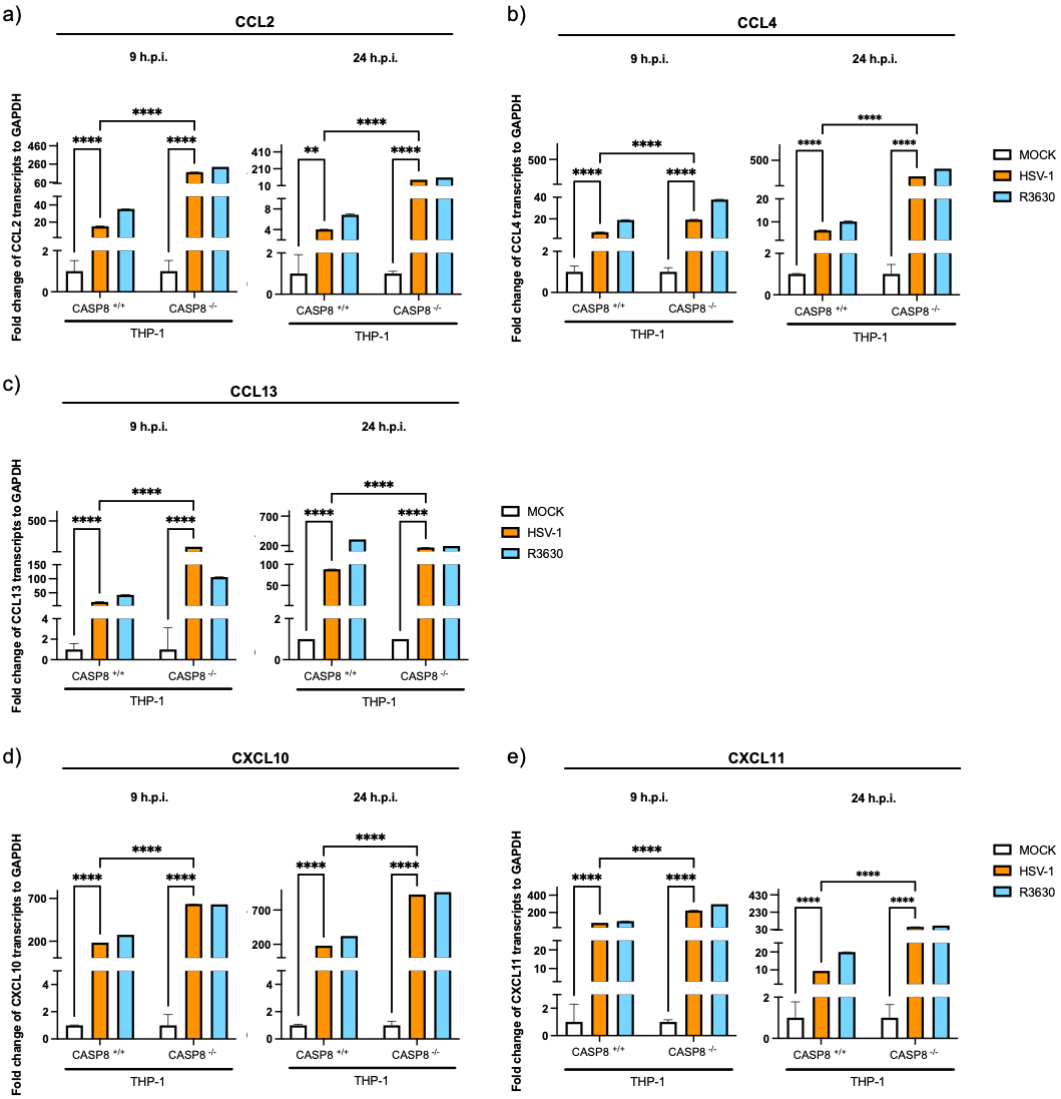

Figure 15. qPCR analysis of chemokine gene expression in CASP8$^{+/+}$ and CASP8$^{-/-}$ THP-1 cells upon HSV-1 infection. Expression profile of chemokines in CASP8$^{+/+}$ and CASP8$^{-/-}$ THP-1 cells infected or not with HSV-1 and R3630 (ΔUs11/Us12) viruses at MOI 50. Total RNA was collected at 9 and 24 h.p.i. (a-e) Chemokine gene expression was analyzed by using qPCR. Asterisks (*, **, ***, ****) indicate the significance of *p-values* less than 0.05, 0.01, 0.001, and 0,0001, respectively.

Given that primary HSV-1 infection consistently elicits a robust chemokine surge (including CXCL10, CXCL9, CCL2, CCL3, and CCL5) across tissues and immune contexts (Azher et al., 2017; Carr and Tomanek, 2006; Pontejo et al., 2018; Smith et al., 2022), we expected an overall increase in these transcripts upon infection, in fact all chemokines were found to be more highly expressed following viral infection. Still, more interestingly, all five chemokines were expressed at higher

levels in CASP8$^{-/-}$ THP-1 cells compared to CASP8$^{+/+}$ THP-1 controls, both at 9 and 24 h.p.i., suggesting that caspase-8 may exert a dampening effect on HSV-1-induced inflammatory responses. This chemokine "overload" in the absence of caspase-8 indicates that their transcriptional activation is not dependent on caspase-8, but rather that caspase-8 may act to limit or resolve the inflammatory cascade triggered by HSV-1 infection. This aligns with findings highlighting the dual roles of caspase-8 in both promoting and restraining inflammation, depending on the context and interaction with signaling adaptors such as RIPK1, FLIP, and FADD (Fritsch et al., 2019; Kaiser et al., 2011). Furthermore, no significant differences were observed in chemokine expression between infections with wild-type HSV-1 and the R3630 mutant, supporting the conclusion that Us11 and Us12 do not significantly regulate chemokine expression in this model. Together, these data indicate that caspase-8 is dispensable for the induction of chemokines during HSV-1 infection of THP-1 cells. However, the higher chemokine levels observed in CASP8$^{-/-}$ cells may be an indirect consequence of greater viral burden (consistent with the enhanced intracellular accumulation of viral transcripts and proteins in the knockout), rather than evidence of a direct caspase-8-mediated brake on chemokine signaling. Thus, caspase-8 presence may indirectly limit excessive chemokine expression, thereby contributing to the fine-tuning of the inflammatory response during viral infection.

2.8.3. Caspase-8 deficiency enhances NF-κB activation during HSV-1 infection

Given the increased chemokine expression observed in HSV-1-infected CASP8$^{-/-}$ THP-1 cells, we next investigated whether this inflammatory amplification could be attributed to upstream changes in the NF-κB pathway. NF-κB is a key transcriptional regulator of innate immune responses, and its activation is known to be triggered by HSV-1 infection in various cell types, including monocytes and dendritic cells (Alandijany, 2019). In the context of viral infections, caspase-8 has been reported to act both as a modulator and amplifier of NF-κB signaling,

depending on its interaction with adaptor proteins such as RIPK1 and FADD (Fritsch et al., 2019; Kaiser et al., 2011).

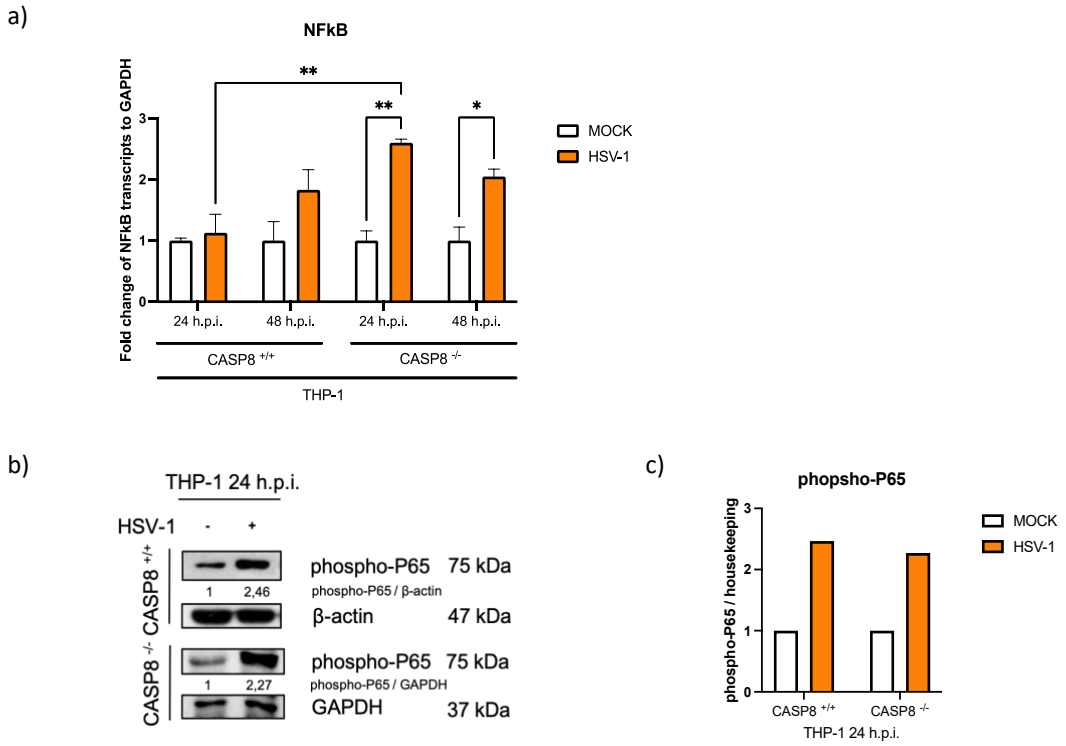

Figure 16. Analysis of NF-κB activation in CASP8$^{+/+}$ and CASP8$^{-/-}$ THP-1 cells during HSV-1 infection. (a) NF-kB levels were measured by qPCR in CASP8$^{+/+}$ and CASP8$^{-/-}$ THP-1 cells infected or not with HSV-1 virus at MOI 50. Total RNA was collected at 24 and 48 h.p.i. Asterisks (*, **, ***, ****) indicate the significance of *p-values* less than 0.05, 0.01, 0.001, and 0,0001, respectively. (b) Western blot analysis of phospho-P65 in CASP8$^{+/+}$ and CASP8$^{-/-}$ THP-1 cells infected or not with HSV-1 virus at MOI 50 and collected at 24 h.p.i. GAPDH and β-actin were used as loading controls. (c) The graph represents the relative fold change of phospho-P65 band intensity over the housekeeping band intensity. The membranes were probed with antibodies directed to phospho-P65 protein. The band intensity of phospho-P65 was determined using ImageLab Bio-Rad software, expressed as a fold change relative to the housekeeping gene.

To assess NF-κB activation at the transcriptional level, we measured NFKB1 mRNA expression by qPCR in CASP8$^{+/+}$ and CASP8$^{-/-}$ THP-1 cells infected at MOI 50 with HSV-1, at 24 and 48 h.p.i. (Figure 16a). Infection induced an evident upregulation of NFKB1 transcripts in both cell lines, with a notably more substantial increase in CASP8$^{-/-}$ THP-1 cells at 24 h.p.i. Collectively, these data

confirm that HSV-1 elicits a robust NF-κB response in THP-1 cells and indicate that caspase-8 loss further amplifies this response, as reflected by the stronger induction of NFKB1 transcripts (particularly at 24 h.p.i.) in CASP8$^{-/-}$ cells. This enhanced NF-κB transcriptional activity aligns with the exaggerated chemokine output observed in the knockouts. These findings support a model in which caspase-8 is not required for NF-κB/chemokine induction. The amplified response in CASP8$^{-/-}$ cells is compatible with indirect effects of altered infection dynamics and greater viral burden that secondarily enhance NF-κB-dependent transcription.

To determine whether this transcriptional upregulation correlated with enhanced NF-κB signaling activity, we analyzed the phosphorylation status of the NF-κB p65 subunit by Western blot. Protein lysates from HSV-1-infected (MOI 50) and mock-infected CASP8$^{+/+}$ and CASP8$^{-/-}$ THP-1 cells were probed with an antibody specific for phospho-p65 (Figure 16b). Densitometric analysis normalized to GAPDH and β-actin showed a similar accumulation of phosphorylated p65 in CASP8$^{-/-}$ cells and wild-type THP-1 cells upon infection with HSV-1 (Figure 16c).

These findings indicate that in THP-1 cell caspase-8 deficiency enhances NF-κB transcriptional activation in response to HSV-1 infection, as reflected by the stronger upregulation of NFKB1 mRNA in CASP8$^{-/-}$ THP-1 cells. However, this effect does not appear to be mediated by increased p65 phosphorylation, suggesting that caspase-8 primarily influences NF-κB activity at the transcriptional rather than the post-translational level, pointing to a regulatory role of caspase-8 in restraining NF-κB-driven inflammatory gene expression during HSV-1 infection.

2.8.4. NF-κB pathway is required for chemokine induction during HSV-1 infection in THP-1 cells

To validate the involvement of NF-κB signaling in chemokine regulation during HSV-1 infection, we employed a genetic approach using THP-1 cells stably expressing a dominant-negative mutant of IκBα (DN IκBα). IκBα is a central inhibitor of NF-κB: under basal conditions, it binds the NF-κB p65/p50 heterodimer in the cytoplasm and prevents its nuclear translocation. Upon stimulation, including

viral infection, the IKK complex phosphorylates IκBα at Ser32 and Ser36, marking it for ubiquitination and proteasomal degradation. This degradation allows NF-κB to enter the nucleus and initiate the transcription of proinflammatory genes (Bonizzi and Karin, 2004; Hayden and Ghosh, 2011; Liu et al., 2017). The DN IκBα variant harbors point mutations at critical phosphorylation sites, rendering it resistant to degradation. As a result, NF-κB remains sequestered in the cytoplasm even upon stimulation, and downstream gene expression is strongly impaired (Venuti et al., 2019). This system enables a direct assessment of the dependency of chemokine induction on NF-κB activation.

THP-1 wild-type and DN IκBα cells were infected with HSV-1 at MOI 50 at 37 °C, at 24 h.p.i., samples were collected, and total-RNA was processed for gene expression analysis using qPCR. We analyzed the mRNA levels of five chemokines known to be responsive to HSV-1 infection and to NF-κB activity: CCL4, CCL2, CCL13, CXCL10, and CXCL11.

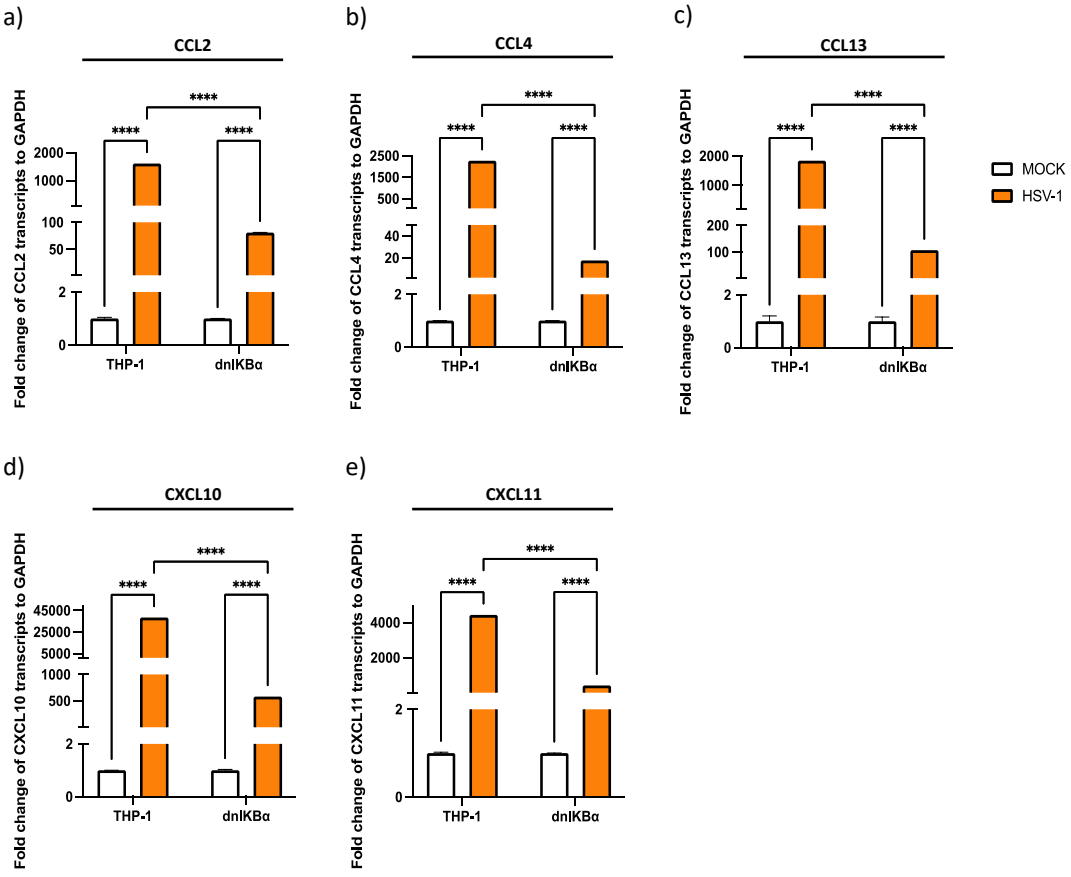

Figure 17. qPCR analysis of chemokine gene expression in HSV-1-infected THP-1 wild-type and DN IκBα cells. THP-1 cells were infected or not with HSV-1 viruses at MOI of 50. Total RNA was collected at 24 h.p.i. Chemokine gene expression was analyzed by qPCR. (a-e) Gene expression values were normalized to the housekeeping gene GAPDH. Asterisks (*, **, ***, ****) indicate the significance of *p-values* less than 0.05, 0.01, 0.001, and 0,0001, respectively.

In both wild-type and DN IκBα THP-1 cells, infection with HSV-1 led to increased expression of all tested chemokines compared to mock-infected controls (Figure 17a-e). However, the magnitude of induction was markedly lower in DN IκBα cells. This reduction was consistent across all targets, including CXCL10 and CCL2, which are classical NF-κB/AP-1-regulated genes (Alandijany, 2019; Melchjorsen et al., 2006). These data show that NF-κB activity is necessary for the full amplitude of chemokine induction during HSV-1 infection of THP-1 cells. Stabilizing IκBα with the dominant-negative mutant consistently blunted the upregulation of CCL2, CCL4, CCL13, CXCL10, and CXCL11 at 24 h.p.i., establishing a causal link between NF-κB activation and chemokine transcription in this setting. The residual increase observed in DN IκBα cells indicates that, under these conditions, chemokine expression is only partially dependent on NF-κB, either because the blockade is incomplete or because additional NF-κB-independent inputs contribute, making NF-κB a major, but not exclusive, determinant of the response.

2.8.5. HSV-1-induced chemokine expression requires active viral replication

To clarify the mechanism of chemokine induction during HSV-1 infection, we examined whether active viral replication is essential or if viral entry alone suffices to elicit the production of proinflammatory mediators. Establishing this distinction is needed for assessing whether chemokine production relies on viral gene expression and replication or results from immediate innate detection of incoming viral particles.

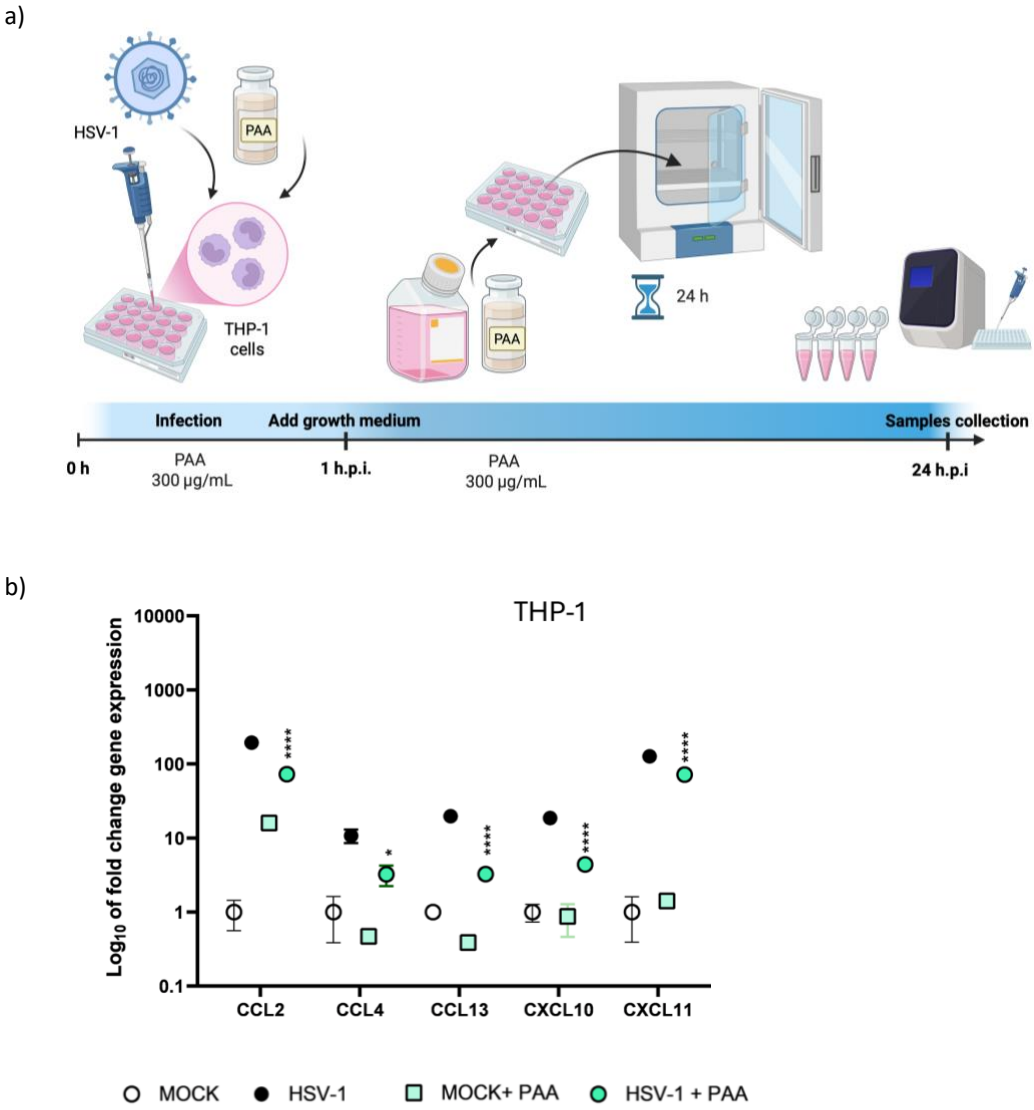

Figure 18. qPCR analysis of chemokine gene expression in HSV-1-infected THP-1 cells. (a) Graphical representation of the experiment workflow: THP-1 cells were infected with HSV-1 (MOI 50) in the presence or absence of phosphonoacetic acid (PAA, 300 µg/mL), a selective inhibitor of viral DNA polymerase. After 1 hour, the viral inoculum was removed and replaced with growth medium containing PAA. At 24 h.p.i., samples were collected, and total RNA was isolated and (b) analysed by qPCR to evaluate the expression levels of CCL2, CCL4, CCL3, CXCL10, and CXCL11. Gene expression values were normalized to the housekeeping gene GAPDH. Asterisks (*, **, ***, ****) indicate the significance of *p-values* less than 0.05, 0.01, 0.001, and 0,0001, respectively.

We used phosphonoacetic acid (PAA), a specific inhibitor of herpesvirus DNA polymerase (Honess and Watson, 1976), either alone or in combination with HSV-1, to treat THP-1 cells and address this inquiry. The PAA concentration tested was 300 µg/mL, which was proven to effectively inhibit HSV-1 genome replication

without inducing cytotoxicity (Honess and Watson, 1976). At 24 h.p.i., total RNA was collected, and qPCR was performed to quantify the mRNA levels of significant inflammatory mediators, including CCL2, CCL4, CCL13, CXCL10, and CXCL11. Compared to untreated infected controls, the results indicated that PAA treatment markedly decreased the transcriptional activation of all assessed targets. The observed decrease occurred in several independent replicates, and it was consistent across all examined chemokines, indicating that active viral DNA replication is essential for the accumulation of these transcripts, rather than merely viral entry or immediate-early processes.

Blocking HSV-1 DNA synthesis with PAA (300 μg/mL) sharply reduced the 24 h.p.i. upregulation of CCL2, CCL4, CCL13, CXCL10, and CXCL11 in THP-1 cells, despite the absence of cytotoxicity (Figure 18b). This reproducible effect indicates that robust chemokine induction depends on productive viral replication and cannot be explained by viral entry or immediate-early events alone. In this system, chemokine overexpression therefore occurs downstream of genome replication and tracks with the replicative phase of the HSV-1 life cycle.

2.8.6. Investigating RIPK1 regulation during HSV-1 infection in caspase-8-knockout cells

The previous sections demonstrated that caspase-8 deficiency amplifies inflammatory signaling in HSV-1-infected knockout THP-1 cells, as evidenced by the increased transcription of chemokines and NF-κB. Furthermore, chemokine induction has been shown to rely on NF-κB signaling, as the dominant-negative inhibition of IκBα suppresses their expression. To further investigate the underlying mechanisms, we examined the expression of RIPK1, a central signaling node that integrates inflammatory and cell death pathways, and which is known to interact functionally with both caspase-8 and NF-κB (Fritsch et al., 2019; Newton et al., 2019). RIPK1 has been implicated in the regulation of chemokine gene expression through NF-κB activation, and its expression is known to be modulated in response to inflammatory stimuli and viral infections (Han et al., 2021; Weinlich et al., 2017).

We therefore sought to determine whether RIPK1 expression is altered during HSV-1 infection in relation to caspase-8, and whether its regulation is dependent on NF-κB. The non-apoptotic cleavage of the p18 subunit from procaspase-8, through direct interaction with Us11, has been observed in different cellular models. It is associated with autophagy restriction via Atg3 cleavage, a process that could support viral fitness (Musarra-Pizzo et al., 2022), and is consistent with, but does not by itself demonstrate, viral immune evasion. On this basis, we decided to examine the expression of RIPK1, also in relation to Us11. Therefore, we included the recombinant virus R3630 in our experimental design.

Indeed, a series of experiments were performed in THP-1 monocytic cells (CASP8$^{+/+}$ and CASP8$^{-/-}$), and HEp-2 epithelial cells (CASP8$^{+/+}$ and CASP8$^{-/-}$). All models were infected with either wild-type HSV-1 or the Us11/Us12-deleted mutant R3630 and harvested at 24 h.p.i. for Western blot and qPCR analysis. Wild-type and CASP8$^{-/-}$ THP-1 cells were infected with either HSV-1 or the mutant strain R3630 at MOI of 50. At 24 h.p.i. samples were harvested and subjected to Western blot analysis.

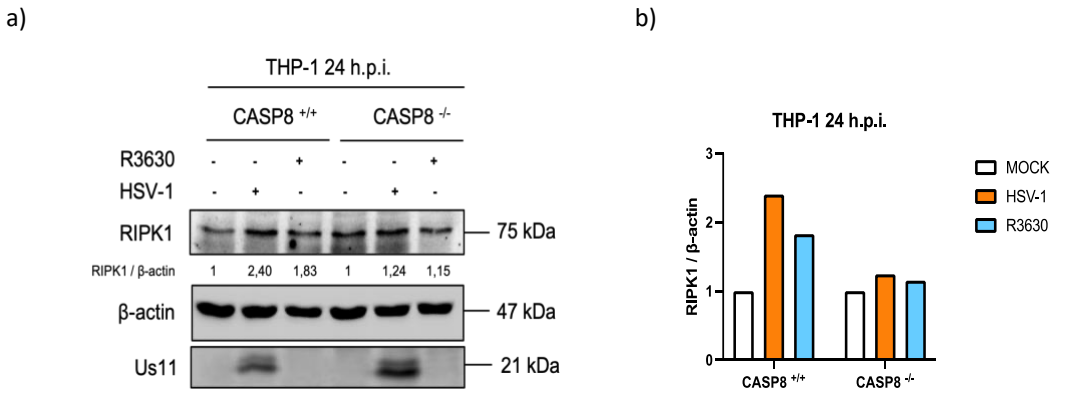

Figure 19. RIPK1 expression upon HSV-1 infection in CASP8$^{+/+}$ and CASP8$^{-/-}$ THP-1 cells at MOI 50. (a) Western blot analysis of RIPK1 in CASP8$^{+/+}$ and CASP8$^{-/-}$ THP-1 cells infected or not with HSV-1 and R3630 (ΔUs11/Us12) viruses at MOI 50 and collected at 24 h.p.i. Us11 was used as a representative viral protein. β-actin was used as a loading control. (b) The graph represents the relative fold change of RIPK1 band intensity over the β-actin band intensity. The membranes were probed with antibodies directed to the RIPK1 protein. The band intensity of RIPK1 was determined using ImageJ Software, expressed as a fold change over the housekeeping gene.

Data demonstrated that at 24 h.p.i., wild-type HSV-1 increased RIPK1 protein abundance in CASP8$^{+/+}$ THP-1 cells, whereas this increase was diminished in CASP8$^{-/-}$ cells. Infection with the Us11/Us12-deleted mutant R3630 did not appreciably change RIPK1 levels in either genotype compared to the wild-type HSV-1 infection (Figure 19a-b).

Similarly, CASP8$^{+/+}$ and CASP8$^{-/-}$ HEp-2 cells were exposed to HSV-1 or the mutant strain R3630 at a multiplicity of infection of 10. One hour later, the inoculum was replaced with fresh culture medium, and cells were harvested at 24 h.p.i. for downstream analyses, including Western blotting and qPCR.

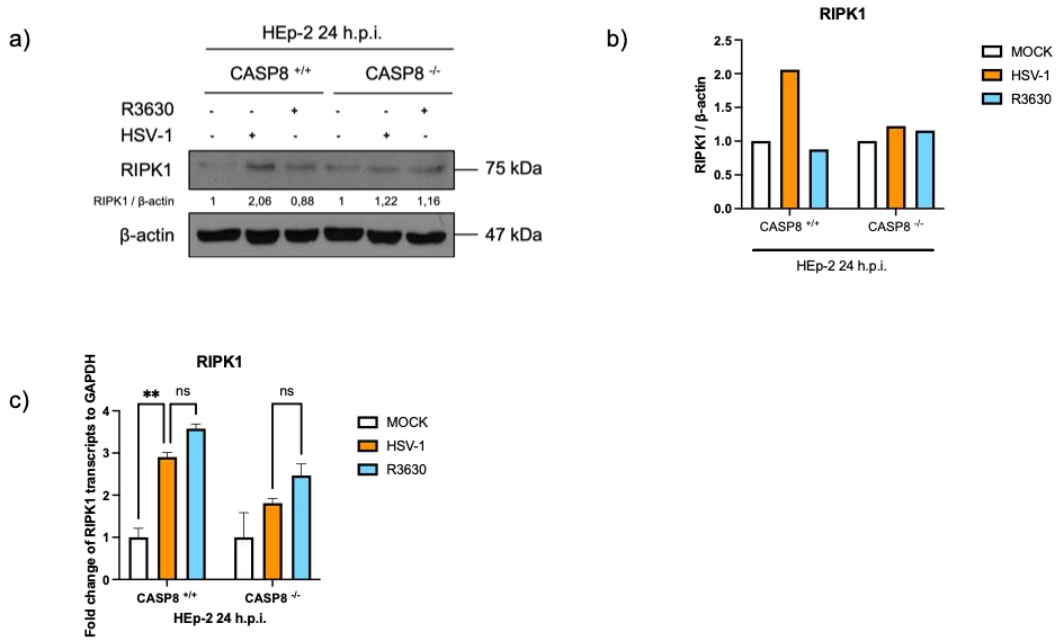

Figure 20. RIPK1 expression upon HSV-1 infection in CASP8$^{+/+}$ and CASP8$^{-/-}$ HEp-2 cells at MOI 10. (a) Western blot analysis of RIPK1 in CASP8$^{+/+}$ and CASP8$^{-/-}$ HEp-2 cells infected or not with HSV-1 and R3630 (ΔUs11/Us12) viruses at MOI 10 and collected at 24 h.p.i. (b) The graph represents the relative fold change of RIPK1 band intensity over the β-actin band intensity. The membranes were probed with antibodies directed to the RIPK1 protein. The band intensity of RIPK1 was determined using ImageJ Software, expressed as a fold change over the housekeeping gene. (c) RIPK1 levels were measured by qPCR in CASP8$^{+/+}$ and CASP8$^{-/-}$ HEp-2 cells infected or not with HSV-1 and R3630 (ΔUs11/Us12) viruses at MOI 10. Total RNA was collected 24 h.p.i.

In HEp-2 cells, RIPK1 protein and transcript levels were significantly upregulated in CASP8$^{+/+}$ cells upon infection with HSV-1 wild-type, and this effect was not that enhanced in CASP8$^{-/-}$ cells (Figure 20a-b). Interestingly, at the protein and

transcriptional level, RIPK1 protein and mRNA did not change significantly with R3630 infection compared to wild-type HSV-1 infection in both CASP8$^{+/+}$ and CASP8$^{-/-}$ cells (Figure 20c), suggesting that caspase-8 contributes to the transcriptional and protein accumulation of RIPK1, while Us11 does not interfere at the transcriptional or protein stabilization level.

Across both cell models, caspase-8 presence was associated with stronger RIPK1 induction following HSV-1 infection, despite their distinct permissivity. In semi-permissive monocytic THP-1 cells (MOI 50), wild-type HSV-1 increased RIPK1 protein in CASP8$^{+/+}$ cells, whereas this increase was blunted in CASP8$^{-/-}$ cells (Figure 19a-b). In permissive epithelial HEp-2 cells (MOI 10), wild-type HSV-1 upregulated RIPK1 at both mRNA and protein levels in CASP8$^{+/+}$ cells, with a less pronounced response in CASP8$^{-/-}$ cells (Figure 20). RIPK1 abundance following R3630 infection was comparable to that of HSV-1 wild-type in both CASP8$^{+/+}$ and CASP8$^{-/-}$ cells, at the protein level in THP-1 cells (Figure 19) and at mRNA levels in HEp-2 cells (Figure 20). Taken together, these results indicate that, under the conditions tested, caspase-8 is required for RIPK1 upregulation during HSV-1 infection. In THP-1 cells, this occurs at the protein level, whereas in HEp-2 cells it is observed at both transcript and protein levels. Us11/Us12 deletion does not detectably impact this axis. Regarding the NF-κB-dependent chemokine responses described above, the data support a model in which caspase-8 promotes RIPK1 expression during HSV-1 infection. Enhanced NFKB1 and chemokine induction in CASP8$^{-/-}$ cells likely reflect indirect, infection-driven effects, rather than increased proximal NF-κB activation.

2.8.7. Investigating the role of caspase-8 in HSV-1 egress using a dual-fluorescent recombinant virus

HSV-1 uses several mechanisms to spread from infected to uninfected cells (Agelidis and Shukla, 2015), notably through the production of secreted vesicles, such as virion-like structures composed of viral envelopes and tegument proteins (McLauchlan et al., 1992) and extracellular vesicles (EVs), including exosome-like

structures that contain both viral and host components (Kalamvoki and Deschamps, 2016). In addition, HSV-1 exploits host intracellular trafficking machinery for morphogenesis and egress. Rab GTPases, which are master regulators of vesicle transport, have emerged as key players in these processes. Rab1 and Rab43, for example, regulate glycoprotein trafficking and maintain Golgi integrity, respectively, both of which are essential for proper viral assembly (Raza et al., 2018). Moreover, Rab5 and Rab11 are involved in endocytic pathways that supply membranes for secondary envelopment of cytoplasmic capsids; silencing these proteins markedly reduces virion production, indicating that HSV-1 utilizes Rab-regulated endosomal tubules during egress (Raza et al., 2018). Recent evidence has highlighted an additional level of complexity in HSV-1 egress mechanisms involving host cell death pathways. In particular, caspase-8 has emerged as a key regulator not only of HSV-1-induced apoptosis, but also of viral particle release through the modulation of autophagy. It was shown that caspase-8-deficient monocytes and fibroblasts exhibited a significant reduction in extracellular HSV-1 titers despite robust viral gene expression, due to enhanced autophagic activity that sequestered virions in LC3-positive vesicles and impaired their release (Marino-Merlo et al., 2023). This study supports a non-canonical role for caspase-8 in counteracting autophagy to ensure efficient viral egress. These findings suggest that the absence of caspase-8 may alter intracellular trafficking events involved in virion maturation and export, independent of its classical pro-apoptotic function.

Although our previous findings revealed that caspase-8 deficiency does not significantly impair HSV-1 replication or directly induce chemokine production and NF-κB activation in THP-1 cells, they also highlighted an enhanced accumulation of viral proteins and transcripts in CASP8$^{-/-}$ cells. These observations raise the possibility that caspase-8 may contribute to stages of the viral life cycle beyond genome replication or immediate-early gene expression. To address whether caspase-8 supports HSV-1 replication and spread by influencing late events in the viral life cycle, we designed, through *en passant* BAC mutagenesis (Tischer et al., 2010), two single-fluorescent recombinant HSV-1 viruses. These viruses carry a distinct fluorescent tag: one has mNeonGreen inserted between codons 1 and 2 of *UL35* (VP26, a capsid protein), and the other has mScarlet,

inserted between codons 6 and 7 of *UL22* (gH, an envelope glycoprotein), as suggested by De Oliveira et al., 2008, to not interfere with viral replication (Figure 21a and b), This allows the respective visualization of the capsid and envelope structures in the nucleus and membrane compartments.

Briefly, as outlined in the Materials and Methods section, the shuttle plasmids were employed for the recombination procedure (Figure 21a and b). Following purification, the PCR product was used to transform GS1783 cells harboring the HSV-1 F strain BAC. Transformed bacteria were plated on LB agar supplemented with chloramphenicol and kanamycin. The obtained bacterial colonies were screened by restriction enzyme digestion and analytical PCR. Verified positive clones were then subjected to the second recombination step. This step requires the induction of I-SceI recombinase expression, achieved by adding 2% (w/v) L-arabinose and incubating the culture at 42 °C. Recombinant bacteria were subsequently plated on LB agar containing 1% L-arabinose and chloramphenicol. Colonies were then examined for the loss of kanamycin resistance through restriction digestion (Figure 21c and d), analytical PCR, and sequencing.

This approach enables a dynamic analysis of HSV-1 maturation, intracellular trafficking, and egress, as well as real-time and single-cell level monitoring of viral replication through direct fluorescence detection.

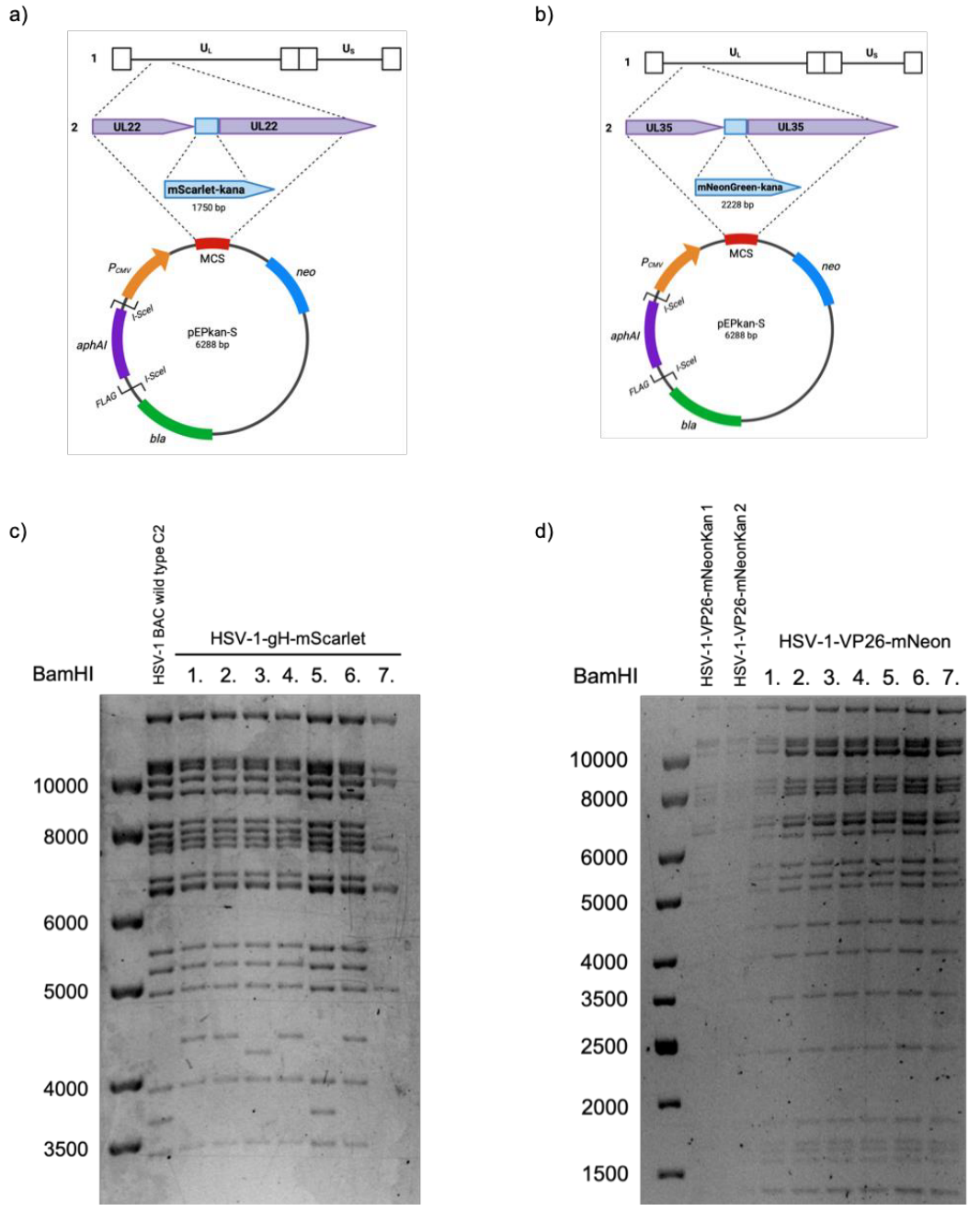

Figure 21. *En passant* mutagenesis of HSV-1-gH-mScarlet and HSV-1-VP26-mNeonGreen recombinants. (a) (b) (1) linear representation of the HSV-1 genome. White rectangles represent the inverted repeats flanking the unique sequences (UL and US). (a) (2) pEPkan-S DNA plasmid contains the insertion of the mScarlet sequence, inserted between codons 6 and 7 of gH (*UL22*). (b) (2) pEPkan-S DNA plasmid contains the insertion of the mNeonGreen sequence, inserted between codons 1 and 2 of VP26 (*UL35*) (Adapted from Tischer et al., 2010). (c) (d) Second recombination. The *en passant* cassette was excised by inducing the expression of I-SceI and the recombinase system. Resolved clones were selected against the presence of kanamycin resistance. BAC DNA was digested for 1 hour at 37 °C with BamHI and run on a BAC gel. (c) Lane 1 represents HSV-1 BAC wild type with BamHI restriction site at 3700 bp; lanes 2, 3, 4, 5, 6, 7 represent HSV-1 gH-mScarlet with BamHI restriction site at 4500 bp. The left panel displays molecular weights. (d) Lanes 1 and 2 represent the co-integrates 1 HSV-1 VP26-mNeonGreen-kan with BamHI restriction

site at 7900 bp; lanes 3, 4, 5, 6, 7, 8, 9 represent HSV-1-gH-mScarlet with BamHI restriction site at 6400 bp. The left panel displays molecular weights.

Live imaging experiments were performed using the HEp-2 permissive cell line, both wild-type ($CASP8^{+/+}$) and $CASP8^{-/-}$ cells. Cells were seeded in a µ-Dish 35 mm Quad (ibidi), an imaging dish with four compartments, allowing simultaneous observation of multiple conditions and facilitating the identification of potential differences between the cell lines. HEp-2 $CASP8^{+/+}$ and $CASP8^{-/-}$ cells were infected with HSV-1 VP26-mNeonGreen at MOI 10 for 1 hour at 37 °C. Live-cell imaging was carried out using the Nikon TI2 Spinning Disk system over 27 h.p.i. (Figure 22a). The accumulation of viral DNA in HSV-1-infected cells was then assessed, and following quantification, the resultant two graphs (Figure 22b, 22c) showed that the number of HSV-1 *foci* did not differ significantly between $CASP8^{+/+}$ and $CASP8^{-/-}$ cells; however, a statistically significant difference was observed in the area of the *foci*. This suggests that the accumulation of viral progeny may not differ in quantity but rather in its spatial distribution within the nucleus, pointing toward impaired viral egress in the absence of caspase-8. This is made more explicit in Figure 22d, where HEp-2 $CASP8^{+/+}$ cells were co-infected with HSV-1 VP26-mNeonGreen and HSV-1 gH-mScarlet at MOI 5 for 1 hour at 37 °C. As already demonstrated by De Oliveira et al., 2008, the VP26 capsid fusion proteins were initially observed throughout the nucleus and later accumulated in viral replication compartments, forming small foci at the periphery of these compartments that expanded and coalesced over time into much larger structures. The envelope glycoprotein H (gH) was first observed accumulating in a vesicular pattern in the cytoplasm and was then incorporated primarily into the cellular membrane.

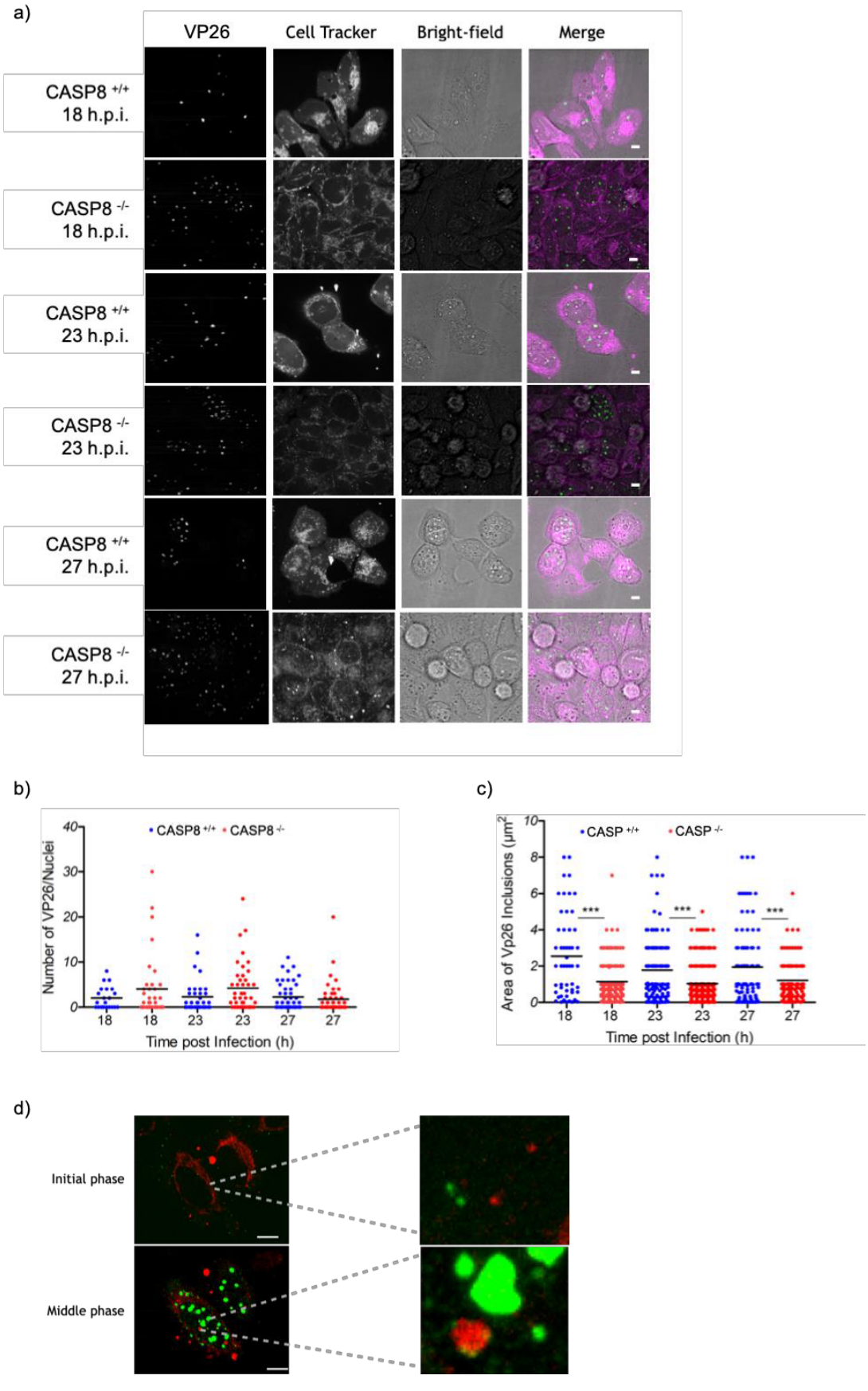
a)
VP26
Cell Tracker
Bright-field
Merge
CASP8 +/+ 18 h.p.i.
CASP8 -/- 18 h.p.i.
CASP8 +/+ 23 h.p.i.
CASP8 -/- 23 h.p.i.
CASP8 +/+ 27 h.p.i.
CASP8 -/- 27 h.p.i.
b)
CASP8 +/+
CASP8 -/-
Number of VP26/Nuclei
Time post Infection (h)
c)
CASP +/+
CASP -/-
Area of Vp26 Inclusions (µm²)
***
Time post Infection (h)
d)
Initial phase
Middle phase

Figure 22. Live imaging of HEp-2 CASP8$^{+/+}$ and CASP8$^{-/-}$ cells infection. (a) HEp-2 CASP8$^{+/+}$ and CASP8$^{-/-}$ cells, using the CellTracker™ Deep Red Dye, were infected with HSV-1 VP26-mNeonGreen at MOI 10 and imaged in live cell imaging by confocal microscopy at 18, 23, and 27 h.p.i. The variation in the number of VP26 between CASP8$^{+/+}$ and CASP8$^{-/-}$ is not statistically relevant (b), but it is in terms of their area (c). (d) HEp-2 cells were co-infected with HSV-1 VP26-mNeonGreen and HSV-1 gH-mScarlet at MOI 5 and imaged in live cell imaging by confocal microscopy up to 60 h.p.i. Scale bar is 20 μm. On the left, frames from the initial and middle phases of infection; on the right, corresponding enlargements.

Taken together, live imaging with capsid- (VP26-mNeonGreen) and envelope- (gH-mScarlet) tagged HSV-1 indicates that loss of caspase-8 does not reduce the number of nuclear replication foci but limits their growth/expansion, pointing to a defect that emerges after genome replication. In CASP8$^{+/+}$ cells, VP26 foci were seen progressively expand and coalesce, and gH displayed the expected vesicular accumulation before membrane incorporation. Paired with the unchanged focus counts yet smaller focus areas in CASP8-/- cells, this supports a role for caspase-8 in coordinating late maturation and egress steps rather than early nuclear replication.

The next step was the generation of a double recombinant virus that simultaneously encodes two different fluorescent proteins in the two viral proteins: the envelope glycoprotein (gH), which is likely to localize at the cellular membrane, and the capsid protein (VP26), which is expected to localize within the nuclear compartment. Following confirmation of the expected restriction pattern by BAC gel electrophoresis (Figure 23a), deep sequencing was performed to verify the correct insertion of the fluorescent tags (mScarlet and mNeonGreen) and to ensure that no undesired mutations had occurred in the significant genes of the viral cascade (Figure 23b).

a)

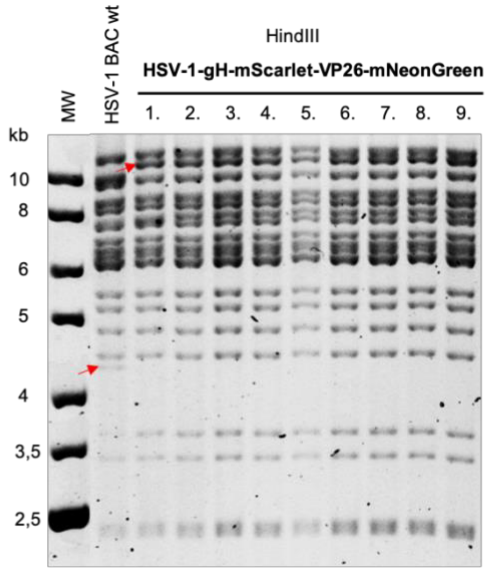
HindIII
HSV-1-gH-mScarlet-VP26-mNeonGreen
MW
HSV-1 BAC wt
1. 2. 3. 4. 5. 6. 7. 8. 9.
kb
10
8
6
5
4
3,5
2,5

b)

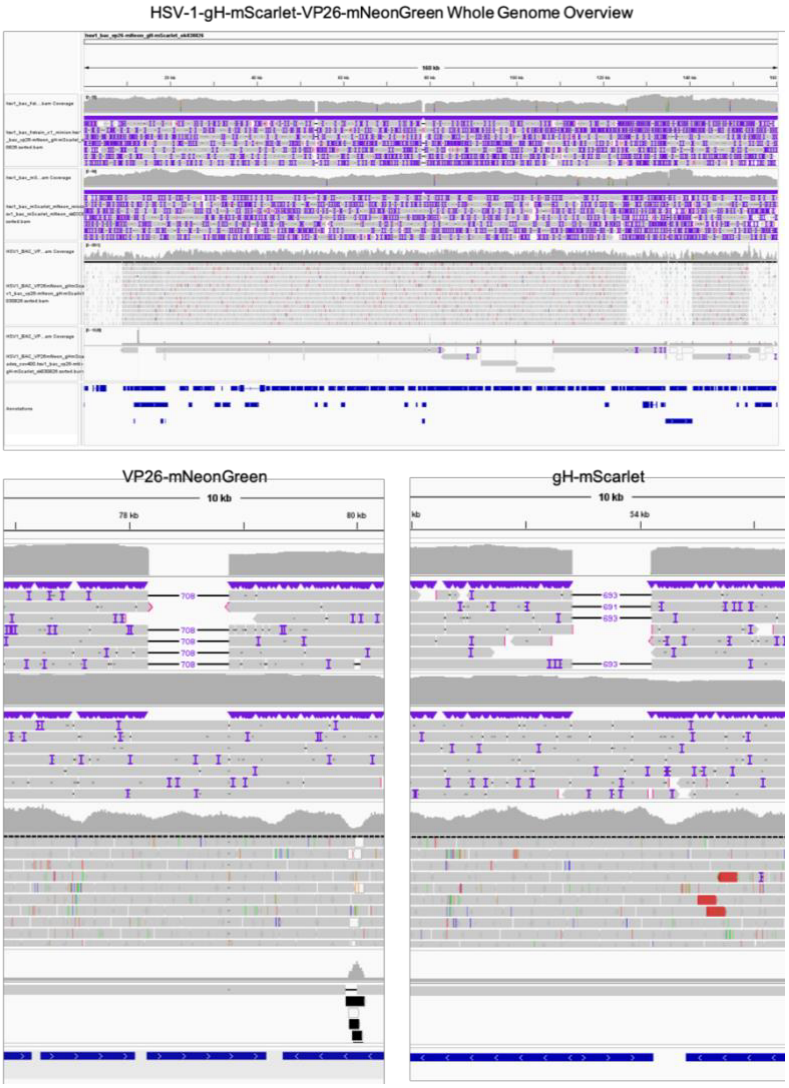
HSV-1-gH-mScarlet-VP26-mNeonGreen Whole Genome Overview
VP26-mNeonGreen
10 kb
gH-mScarlet
10 kb

Figure 23. *En passant* mutagenesis of HSV-1 gH-mScarlet VP26-mNeonGreen recombinant. (a) Second recombination. *En passant* cassette was excised by inducing the expression of I-SceI and the recombinase system. Resolved clones were selected against the presence of kanamycin resistance. BAC DNA was digested for 1 hour at 37 °C with HindIII. Lanes 1 and 2 represent HSV-1 BAC wild-type clones with HindIII restriction site at 4500 bp; lanes 3, 4, 5, 6, 7, 8, 9, 10, 11 represent HSV-1 gH-mScarlet VP26-mNeonGreen with HindIII restriction site over 10000 bp. The left panel displays molecular weights. (b) Analysis of Nanopore and Illumina sequencing of HSV-1 gH-mScarlet VP26-mNeonGreen, focusing on the gH and VP26 genes, resulted in frame. No mutations were found in coding genes.

To verify that BAC mutagenesis did not alter viral fitness, we characterized the HSV-1 BAC wild type, the single-tagged (gH-mScarlet, VP26-mNeonGreen) recombinants, and the double-tagged recombinant in VERO cells infected at MOI 1. Replication was quantified by a plaque reduction assay with titration of total viral particles at 9, 24, and 48 h.p.i., showing growth kinetics that overlapped with those of the BAC wild type (Figure 24b). As expected for envelope-tagged variants (Fan et al., 2018, p. 2), plaque morphology was altered, and microplaques were observed for gH-mScarlet and the double recombinant (Figure 24a) without impacting viral yields. Viral gene expressions were profiled by qPCR at 9, 18, 24, and 48 h.p.i. (ICP0, UL42, Us11; respectively α, β, and γ), revealing comparable temporal patterns across all viruses (Figures 24d, e, and f). Consistently, Western blotting of viral proteins representing α, β, and γ kinetic classes (ICP0, UL42, gD), with GAPDH as loading control, confirmed similar accumulation over time (Figure 24g). Finally, fluorescence microscopy of infected monolayers (MOI 1) revealed robust mScarlet and mNeonGreen signals, visually confirming the correct insertion and expression of both fluorescent tags (Figure 24c).

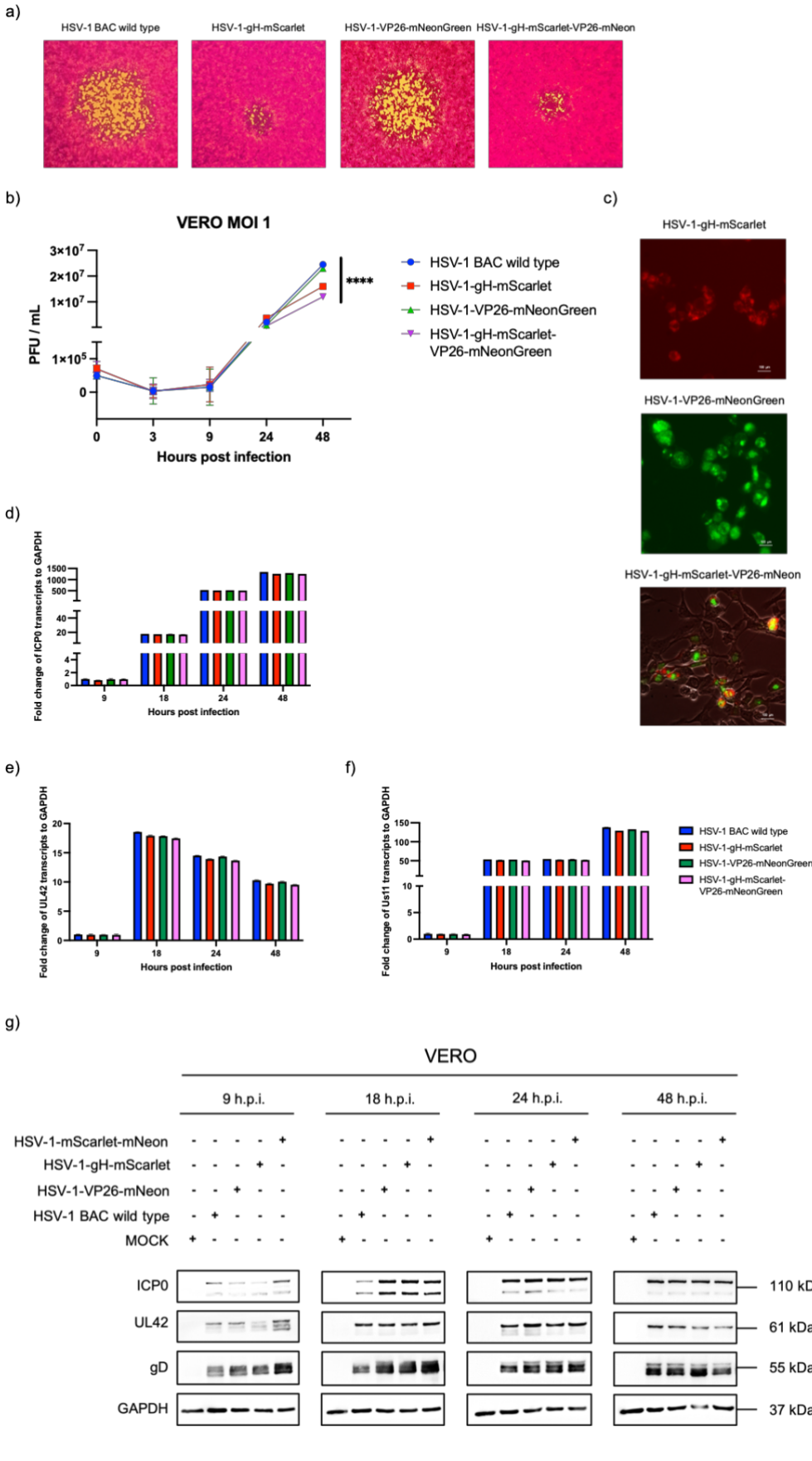
a)
HSV-1 BAC wild type
HSV-1-gH-mScarlet
HSV-1-VP26-mNeonGreen
HSV-1-gH-mScarlet-VP26-mNeon
b)
VERO MOI 1
PFU / mL
3×10^7
2×10^7
1×10^7
1×10^5
0
****
0
3
9
24
48
Hours post infection
HSV-1 BAC wild type
HSV-1-gH-mScarlet
HSV-1-VP26-mNeonGreen
HSV-1-gH-mScarlet-VP26-mNeonGreen
c)
HSV-1-gH-mScarlet
HSV-1-VP26-mNeonGreen
HSV-1-gH-mScarlet-VP26-mNeon
d)
Fold change of ICP0 transcripts to GAPDH
1500
1000
500
40
20
4
2
0
9
18
24
48
Hours post infection
e)
Fold change of UL42 transcripts to GAPDH
20
15
10
5
0
9
18
24
48
Hours post infection
f)
Fold change of Us11 transcripts to GAPDH
150
100
50
10
5
0
9
18
24
48
Hours post infection
HSV-1 BAC wild type
HSV-1-gH-mScarlet
HSV-1-VP26-mNeonGreen
HSV-1-gH-mScarlet-VP26-mNeonGreen
g)
VERO
9 h.p.i.
18 h.p.i.
24 h.p.i.
48 h.p.i.
HSV-1-mScarlet-mNeon
HSV-1-gH-mScarlet
HSV-1-VP26-mNeon
HSV-1 BAC wild type
MOCK
ICP0
UL42
gD
GAPDH
110 kDa
61 kDa
55 kDa
37 kDa

Figure 24. HSV-1 recombinants characterization. (a) (b) Evaluation of HSV-1 recombinants' replication efficiency in VERO cells by plaque reduction assay. VERO cells were infected with HSV-1 BAC wild type, HSV-1 gH-mScarlet, HSV-1 VP26-mNeonGreen, and HSV-1 gH-mScarlet-VP26-mNeonGreen viruses at MOI 1 and harvested at different times p.i. (a) Plaque morphological changes (microplaques) were displayed in HSV-1 gH-mScarlet and HSV-1 gH-mScarlet-VP26-mNeonGreen. (b) Samples were harvested at 9, 24, and 48 h.p.i., and viral yield was assessed by titration of total viral particles. Data are expressed as mean (± SD) of triplicates. (c) Panel shows the fluorescence emission in VERO cells infected at MOI 1 with HSV-1 recombinants. Scale bar is 100 μm. (d) (e) (f) qPCR time-course analysis of ICP0 (α), UL42 (β), and Us11 (γ) viral genes in VERO cells infected with HSV-1 BAC wild type, HSV-1 gH-mScarlet, HSV-1 VP26-mNeonGreen, and HSV-1 gH-mScarlet-VP26-mNeonGreen viruses at MOI 1, and collected at 9, 18, 24, and 48 h.p.i. Asterisks (*, **, ***, ****) indicate the significance of *p-values* less than 0.05, 0.01, 0.001, and 0,0001, respectively. (g) Western blot analysis of ICP0 (α), UL42 (β), and gD (γ) viral proteins in VERO cells infected or not with HSV-1 BAC wild type, HSV-1 gH-mScarlet, HSV-1 VP26-mNeonGreen, and HSV-1 gH-mScarlet-VP26-mNeonGreen viruses at MOI 1 and collected at 9, 18, 24, and 48 h.p.i. GAPDH was used as a loading control.

2.9. Discussion

Caspase-8 has long been recognized as a pivotal player in the extrinsic apoptosis pathway, yet growing evidence highlights its non-apoptotic functions during viral infections (Han et al., 2021; Musarra-Pizzo et al., 2022; Weinlich et al., 2017). In this study, we investigated the role of caspase-8 in the context of HSV-1 infection using CRISPR-Cas9-generated caspase-8-knockout THP-1 cells and a panel of wild-type and mutant HSV-1 strains. Our data collectively indicate that caspase-8 exerts a modulatory effect on intracellular viral replication, inflammatory gene expression, and signal transduction during HSV-1 infection in monocytic cells.

The absence of caspase-8 significantly enhanced the intracellular accumulation of HSV-1 gene products, as shown by increased levels of representative immediate-early (ICP0), early (UL42), and late (Us11 and gD) transcripts and proteins in $CASP8^{-/-}$ THP-1 cells compared to wild-type controls. Importantly, the same pattern was observed upon infection with both the wild-type virus and the Us11/Us12-deleted strain R3630, suggesting that caspase-8 limits viral gene expression independently of the presence of the Us11 immune-evasion gene. Despite the accumulation of HSV-1 proteins and transcripts, no pronounced differences were observed in cytopathic effects or in the total production of infectious virus across multiple time points and MOIs, indicating that caspase-8 does not markedly influence overall infectious yield under the tested conditions.

In parallel, we examined the impact of caspase-8 deficiency on inflammatory gene expression during HSV-1 infection. The lack of caspase-8 resulted in elevated expression of several chemokines, including CCL2, CCL4, CCL13, CXCL10, and CXCL11. These results indicate that chemokine transcription is not directly dependent on caspase-8, but instead that caspase-8 acts to moderate the magnitude of the inflammatory response. This finding aligns with previous reports suggesting that caspase-8 serves as a regulator capable of dampening inflammation through its interactions with other signaling proteins, including RIPK1 and FLIP (Fritsch et al., 2019; Kaiser et al., 2011).

To further explore the mechanism underlying chemokine overexpression, we analyzed the activation of the NF-κB pathway. Our findings demonstrated that caspase-8 deficiency correlates with increased NF-κB activity during HSV-1 infection, as evidenced by the upregulation of NF-κB transcripts in CASP8$^{-/-}$ THP-1 cells. However, this does not correspond to enhanced phosphorylation of the p65 subunit. These data support an indirect model whereby a greater intracellular viral burden (caused by the absence of caspase-8) amplifies PRR-driven transcription (including NF-κB-dependent chemokines), rather than a direct caspase-8-mediated suppression of chemokine signaling (Alandijany, 2019; Fritsch et al., 2019).

The critical role of NF-κB in chemokine induction was confirmed using THP-1 cells expressing a dominant-negative IκBα mutant. Blocking NF-κB nuclear translocation via this dominant-negative approach led to a marked reduction in the expression of CCL2, CCL4, CCL13, CXCL10, and CXCL11 during HSV-1 infection. This confirms that NF-κB is necessary for full activation of the chemokine response in this model, and positions caspase-8 as an upstream modulator of this axis.

Additionally, we aimed to determine whether active viral replication was necessary for chemokine induction or whether viral entry alone was sufficient for this purpose. By treating infected THP-1 cells with the DNA polymerase inhibitor phosphonoacetic acid (PAA), we demonstrated that active viral replication is required for the upregulation of all tested inflammatory mediators. The suppression of chemokine transcription by PAA treatment across multiple experimental replicates indicates that viral gene expression, rather than simply virion entry, drives inflammatory signaling during HSV-1 infection in monocytic cells.

We then investigated the potential link between caspase-8, RIPK1, and viral gene expression during HSV-1 infection. In wild-type THP-1 and HEp-2 cells, infection with HSV-1 led to increased levels of RIPK1 (protein in THP-1 cells; mRNA and protein in HEp-2), whereas this upregulation was diminished in CASP8$^{-/-}$ counterparts. RIPK1 protein and mRNA levels following infection with the Us11/Us12-deleted mutant R3630 were comparable to those induced by wild-type HSV-1 in both CASP8$^{+/+}$ and CASP8$^{-/-}$ cells, indicating that caspase-8 supports RIPK1 transcriptional induction, while Us11 deletion does not measurably alter

RIPK1 expression or stability relative compared to wild-type HSV-1 under the conditions tested.

Finally, to explore a possible role of caspase-8 in HSV-1 egress, we constructed two single- and a double-fluorescent recombinant viruses expressing a capsid protein (VP26) and an envelope glycoprotein (gH), each tagged with a distinct fluorescent marker. The imaging data of $CASP8^{+/+}$ and $CASP8^{-/-}$ HEp-2 cells infected with a fluorescent recombinant virus suggest that while caspase-8 deficiency does not alter the number of HSV-1 replication foci, it affects their spatial distribution and capsid localization, indicating a defect in viral egress rather than genome replication.

In conclusion, this study reveals that caspase-8 plays a multifaceted regulatory role during HSV-1 infection in the monocytic cell model. While its absence does not substantially affect viral release or cytopathic effects, caspase-8 deficiency leads to increased viral gene expression, enhanced NF-κB activity, and elevated chemokine production. These findings suggest that caspase-8 contributes to intrinsic antiviral defense by restraining viral replication and tempering inflammatory responses. Additionally, RIPK1 expression is disrupted in the absence of caspase-8, further supporting its involvement in coordinating immune signaling. Finally, the use of fluorescent recombinant HSV-1 viruses provided preliminary insights into alterations in virion maturation and trafficking, highlighting caspase-8 as a potential modulator of viral egress. Overall, our study underscores the significance of caspase-8 as a pivotal modulator in the interplay between viral infection and host innate immunity, with implications for understanding viral pathogenesis and immune regulation in myeloid cells.

Chapter III
Emerging HSV-1 Natural Therapies

In addition to the main project focused on HSV-1 infection of monocytic cells and the role of caspase-8 pathways, this thesis also includes a set of complementary studies investigating the antiviral activity of selected natural compounds and food by-products. These investigations, presented in Chapters III and IV, derive from independent and previously published works (Ingegneri et al., 2023 and Pennisi et al., 2023) and were pursued as side projects during the doctoral program. Accordingly, these chapters are more concise and primarily descriptive, with a focus on antiviral efficacy rather than in-depth mechanistic dissection. Their inclusion aims to broaden the scope of the thesis by highlighting alternative antiviral strategies against HSV-1, without detracting from the central experimental and conceptual framework developed in the preceding chapters.

HSV-1 treatment has long relied on compounds targeting viral DNA synthesis, primarily categorized into acyclic guanosine analogues (e.g., acyclovir, ganciclovir, famciclovir), acyclic nucleotide analogues (e.g., cidofovir), and pyrophosphate analogues (e.g., foscarnet) (Jiang et al., 2016; Reardon, 1989; Wagstaff and Bryson, 1994). Prolonged use, especially of acyclovir, has led to the emergence of resistant HSV-1 strains, primarily in immunocompromised hosts (Jiang et al., 2016), leaving TK-independent agents, such as cidofovir and foscarnet, as alternatives (Morfin and Thouvenot, 2003).

New strategies include natural compounds that have garnered substantial attention in biomedical research due to their therapeutic potential. Plant-derived polyphenols show antiviral effects (Bhaskarachary et al., 2015). For example, phenolics inhibit HSV-1 binding to glycosaminoglycan receptors (El-Toumy et al., 2018), quercetin blocks viral entry and suppresses NF-κB signaling, effective even against acyclovir-resistant strains (Hung et al., 2015), and curcumin downregulates immediate-early gene expression via interference with VP16-dependent transcription (Kutluay et al., 2008).

3.1. Antiviral properties of olive leaf extracts and oleuropein

Among Mediterranean medicinal plants, *Olea europaea L.* (olive tree) stands out for its multifaceted bioactivities, including antioxidant, anti-inflammatory, antimicrobial, and antiviral properties. These beneficial effects are primarily attributed to a rich profile of phenolic compounds, including oleuropein, hydroxytyrosol, and flavonoids (Romani et al., 2019; Zhang et al., 2022). Reactive oxygen species (ROS) contribute to DNA damage, lipid peroxidation, and protein oxidation, acting as major drivers of carcinogenesis and viral pathogenesis. As such, enhancing antioxidant defenses through phytocompounds can be a strategic approach to prevent oxidative stress-related diseases (Sharifi-Rad et al., 2020; Zahra et al., 2021). Notably, polyphenols from olive leaves can modulate redox signaling and gene expression in cancer cells (Rahman et al., 2006), while also exerting antiviral effects against various viruses, including HSV-1 (Ben-Amor et al., 2021a; Musarra-Pizzo et al., 2020).

3.2. Aim of the study

This study aimed to evaluate the antiviral activities of hydroethanolic leaf extracts from two varieties of *Olea europaea L.* (the cultivated *var. sativa* (OESA) and the wild *var. sylvestris* (OESY)) using HeLa cells as a cancer model. Additionally, the antiviral potential of the purified compound oleuropein was assessed, with a focus on its role in modulating intracellular signaling pathways during HSV-1 infection.
The rationale for this investigation is grounded in the increasing clinical relevance of antiviral drug resistance. Although nucleoside analogues such as acyclovir remain the first-line therapy for HSV infections, their extensive and prolonged use, particularly in patients with recurrent disease or immunocompromised conditions, has led to the emergence of resistant viral strains, most commonly associated with mutations in the viral thymidine kinase (UL23) or viral polymerase (UL30) genes (Jiang et al., 2016; Morfin and Thouvenot, 2003; Piret and Boivin, 2011). Resistance to acyclovir frequently confers cross-resistance to other thymidine kinase–dependent analogues, leaving limited therapeutic alternatives (Jiang et al.,

2016; Piret and Boivin, 2011). In this context, plant-derived natural products have attracted increasing attention as potential sources of antiviral agents with alternative mechanisms of action and lower toxicity compared with conventional nucleoside analogues (Bhaskarachary et al., 2015). Polyphenol-rich extracts and some compounds have been reported to interfere with multiple stages of the HSV-1 life cycle, and in some cases to retain activity against acyclovir-resistant strains (El-Toumy et al., 2018; Hung et al., 2015; Kutluay et al., 2008). Accordingly, these analyses were designed to characterize the antiviral potential of olive-derived extracts and oleuropein compound, with limited mechanistic exploration focused on selected intracellular signaling pathways previously implicated in HSV-1 replication.

3.3. Materials and Methods

Methods were performed as previously described in Ingegneri et al., 2023 and Pennisi et al., 2023 - MDPI, Basel, Switzerland, distributed under the terms of the Creative Commons Attribution (CC BY) license.

Cell lines and viruses

HeLa cells (human cervical epithelial carcinoma cell line) were cultured in RPMI 1640 medium (Gibco) supplemented with 10% (v/v) fetal calf serum (FCS) and 2 mM L-glutamine. VERO cells (American Type Culture Collection) were maintained in minimal essential medium (EMEM) supplemented with 6% fetal bovine serum (FBS) (Lonza). Both cell lines were incubated at 37 °C in a humidified atmosphere containing 5% CO_2. The HSV-1 prototype strain (F), employed for the in vitro experiments, was kindly provided by Dr. Bernard Roizman (University of Chicago). Viral stocks were propagated and titrated in VERO cells.

Plant materials

Olive leaf samples from *Olea europaea* var. *sativa* (OESA) and *Olea europaea* var. *sylvestris* (OESY) were obtained from the Chemlali SFAX variety in Tunisia. The leaves were collected under identical pedoclimatic conditions in October 2018. After harvesting, the olive leaves were air-dried at room temperature, and 100 g of dried material was extracted overnight with a 50:50 (v/v) water-ethanol solution under gentle stirring. The hydroethanolic extracts were then filtered through a cellulose filter, lyophilized, and stored at -80 °C until use. The extracts had been previously characterized using LC-DAD-ESI-MS analysis (Phenomenex) (Ben-Amor et al., 2021b). Oleuropein was isolated from fresh olive leaves (*Olea europaea* L.) by boiling 50 g of leaves in 250 mL of water for 2 h. The resulting solution was concentrated under vacuum, and the residue was extracted and purified using hot acetone (Bianco et al., 1999a, 1999b).

Cell proliferation assay

HeLa cell viability after treatment with OESA and OESY was evaluated using a CCK-8 assay (ab228554; Abcam) according to the manufacturer's instructions. The WST-8/CCK8 tetrazolium salt is metabolically reduced by cellular dehydrogenases, resulting in the formation of an orange formazan dye that is soluble in the culture medium. The intensity of the formazan signal, measured as absorbance at 460 nm, is directly proportional to the number of viable and metabolically active cells.

HeLa cells (2×10^4 cells/mL) or Vero cells (2.5×10^4 cells/mL) were seeded in 96-well microtiter plates and incubated at 37 °C in a 5% CO_2 atmosphere for 24 h. Subsequently, cells were treated with serial dilutions of OESA and OESY (0.1, 0.2, 0.4, 1, 5, 10, and 20 mg/mL) and oleuropein (25, 50, 100, 150, 200, 300, and 400 µg/mL), or of BSE (50, 100, 150, 200, and 300 µg/mL) for 72 h. After treatment, CCK-8 tetrazolium salt was added, and cells were incubated for an additional 4 hours under the same conditions. Absorbance was measured at 460 nm using a GloMax® Discover Microplate Reader (Promega), and cell viability was expressed as a percentage relative to untreated controls.

Plaque assay

Confluent monolayers of VERO cells were prepared in 24-well plates. Infected samples were subjected to three freeze-thaw cycles and subsequently diluted. Then, 100 µL of each dilution was used to infect the cell monolayers, which were incubated for 1 h at 37 °C under gentle agitation. After incubation, the viral inoculum was removed, and cell monolayers were overlaid with Dulbecco's Modified Eagle's Medium supplemented with 0.8% methylcellulose, with or without BSE at different concentrations (100, 150, and 200 µg/mL). DMSO (1%) was used as a control. Following a 72 h incubation, cells were stained with crystal violet and examined using an inverted microscope (Leica DMIL) for plaque detection. Data were collected in triplicate and expressed as mean ± standard deviation (SD) for each dilution.

Viral infection

HeLa cells (4×10^5 cells/well) and the virus were pre-treated with oleuropein at concentrations of 150 μg/mL, 300 μg/mL, and 400 μg/mL for 1 h at 37 °C. Subsequently, the pre-treated virus was used to infect the pre-treated cells at a multiplicity of infection (MOI) of 10. After 1 h of adsorption at 37 °C, the viral inoculum was replaced with fresh growth medium containing the respective concentrations of oleuropein. Acyclovir (50 μM) served as a positive control. Samples were collected 24 h post-infection.

Cell lysis and immunoblotting

Samples were lysed in 1X SDS sample buffer, sonicated, and then boiled for 5 minutes. Equal amounts of protein extracts were separated by SDS-PAGE, transferred onto membranes (Bio-Rad Life Science Research), and analyzed by immunoblotting (Pennisi et al., 2022). Protein bands were detected using the Immobilon Classico Western HRP substrate (Merck, Millipore Darmstadt). Densitometric quantification of band intensities was performed with ImageJ software. The intensity of each target protein was normalized to GAPDH levels and graphically represented using GraphPad Prism 6 software (GraphPad Software).

Antibodies

Anti-GAPDH (sc-32233), anti-HSV-1 UL42 (sc-53333), and anti-ICP0 (sc-56985) antibodies were obtained from Santa Cruz Biotechnology. Phospho-c-Jun (Ser73) (D47G9) and phospho-c-Fos (Ser32) (D82C12) antibodies were purchased from Cell Signaling Technology, while anti-PKR (phospho-T446, ab32036) was obtained from Abcam. The monoclonal anti-Us11 antibody was kindly provided by Professor Bernard Roizman. HRP-conjugated goat anti-mouse IgG secondary antibody was purchased from Millipore.

Viral DNA extraction and qPCR

Viral DNA was extracted using a phenol/chloroform solution and precipitated from the organic phase (EL-Aguel et al., 2022). The resulting DNA pellet was washed twice with 0.1 M trisodium citrate in 10% ethanol and subsequently dissolved in 8

mM NaOH. DNA concentration was determined by fluorometric analysis using the Qubit double-stranded DNA (dsDNA) High Sensitivity Assay Kit, following the manufacturer's instructions. Viral DNA amplification was performed using the TaqMan™ Universal Master Mix II (Applied Biosystems) in a 50 µL reaction mixture containing: TaqMan Universal Master Mix II, 100 ng of DNA, HSV-1 forward (10 µM) and reverse (10 µM) primers (Fw 5′-catcaccgacccggagagggac; Rev 5′-gggccaggcgcttgttggtgta), and a TaqMan probe (5 µM) (5′-6FAM-ccgccgaactgagcagacacccgcgc-TAMRA, where 6FAM is 6-carboxyfluorescein and TAMRA is 6-carboxytetramethylrhodamine). The amplification was carried out using the Applied Biosystems 7300 Real-Time PCR System under the following conditions: 10 minutes at 95°C, followed by 40 cycles of 60 seconds at 95°C, 30 seconds at 60°C, and 30 seconds at 72 °C. Absolute quantification by Real-Time PCR using the specific TaqMan probe was used to detect viral DNA. Viral load was determined from the threshold cycle (CT) based on a standard curve generated in parallel and expressed as the concentration in µg of DNA/µL.

RNA extraction and Reverse transcription

Total RNA was extracted using TRIzol® reagent (Life Technologies) following the manufacturer's instructions. For DNase treatment before cDNA synthesis, 1 µg of RNA was incubated at 37 °C for 2 h in a reaction containing 5 µL of 10X DNase I Buffer, 2 µL of recombinant RNase-free DNase I (10 U) (2270A, TaKaRa), and 20 U of RNase inhibitor (N251A, Promega)(EL-Aguel et al., 2022). Subsequently, 1 µg of total RNA was reverse-transcribed into cDNA using ReverTra Ace® qPCR RT Master Mix (FSQ-201, Toyobo, Kita-ku, Osaka, Japan) under the following conditions: 37 °C for 15 min, followed by 50 °C for 5 min, and 98 °C for 5 min.

Quantitative polymerase chain reaction (qPCR)

cDNA samples were used for quantitative Real-Time PCR performed on the Applied Biosystems 7300 Real-Time PCR System (Foster City, CA, USA). The thermal cycling conditions were as follows: initial incubation at 95 °C for 10 min, followed by 30 cycles of denaturation at 95 °C for 15 s, annealing at 60 °C for 35 s,

and elongation at 72 °C for 45 s. cDNA copy numbers were normalized to GAPDH expression levels. The primers used for RT-PCR are in Table 2.

Each quantitative Real-Time PCR experiment included a minus-reverse transcriptase control.

Quantification and statistical analysis

All chemical analyses and in vitro assays were performed in three independent experiments, each conducted in triplicate (n = 3), and the data are presented as the mean ± standard deviation (SD). Statistical analyses were conducted using GraphPad Prism 8 software (GraphPad Software, San Diego, CA, USA) with one-way analysis of variance (ANOVA) followed by Student-Newman-Keuls and Tukey's post hoc tests, using SigmaPlot 12.0 software (Systat Software Inc.). Statistical significance was indicated by asterisks (*, **, ***, ****), corresponding to *p-values* < 0.1, < 0.01, < 0.001, and < 0.0001, respectively. The half-maximal cytotoxic concentration (CC_{50}) and half-maximal effective concentration (EC_{50}) were determined using non-linear regression analysis.

3.4. Results

The following results have been previously published (Pennisi et al., 2023, MDPI, Basel, Switzerland), and are reproduced here under the terms of the Creative Commons Attribution (CC BY) license.

3.4.1. Antiviral activity of OESA and OESY

Cell viability assays demonstrated a dose-dependent cytotoxic effect, with OESY exhibiting higher cytotoxicity (IC_{50} = 0.848 mg/mL) compared to OESA (IC_{50} = 2.66 mg/mL). For subsequent experiments, subtoxic concentrations of 0.2 mg/mL and 0.4 mg/mL were selected (Figure 25).

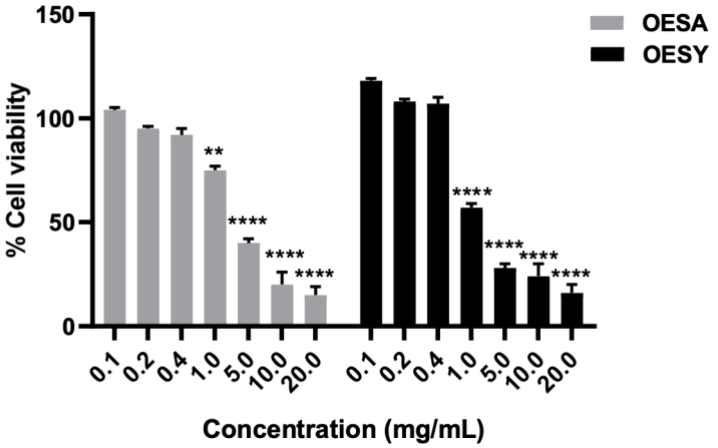

Figure 25. Cytotoxic effects of OESA and OESY on HeLa cells. The impact of OESA and OESY on cell growth was assessed using a CCK-8 assay. HeLa cells were treated with serial dilutions of OESA and OESY (0.1, 0.2, 0.4, 1, 5, 10, and 20 mg/mL) for 72 h, followed by incubation with CCK-8 tetrazolium salt solution in the dark for 4 h. Absorbance was measured at 460 nm, and cell viability was calculated relative to untreated controls. Data are presented as mean ± standard deviation (n = 3). ** $p < 0.01$, **** $p < 0.0001$. Reproduced from Pennisi et al., 2023, MDPI, Basel, Switzerland. This article is an open-access article distributed under the terms and conditions of the Creative Commons Attribution (CC BY) license.

To evaluate the antiviral activity of OESA and OESY, intracellular HSV-1 production was measured in HeLa cells after 24 h of treatment and infection. At 24 h post-infection, intracellular viral particles were released by freeze-thaw cycles, and titers were determined by PFU assays in Vero cells (Figure 26). Both extracts significantly reduced viral titers compared to untreated controls, indicating impaired HSV-1 replication. Furthermore, both extracts markedly decreased viral DNA levels (**$p < 0.01$) (Figure 27).

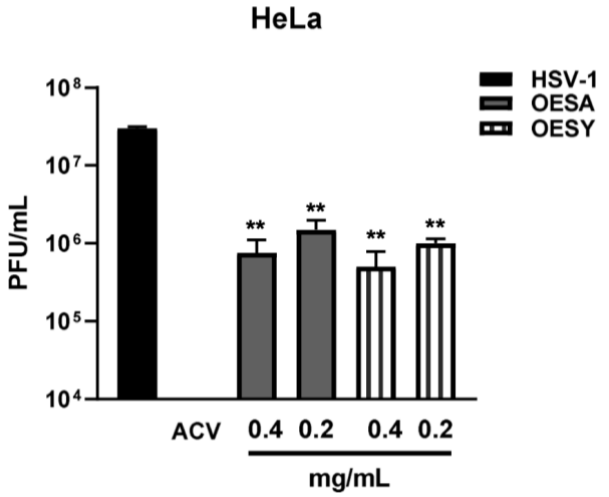

Figure 26. Evaluation of viral titers in HeLa cells after OESA and OESY treatment. HeLa cells (4×10^5 cells/well) and HSV-1 were pre-treated with OESA or OESY (0.2 and 0.4 mg/mL) for 1 h at 37 °C. Then, the pre-treated virus was used to infect pre-treated cells (MOI = 10). After 1 h, the inoculum was replaced with fresh medium containing the same extract concentrations, and acyclovir (50 µM) served as a positive control. At 24 hours post-infection, samples were collected, and intracellular viral particles were released through freeze-thaw cycles. Titer determination was performed by plaque assays on VERO cells. Data represent the mean ± SD of three independent experiments; ** $p < 0.01$ vs. HSV-1 +DMSO. Reproduced from Pennisi et al., 2023, MDPI, Basel, Switzerland. This article is an open-access article distributed under the terms and conditions of the Creative Commons Attribution (CC BY) license.

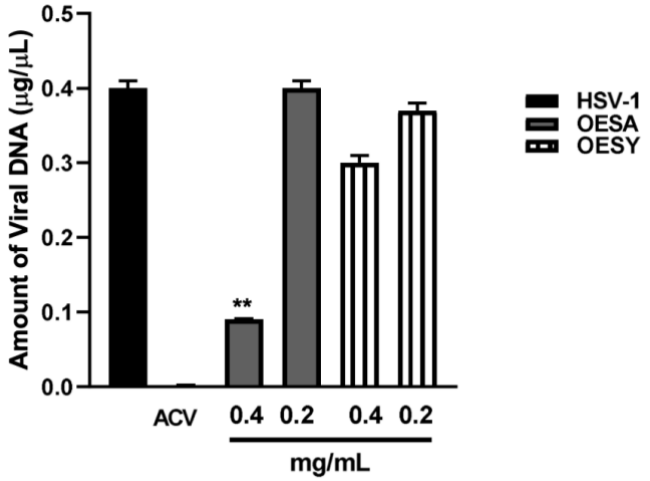

Figure 27. Absolute quantification of viral DNA. HeLa cells and HSV-1 were pre-treated with OESA or OESY (0.2 and 0.4 mg/mL) for 1 hour at 37 °C. Then, the pre-treated virus was used to infect pre-treated cells (MOI = 10). After 1 h, the inoculum was replaced with fresh medium containing the same extract concentrations, with acyclovir (50 µM) as a positive control. At 24 h post-infection, viral DNA was extracted and quantified by absolute Real-Time PCR using a TaqMan probe. Results are expressed as DNA concentration (µg/µL) and represent the mean ± SD of three independent experiments; ** $p < 0.01$ vs. HSV-1 +DMSO. Reproduced from Pennisi et al., 2023, MDPI, Basel, Switzerland. This article is an open-access article distributed under the terms and conditions of the Creative Commons Attribution (CC BY) license.

3.4.2. Antiviral activity of OESA and OESY compounds

Since OESA treatment showed a more substantial inhibitory effect on viral DNA accumulation compared to OESY, we investigated whether its polyphenol content, particularly oleuropein, was responsible for blocking HSV-1 replication. This choice was supported by phytochemical characterization (Ben-Amor et al., 2021b), which identified oleuropein as one of the most abundant compounds in OESA but absent in OESY. First, a viability assay was performed on HeLa cells treated with various oleuropein concentrations (25-400 µg/mL), demonstrating good tolerability across all tested doses (Figure 28). Non-toxic concentrations were then used to assess antiviral activity (Figure 29a). Oleuropein significantly reduced HSV-1 titers at 300 µg/mL and 400 µg/mL. Moreover, treatment with 300 µg/mL and 400 µg/mL of oleuropein led to a marked decrease in viral transcripts and proteins from all three phases of the replication cycle (Figure 29b, 29c). These findings suggest that oleuropein interferes with multiple stages of HSV-1 replication.

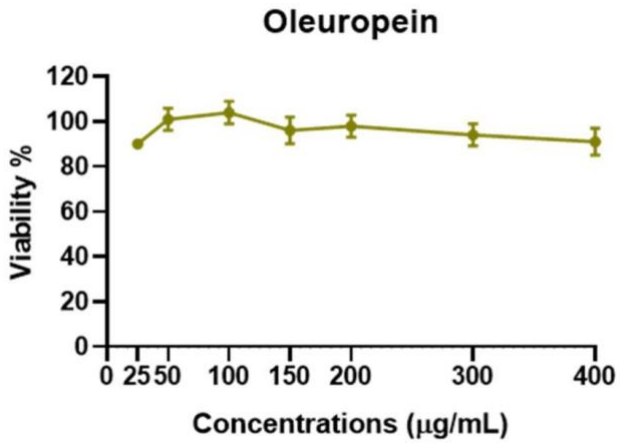

Figure. 28. Cytotoxicity assay of oleuropein. HeLa cells were treated with various concentrations of oleuropein (25, 50, 100, 150, 200, 300, and 400 µg/mL) for 72 hours. Cell viability was then assessed and expressed as a percentage relative to untreated controls. Data represent the mean ± SD of three independent experiments. Reproduced from Pennisi et al., 2023, MDPI, Basel, Switzerland. This article is an open-access article distributed under the terms and conditions of the Creative Commons Attribution (CC BY) license.

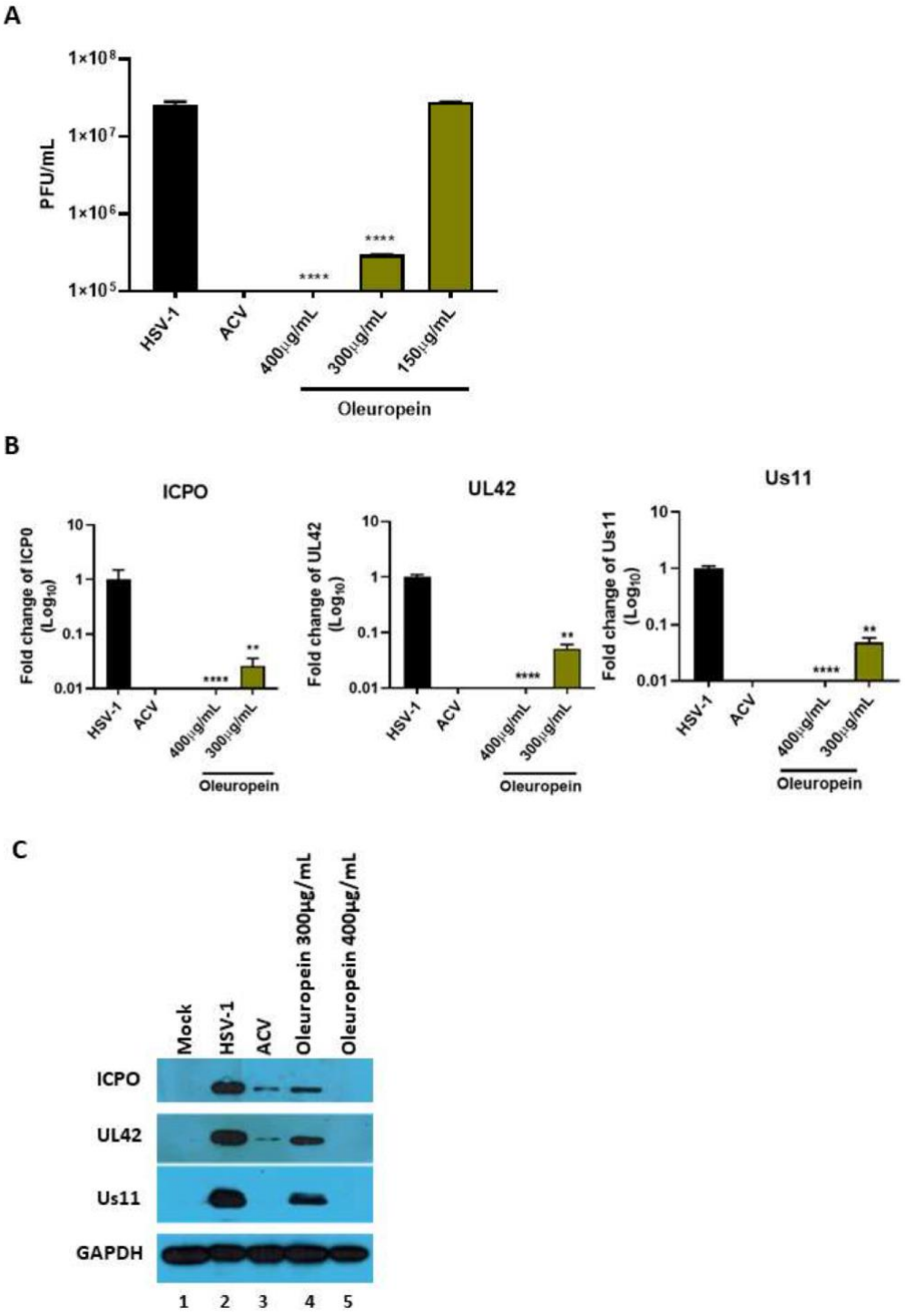

Figure 29. Antiviral activity of oleuropein. (A) HeLa cells (4×10^5 cells/well) and HSV-1 were pre-treated with oleuropein (150, 300, and 400 µg/mL) for 1 h at 37 °C, followed by infection at MOI = 10. After 1 h, the inoculum was replaced with fresh medium containing the same concentrations, and acyclovir (50 µM) served as a positive control. Viral titers were measured 24 h post-infection using plaque assays on Vero cells. (B) Relative quantification of viral transcripts (ICP0, UL42, Us11) was performed by Real-Time PCR using the ΔΔCt method, normalized to GAPDH. (C) Western blot analysis of ICP0, UL42, and Us11 proteins, with GAPDH as loading control. Data represent mean ± SD from at least three independent experiments. Statistical

significance was determined by one-way ANOVA (**$p < 0.01$, ****$p < 0.0001$ vs. HSV-1 + DMSO). Reproduced from Pennisi et al., 2023, MDPI, Basel, Switzerland. This article is an open-access article distributed under the terms and conditions of the Creative Commons Attribution (CC BY) license.

3.4.3. Oleuropein suppresses viral replication by modulating PKR-dependent c-Fos and c-Jun activation

The results show that oleuropein treatment after viral adsorption inhibits HSV-1 replication in HeLa cells. Since HSV-1 relies on host signaling pathways, the role of the double-stranded RNA-activated protein kinase R (PKR) was investigated. Although HSV encodes multiple proteins that interfere with PKR activation, the combined effects of these proteins on PKR activation remain unclear (Sciortino et al., 2013).

Western blot analysis (Figure 30a, 30b) revealed that oleuropein treatment (400 μg/mL) in infected cells increases phosphorylated PKR (p-PKR) levels. Given that PKR activation triggers downstream pathways, including the JNK pathway (Bonnet et al., 2000; Gal-Ben-Ari et al., 2019; McLean and Bachenheimer, 1999; Mundschau and Faller, 1995; Watanabe et al., 2013), the phosphorylation of AP-1 transcription factors c-Fos and c-Jun was also analyzed. Oleuropein treatment during HSV-1 infection enhanced p-PKR accumulation, correlating with increased phosphorylation of both c-Fos and c-Jun (Figures 30c and 30d).

These findings suggest that oleuropein promotes p-PKR activation, leading to enhanced phosphorylation of c-Fos and c-Jun, which may contribute to its antiviral mechanism against HSV-1 replication.

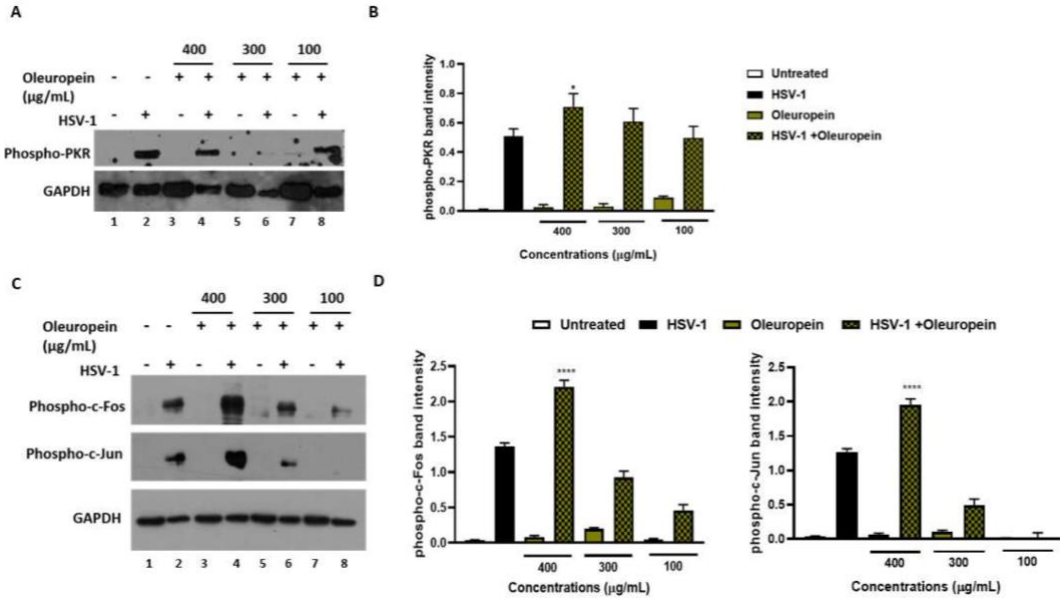

Figure 30. Activation of the innate antiviral response via phospho-PKR, phospho-c-Jun, and phospho-c-Fos in HSV-1-infected HeLa cells after oleuropein treatment. HeLa cells were infected at MOI = 10 and treated with oleuropein (100, 300, and 400 µg/mL) or left untreated. (A-C) Western blot analysis of phospho-PKR, phospho-c-Jun, and phospho-c-Fos expression; quantification of band intensities is shown in (B) and (D). Data represent mean ± SD from three independent experiments. Statistical significance was determined by one-way ANOVA (*$p < 0.1$, ****$p < 0.001$). Reproduced from Pennisi et al., 2023, MDPI, Basel, Switzerland. This article is an open-access article distributed under the terms and conditions of the Creative Commons Attribution (CC BY) license.

3.5. Discussion

This study demonstrates that both OESA and OESY exert antiviral activity in HeLa cells. OESA was more effective, likely due to its higher oleuropein content, a secoiridoid with recognized pharmacological value (Omar, 2010). In line with previous reports, olive leaf phenolics have been shown to increase endogenous antioxidant defenses (Senturk and Yıldız, 2018; Xie et al., 2022) and inhibit herpesvirus replication (Ben-Amor et al., 2021b; Cometa et al., 2022). Importantly, oleuropein not only reduced HSV-1 gene expression and protein synthesis but also stimulated p-PKR accumulation and downstream AP-1 transcription factors. This signaling pathway is crucial for the antiviral response and can modulate the expression of immune and inflammatory genes (Bonnet et al., 2000; Gal-Ben-Ari et al., 2019). While HSV-1 deploys multiple strategies to inhibit PKR (Langland et al., 2006), oleuropein appears to override such evasion mechanisms.

The relevance of these findings extends to the broader context of current antiviral therapy. Prolonged clinical use of nucleoside analogues, particularly acyclovir, has led to the emergence of drug-resistant HSV strains (Jiang et al., 2016; Morfin and Thouvenot, 2003; Piret and Boivin, 2011). In this scenario, natural compounds are increasingly considered of interest (Bhaskarachary et al., 2015). Although resistance was not directly addressed in the present study, the observed effects of oleuropein on host-driven antiviral responses support the rationale for further investigation of olive-derived compounds as complementary antiviral agents.

Moreover, given the susceptibility of cancer cells to viral manipulation and the potential role of persistent HSV-1 infection in oncogenesis (Kellogg et al., 2021; Sinha and Kundu, 2021), antiviral action of OESA and oleuropein may offer a preventive strategy to mitigate virus-associated cancer progression. However, further studies in additional cellular models and with deeper mechanistic resolution will be required to define their mode of action and translational relevance.

Chapter IV
Antiviral potential of food by-products

4.1. Antiviral properties of almond blanched skin (BS) and blanch water (BW)

Almonds (*Prunus dulcis* Mill. DA Webb) are among the most widely consumed nuts worldwide (Prgomet et al., 2017). They are a significant source of bioactive molecules, particularly polyphenols, which contribute to their health-promoting effects (Mandalari et al., 2010; Prgomet et al., 2017; Smeriglio et al., 2016).
Almond processing generates large amounts of by-products, including hulls, shells, blanched skin (BS), and blanch water (BW). While hulls and shells are often used in the energy or feed sectors, BS and BW are particularly interesting due to their high fibre and polyphenol content (Caltagirone et al., 2021; Garcia-Perez et al., 2021; Smeriglio et al., 2016). Previous research has highlighted the antioxidant, antimicrobial, and antiviral properties of almond by-products (Bisignano et al., 2017; Musarra-Pizzo et al., 2019). However, most studies did not specify the cultivar investigated, limiting the possibility of correlating chemical composition and biological activity with specific varieties.

4.2. Aim of the study

The present work aimed to investigate the antiviral activity of BS and BW obtained from three different Sicilian cultivars (*Fascionello*, *Pizzuta*, and *Tuono*).
This investigation was motivated by the growing limitations of current anti-HSV therapies. Although nucleoside analogues such as acyclovir remain the cornerstone of HSV treatment, their extensive and prolonged clinical use has contributed to the emergence of drug-resistant viral strains, particularly in immunocompromised patients. Resistance is most commonly associated with mutations affecting viral thymidine kinase or DNA polymerase activity, often resulting in cross-resistance to multiple thymidine kinase–dependent drugs and leaving limited therapeutic

alternatives (Jiang et al., 2016; Morfin and Thouvenot, 2003; Piret and Boivin, 2011). In this context, increasing attention has been directed toward natural bioactive compounds as potential sources of antiviral agents with alternative mechanisms of action compared with nucleoside analogues (Bhaskarachary et al., 2015).

Accordingly, this study was designed as a complementary and exploratory investigation to screen the antiviral activity of almond-processing by-products and to determine whether cultivar variability represents a discriminating factor influencing their chemical composition and associated biological activity. Thus, the work aimed to explore the potential valorization of almond-processing by-products, without extensive mechanistic investigation.

4.3. Materials and Methods

Methods were performed as previously described in Ingegneri et al., 2023 - MDPI, Basel, Switzerland, distributed under the terms of the Creative Commons Attribution (CC BY) license, and are outlined in section 3.3.

4.4. Results

The following results have been previously published (Ingegneri et al., 2023 - MDPI, Basel, Switzerland), and are reproduced here under the terms of the Creative Commons Attribution (CC BY) license.

4.4.1. Antiviral Activity of blanched skin extracts (BSE)

None of the extracts exhibited significant cytotoxicity, except at the highest concentration tested (300 µg/mL), which markedly reduced cell proliferation (Figure 31). Accordingly, the calculated CC_{50} values ranged between 300 and 800 µg/mL (Table 4).

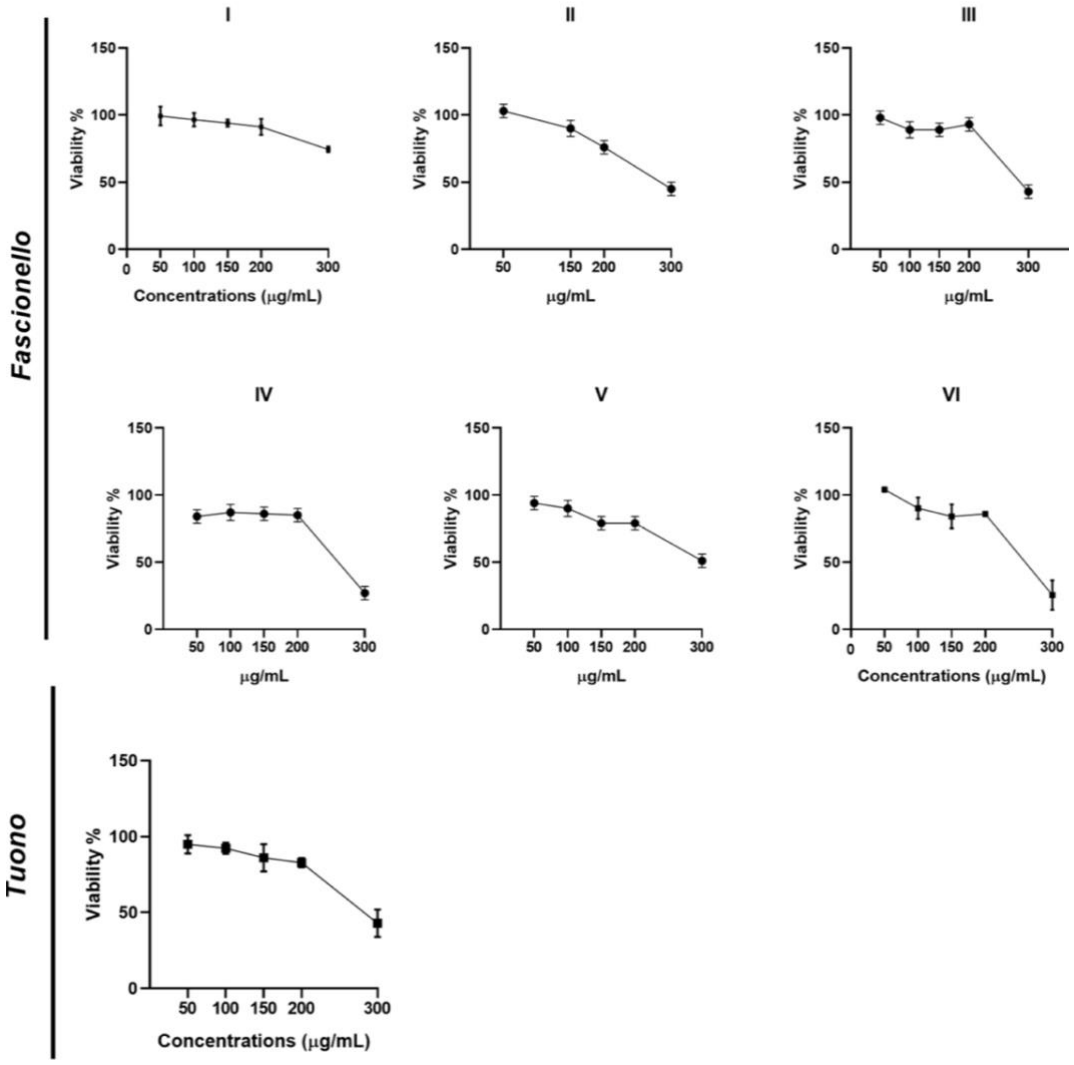

Figure 31. Cell viability assay of VERO cells treated with BSE from Fascionello and Tuono cultivars. Cells were exposed to increasing concentrations of BSE (50, 100, 150, 200, and 300 μg/mL) and collected after 72 h. Viability was expressed as a percentage of viable cells. Data are presented as mean ± SD of triplicate experiments. Roman numerals (I-VI) indicate different producers. Reproduced from Ingegneri et al., 2023, MDPI, Basel, Switzerland. This article is an open-access article distributed under the terms and conditions of the Creative Commons Attribution (CC BY) license.

Cultivar	CC_{50} (μg/mL)	EC_{50} (μg/mL)	SI
	Fascionello		
I	778.57	168.54	4.6
II	289.23	154.75	1.8
III	290.54	165.94	1.7
IV	290.22	155.03	1.8
V	290.19	144.90	2.0
VI	260.25	151.03	1.7
Tuono	290.91	186.52	1.6

CC_{50}: half maximal cytotoxic concentration; EC_{50}: half maximal effective concentration; SI: selectivity index, the ratio of EC_{50}/CC_{50}.

Table 4. Cytotoxicity (CC_{50}), antiviral activity (EC_{50}), and Selectivity index (SI) of blanched skin extracts (BSE). Reproduced from Ingegneri et al., 2023, MDPI, Basel, Switzerland. This article is an open-access article distributed under the terms and conditions of the Creative Commons Attribution (CC BY) license.

The antiviral susceptibility of HSV-1 was evaluated in vitro by plaque reduction assay, with the half-maximal effective concentration (EC_{50}) determined through non-linear regression analysis. Treatment with BSEs from Fascionello and Tuono cultivars resulted in a reduction in plaque number and induced morphological alterations compared to untreated infected controls. All BSEs displayed dose-dependent antiviral activity, with a significant inhibitory effect observed at a concentration of 200 μg/mL. Characteristic plaque morphology changes (Figure 32a, 32b) were evident in treated samples compared to HSV-1 controls.

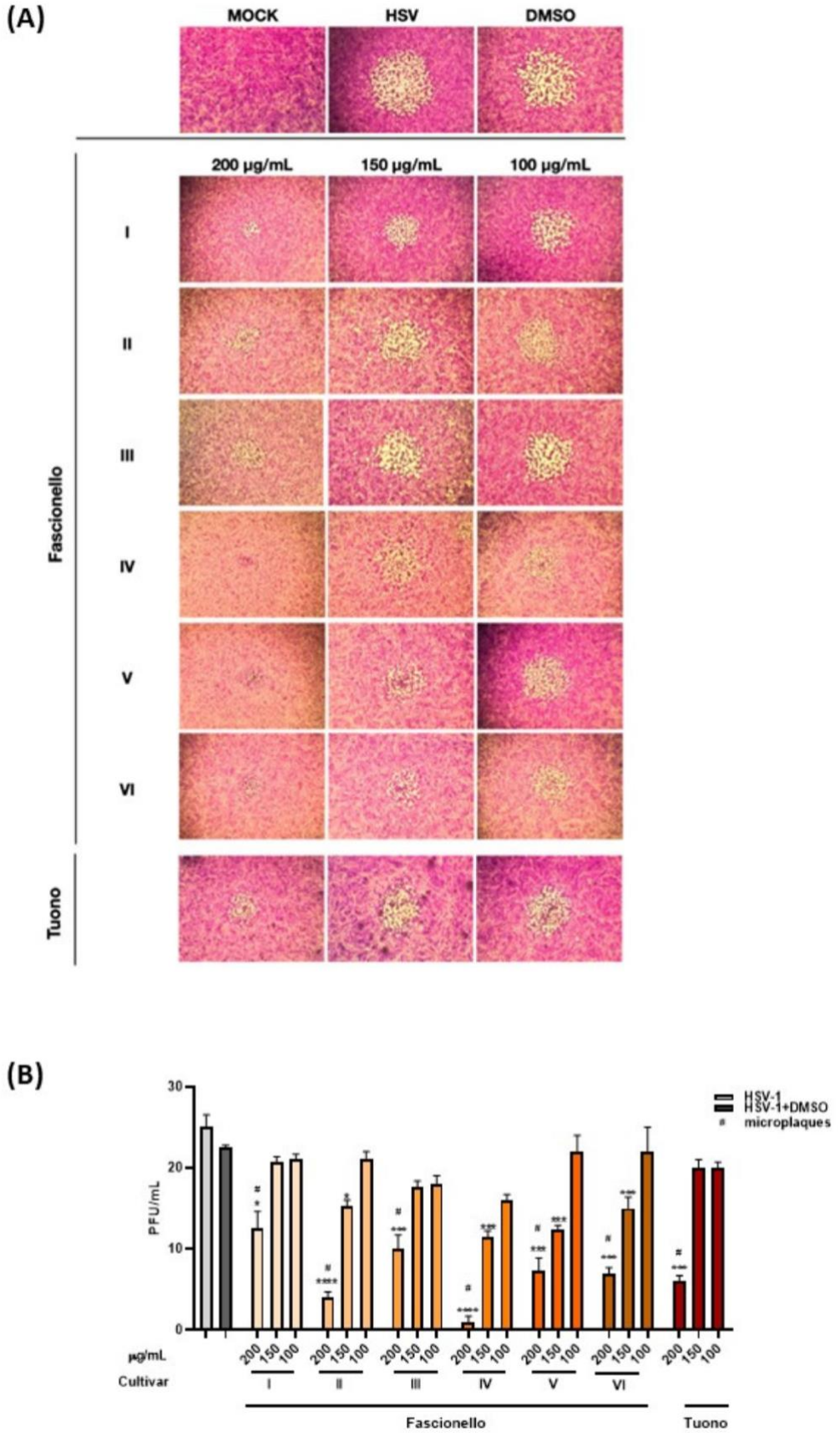
(A)
MOCK
HSV
DMSO
200 µg/mL
150 µg/mL
100 µg/mL
I
II
III
IV
V
VI
Fascionello
Tuono
(B)
HSV-1
HSV-1+DMSO
microplaques
PFU/mL
µg/mL
Cultivar
Fascionello
Tuono

Figure 32. Antiviral effect of BSE on HSV-1 replication assessed by plaque reduction assay. VERO cells were infected with HSV-1 for 1 hour and subsequently treated with BSE from Fascionello and Tuono cultivars at 100, 150, and 200 μg/mL. DMSO (1%) was used as a control. Data are presented as mean ± SD of triplicate experiments. # indicates micro-plaques. * $p < 0.05$, *** $p < 0.001$, **** $p < 0.0001$ vs. HSV-1 + DMSO. Roman numerals (I-VI) refer to different producers. Reproduced from Ingegneri et al., 2023, MDPI, Basel, Switzerland. This article is an open-access article distributed under the terms and conditions of the Creative Commons Attribution (CC BY) license.

4.5. Discussion

This study demonstrated that both BS and BW from Sicilian almond cultivars, rich in polyphenols, which contribute to their antioxidant properties, are associated with antiviral activity, in agreement with previous reports on almond by-products (Bisignano et al., 2017; Mandalari et al., 2013, 2010; Smeriglio et al., 2016). The limited differences observed among cultivars suggest that cultivar type is not the primary determinant of by-product composition. Rather, processing-related parameters, such as blanching conditions as well as environmental and pedoclimatic factors, are likely to exert a stronger influence on polyphenolic profiles and associated biological activity (Garrido et al., 2008; Hughey et al., 2012). The relevance of these findings can be placed within the documented limitations of current anti-HSV therapies (Jiang et al., 2016; Morfin and Thouvenot, 2003; Piret and Boivin, 2011). In this context, plant-derived extracts are of interest as antiviral agents (Bhaskarachary et al., 2015). Although resistance was not directly assessed in this study, the antiviral activity observed for BS and BW supports their further investigation as complementary sources of bioactive compounds. Overall, these results support the relevance of almond-processing by-products as a source of bioactive compounds with antiviral activity. Further studies will be required to better define their biological effects, optimize processing conditions, and evaluate their potential applicability. In conclusion, the recovery of BS and BW aligns with circular economy strategies, providing valuable nutraceutical potential. Their application in the food, pharmaceutical, and cosmetic industries could reduce waste and enhance sustainability.

Chapter V
Study Limitations and Outlook

5.1. Limitations of the study

The present thesis has some limitations that should be acknowledged. First, the mechanistic investigation of caspase-8 function during HSV-1 infection was primarily conducted in a monocytic cell line (THP-1), which, although widely used and relevant for studying innate immune responses, may not fully capture the complexity and heterogeneity of primary myeloid cells. In addition, while the use of caspase-8 knockout models allowed the identification of caspase-8 associated regulatory pathways, it does not exclude the contribution of compensatory mechanisms or parallel signaling routes that may influence viral replication and inflammatory responses. Furthermore, the analysis of NF-κB signaling was focused on transcriptional outputs and selected components of the canonical pathway, such as p65 activation, and did not comprehensively address post-translational regulatory mechanisms or non-canonical NF-κB signaling. Similarly, although alterations in virion trafficking and maturation were suggested by live-cell imaging, these observations remain preliminary and were not explored through detailed ultrastructural or biochemical approaches.

With respect to the studies on plant-derived antiviral compounds, these investigations were designed as complementary projects and were therefore focused on the evaluation of antiviral activity and selected host-response parameters, without extensive mechanistic dissection. A comprehensive mechanistic dissection of their antiviral activity, as well as validation in additional cellular systems, was beyond the scope of the present thesis.

5.2. Future perspectives

Future studies should aim to extend the mechanistic findings on caspase-8 to primary human monocytes, macrophages, and dendritic cells. A deeper characterization of caspase-8 interacting partners, including host and viral proteins, as well as of post-translational modifications that regulate its activity and cleavage, may provide further insight into how caspase-8 integrates antiviral, inflammatory, and pro-survival signaling pathways in myeloid cells. In addition, a more comprehensive analysis of NF-κB signaling, including non-canonical pathways and chromatin-level regulation of chemokine genes, such as histone modifications, could help clarify the molecular basis of caspase-8 mediated control of inflammatory outputs. The preliminary observations suggesting altered virion trafficking and maturation in caspase-8 deficient cells also justify further investigation using advanced imaging approaches and ultrastructural analyses to define the contribution of caspase-8 to late stages of the HSV-1 life cycle.

With regard to the studies on plant-derived antiviral compounds, future work should focus on clarifying their molecular targets within infected cells. From a translational perspective, the antiviral activity observed for olive-derived extracts, oleuropein, and almond by-products supports their potential role as sources of bioactive molecules rather than as immediate therapeutic agents. Further evaluation of bioavailability, stability, toxicity, and efficacy in more physiologically relevant models will be necessary to assess their applicability and possible integration with existing antiviral strategies.

An additional aspect that merits further investigation is the interpretation of antiviral and immunomodulatory effects across different cellular models. The variability observed between monocytic cells, epithelial cells, and cancer-derived cell lines highlights the strong influence of cellular context on HSV-1 replication, innate immune signaling, and responsiveness to antiviral compounds. Differences in permissiveness, basal inflammatory tone, metabolic state, and stress-response pathways are likely to contribute to model-specific outcomes. Systematic comparative studies will be essential to distinguish the specific effects of cell types from the intrinsic antiviral activity of compounds and to better define the biological relevance of these findings.

Conclusions

This thesis provides novel insights into the multifaceted role of caspase-8 during HSV-1 infection, with a primary focus on its function in monocytic cells as regulators of viral replication and host inflammatory responses. Through a combination of genetic, molecular, and imaging approaches, this work dissected the contribution of caspase-8 to the regulation of viral replication, host inflammatory signaling, and immune evasion mechanisms in monocytic cells, a relevant model of HSV-1-host interaction.

Our findings demonstrate that caspase-8 acts as a key modulator of HSV-1 gene expression and innate immune responses in THP-1 monocytic cells. Caspase-8 deficiency led to increased intracellular accumulation of viral proteins and transcripts, indicating a repressive role in viral gene expression. Despite this enhanced intracellular viral load, the loss of caspase-8 did not significantly alter cytopathic effects or extracellular viral release under our experimental conditions, suggesting a predominant impact on intracellular processes rather than virus spread. In parallel, caspase-8 was found to dampen the transcription of pro-inflammatory chemokines (CCL2, CCL4, CCL13, CXCL10, and CXCL11) by restraining NF-κB signaling. In CASP8-knockout cells, increased NF-κB activity was observed at the transcriptional level, although p65 phosphorylation was not markedly elevated. Chemokine overexpression was abrogated by a dominant-negative IκBα mutant and by pharmacological inhibition of viral DNA replication, indicating that NF-κB activity and active viral gene expression are both required for maximal inflammatory output. Together, these results define a regulatory axis in which caspase-8 tempers inflammation by limiting viral replication and modulating NF-κB-driven transcription.

In addition, RIPK1 was identified as a downstream effector of caspase-8 during infection. RIPK1 induction was impaired in CASP8-knockout cells, further supporting the view that caspase-8 coordinates pro-survival and inflammatory checkpoints at the interface of viral sensing and cellular defense. Live-cell imaging with fluorescent recombinant HSV-1 further revealed altered spatial distribution of

viral capsids in CASP8$^{-/-}$ cells, suggesting that caspase-8 may influence late stages of virion trafficking or egress.

In addition to the central mechanistic investigation, this thesis includes complementary studies evaluating the antiviral activity of selected natural compounds. Olive leaf extracts, particularly OESA with high oleuropein content, exhibited potent anti-HSV-1 effects by reducing viral gene expression and protein synthesis while activating PKR and downstream AP-1 transcription factors. These observations support the potential of oleuropein to counteract HSV-1 immune evasion strategies and to stimulate antiviral signaling pathways.

Similarly, almond blanching by-products (both skin and water) were characterized as rich sources of antioxidant polyphenols with measurable antiviral effects. These findings not only validate the biological activity of agricultural waste materials but also highlight their potential application in nutraceutical and pharmaceutical settings, aligning with the principles of a circular economy. These studies, conducted as independent and previously published research lines, broaden the scope of the thesis by examining alternative antiviral approaches without extensive mechanistic dissection.

In conclusion, the primary contribution of this work lies in defining caspase-8 as a central modulator of HSV-1 infection in monocytic cells, integrating control over viral replication, inflammatory signaling, and host survival pathways. The complementary findings on natural compounds, such as oleuropein and polyphenol-rich almond by-products, illustrates the potential of plant-derived compounds as promising candidates of bioactive molecules for the development of novel antiviral strategies, while reinforcing the central mechanistic framework developed in this thesis.

These findings advance our understanding of HSV-1-host interactions and open new avenues for therapeutic intervention based on both molecular immunology and natural product research.

References

Agelidis, A.M., Shukla, D., 2015. Cell Entry Mechanisms of HSV: What we have Learned in Recent Years. Future Virol. 10, 1145–1154. https://doi.org/10.2217/fvl.15.85

Ahmad, I., Wilson, D.W., 2020. HSV-1 Cytoplasmic Envelopment and Egress. Int. J. Mol. Sci. 21, 5969. https://doi.org/10.3390/ijms21175969

Alam, A., Cohen, L.Y., Aouad, S., Sékaly, R.-P., 1999. Early Activation of Caspases during T Lymphocyte Stimulation Results in Selective Substrate Cleavage in Nonapoptotic Cells. J. Exp. Med. 190, 1879–1890. https://doi.org/10.1084/jem.190.12.1879

Alandijany, T., 2019. Host Intrinsic and Innate Intracellular Immunity During Herpes Simplex Virus Type 1 (HSV-1) Infection. Front. Microbiol. 10, 2611. https://doi.org/10.3389/fmicb.2019.02611

Alvarado-Kristensson, M., Melander, F., Leandersson, K., Rönnstrand, L., Wernstedt, C., Andersson, T., 2004. p38-MAPK Signals Survival by Phosphorylation of Caspase-8 and Caspase-3 in Human Neutrophils. J. Exp. Med. 199, 449–458. https://doi.org/10.1084/jem.20031771

Amaral, M.P., Bortoluci, K.R., 2020. Caspase-8 and FADD: Where Cell Death and Inflammation Collide. Immunity 52, 890–892. https://doi.org/10.1016/j.immuni.2020.05.008

Arvin, A., Campadelli-Fiume, G., Mocarski, E., Moore, P.S., Roizman, B., Whitley, R., Yamanishi, K. (Eds.), 2007. Human Herpesviruses: Biology, Therapy, and Immunoprophylaxis. Cambridge University Press, Cambridge.

Aslani, A., Olsson, M., Elias, P., 2002. ATP-dependent Unwinding of a Minimal Origin of DNA Replication by the Origin-binding Protein and the Single-strand DNA-binding Protein ICP8 from Herpes Simplex Virus Type I *. J. Biol. Chem. 277, 41204–41212. https://doi.org/10.1074/jbc.M208270200

Aubert, M., Blaho, J.A., 2003. Viral oncoapoptosis of human tumor cells. Gene Ther. 10, 1437–1445. https://doi.org/10.1038/sj.gt.3302004

Aubert, M., Blaho, J.A., 1999. The Herpes Simplex Virus Type 1 Regulatory Protein ICP27 Is Required for the Prevention of Apoptosis in Infected Human Cells. J. Virol. 73, 2803–2813. https://doi.org/10.1128/jvi.73.4.2803-2813.1999

Azher, T.N., Yin, X.-T., Stuart, P.M., 2017. Understanding the Role of Chemokines and Cytokines in Experimental Models of Herpes Simplex Keratitis. J. Immunol. Res. 2017, 1–5. https://doi.org/10.1155/2017/7261980

Balachandran, S., Roberts, P.C., Kipperman, T., Bhalla, K.N., Compans, R.W., Archer, D.R., Barber, G.N., 2000. Alpha/Beta Interferons Potentiate Virus-Induced Apoptosis through Activation of the FADD/Caspase-8 Death Signaling Pathway. J. Virol. 74, 1513–1523. https://doi.org/10.1128/jvi.74.3.1513-1523.2000

Bell, B.D., Leverrier, S., Weist, B.M., Newton, R.H., Arechiga, A.F., Luhrs, K.A., Morrissette, N.S., Walsh, C.M., 2008. FADD and caspase-8 control the outcome of autophagic signaling in proliferating T cells. Proc. Natl. Acad. Sci. 105, 16677–16682. https://doi.org/10.1073/pnas.0808597105

Ben-Amor, I., Gargouri, B., Attia, H., Tlili, K., Kallel, I., Musarra-Pizzo, M., Sciortino, M.T., Pennisi, R., 2021a. In Vitro Anti-Epstein Barr Virus Activity of Olea europaea L. Leaf Extracts. Plants 10, 2445. https://doi.org/10.3390/plants10112445

Ben-Amor, I., Musarra-Pizzo, M., Smeriglio, A., D'Arrigo, M., Pennisi, R., Attia, H., Gargouri, B., Trombetta, D., Mandalari, G., Sciortino, M.T., 2021b. Phytochemical Characterization of Olea europea Leaf Extracts and Assessment of Their Anti-Microbial and Anti-HSV-1 Activity. Viruses 13, 1085. https://doi.org/10.3390/v13061085

Bhaskarachary, K., Naveena, N., Kalpagam, P., 2015. Potential Benefits of Plant Metabolites for Human Health. Indian J. Nutr. Diet.

Bianco, A.D., Muzzalupo, I., Piperno, A., Romeo, G., Uccella, N., 1999a. Bioactive Derivatives of Oleuropein from Olive Fruits. J. Agric. Food Chem. 47, 3531–3534. https://doi.org/10.1021/jf981240p

Bianco, A.D., Piperno, A., Romeo, G., Uccella, N., 1999b. NMR Experiments of Oleuropein Biomimetic Hydrolysis. J. Agric. Food Chem. 47, 3665–3668. https://doi.org/10.1021/jf981241h

Bidère, N., Snow, A.L., Sakai, K., Zheng, L., Lenardo, M.J., 2006. Caspase-8 Regulation by Direct Interaction with TRAF6 in T Cell Receptor-Induced NF-κB Activation. Curr. Biol. 16, 1666–1671. https://doi.org/10.1016/j.cub.2006.06.062

Bisignano, C., Mandalari, G., Smeriglio, A., Trombetta, D., Musarra Pizzo, M., Pennisi, R., Sciortino, M.T., 2017. Almond Skin Extracts Abrogate HSV-1 Replication by Blocking Virus Binding to the Cell. Viruses 9, 178. https://doi.org/10.3390/v9070178

Boehmer, P., Nimonkar, A., 2003. Herpes Virus Replication. IUBMB Life 55, 13–22. https://doi.org/10.1080/1521654031000070645

Boehmer, P.E., Dodson, M.S., Lehman, I.R., 1993. The herpes simplex virus type-1 origin binding protein. DNA helicase activity. J. Biol. Chem. 268, 1220–1225. https://doi.org/10.1016/S0021-9258(18)54063-1

Boehmer, P.E., Lehman, I.R., 1997. HERPES SIMPLEX VIRUS DNA REPLICATION. Annu. Rev. Biochem. 66, 347–384. https://doi.org/10.1146/annurev.biochem.66.1.347

Bonizzi, G., Karin, M., 2004. The two NF-κB activation pathways and their role in innate and adaptive immunity. Trends Immunol. 25, 280–288. https://doi.org/10.1016/j.it.2004.03.008

Bonnet, M.C., Weil, R., Dam, E., Hovanessian, A.G., Meurs, E.F., 2000. PKR Stimulates NF-κB Irrespective of Its Kinase Function by Interacting with the IκB Kinase Complex. Mol. Cell. Biol. 20, 4532–4542. https://doi.org/10.1128/MCB.20.13.4532-4542.2000

Bosnjak, L., Miranda-Saksena, M., Koelle, D.M., Boadle, R.A., Jones, C.A., Cunningham, A.L., 2005. Herpes Simplex Virus Infection of Human Dendritic Cells Induces Apoptosis and Allows Cross-Presentation via Uninfected Dendritic Cells1. J. Immunol. 174, 2220–2227. https://doi.org/10.4049/jimmunol.174.4.2220

Branco, F.J., Fraser, N.W., 2005. Herpes Simplex Virus Type 1 Latency-Associated Transcript Expression Protects Trigeminal Ganglion Neurons from Apoptosis. J. Virol. 79, 9019–9025. https://doi.org/10.1128/jvi.79.14.9019-9025.2005

Cai, Z., Jitkaew, S., Zhao, J., Chiang, H.-C., Choksi, S., Liu, J., Ward, Y., Wu, L., Liu, Z.-G., 2014. Plasma membrane translocation of trimerized MLKL protein is required for TNF-induced necroptosis. Nat. Cell Biol. 16, 55–65. https://doi.org/10.1038/ncb2883

Caltagirone, C., Peano, C., Sottile, F., 2021. Post-harvest Industrial Processes of Almond (Prunus dulcis L. Mill) in Sicily Influence the Nutraceutical Properties of By-Products at Harvest and During Storage. Front. Nutr. 8. https://doi.org/10.3389/fnut.2021.659378

Campbell, M.E.M., Palfreyman, J.W., Preston, C.M., 1984. Identification of herpes simplex virus DNA sequences which encode a trans-acting polypeptide responsible for stimulation of immediate early transcription. J. Mol. Biol. 180, 1–19. https://doi.org/10.1016/0022-2836(84)90427-3

Cao, L., Mu, W., 2021. Necrostatin-1 and necroptosis inhibition: Pathophysiology and therapeutic implications. Pharmacol. Res. 163, 105297. https://doi.org/10.1016/j.phrs.2020.105297

Cardone, G., Heymann, J.B., Cheng, N., Trus, B.L., Steven, A.C., 2012. Procapsid Assembly, Maturation, Nuclear Exit: Dynamic Steps in the Production of Infectious Herpesvirions, in: Rossmann, M.G., Rao, V.B. (Eds.), Viral Molecular Machines. Springer US, Boston, MA, pp. 423–439. https://doi.org/10.1007/978-1-4614-0980-9_19

Carpenter, D., Hsiang, C., Brown, D.J., Jin, L., Osorio, N., BenMohamed, L., Jones, C., Wechsler, S.L., 2007. Stable cell lines expressing high levels of the herpes simplex virus type 1 LAT are refractory to caspase 3 activation and DNA laddering following cold shock induced apoptosis. Virology 369, 12–18. https://doi.org/10.1016/j.virol.2007.07.023

Carr, D.J.J., Chodosh, J., Ash, J., Lane, T.E., 2003. Effect of Anti-CXCL10 Monoclonal Antibody on Herpes Simplex Virus Type 1 Keratitis and Retinal Infection. J. Virol. 77, 10037–10046. https://doi.org/10.1128/JVI.77.18.10037-10046.2003

Carr, D.J.J., Tomanek, L., 2006. Herpes Simplex Virus and the Chemokines That Mediate the Inflammation, in: Lane, T.E. (Ed.), Chemokines and Viral Infection, Current Topics in Microbiology and Immunology. Springer Berlin Heidelberg, Berlin, Heidelberg, pp. 47–65. https://doi.org/10.1007/978-3-540-33397-5_3

Cartier, A., Broberg, E., Komai, T., Henriksson, M., Masucci, M.G., 2003. The herpes simplex virus-1 Us3 protein kinase blocks CD8T cell lysis by preventing the cleavage of Bid by granzyme B. Cell Death Differ. 10, 1320–1328. https://doi.org/10.1038/sj.cdd.4401308

Cassady, K.A., Gross, M., 2002. The Herpes Simplex Virus Type 1 US11 Protein Interacts with Protein Kinase R in Infected Cells and Requires a 30-Amino-Acid Sequence Adjacent to a

Kinase Substrate Domain. J. Virol. 76, 2029–2035. https://doi.org/10.1128/jvi.76.5.2029-2035.2002
Cathelin, S., Rébé, C., Haddaoui, L., Simioni, N., Verdier, F., Fontenay, M., Launay, S., Mayeux, P., Solary, E., 2006. Identification of Proteins Cleaved Downstream of Caspase Activation in Monocytes Undergoing Macrophage Differentiation *. J. Biol. Chem. 281, 17779–17788. https://doi.org/10.1074/jbc.M600537200
Chang, D.W., 2003. Interdimer processing mechanism of procaspase-8 activation. EMBO J. 22, 4132–4142. https://doi.org/10.1093/emboj/cdg414
Chang, D.W., 2002. c-FLIPL is a dual function regulator for caspase-8 activation and CD95-mediated apoptosis. EMBO J. 21, 3704–3714. https://doi.org/10.1093/emboj/cdf356
Chaudhary, P.M., Eby, M.T., Jasmin, A., Kumar, A., Liu, L., Hood, L., 2000. Activation of the NF-κB pathway by Caspase 8 and its homologs. Oncogene 19, 4451–4460. https://doi.org/10.1038/sj.onc.1203812
Chi, J.H.I., Wilson, D.W., 2000. ATP-Dependent Localization of the Herpes Simplex Virus Capsid Protein VP26 to Sites of Procapsid Maturation. J. Virol. 74, 1468–1476. https://doi.org/10.1128/jvi.74.3.1468-1476.2000
Chou, J., Chen, J.J., Gross, M., Roizman, B., 1995. Association of a M(r) 90,000 phosphoprotein with protein kinase PKR in cells exhibiting enhanced phosphorylation of translation initiation factor eIF-2 alpha and premature shutoff of protein synthesis after infection with gamma 134.5- mutants of herpes simplex virus 1. Proc. Natl. Acad. Sci. 92, 10516–10520. https://doi.org/10.1073/pnas.92.23.10516
Chun, H.J., Zheng, L., Ahmad, M., Wang, J., Speirs, C.K., Siegel, R.M., Dale, J.K., Puck, J., Davis, J., Hall, C.G., Skoda-Smith, S., Atkinson, T.P., Straus, S.E., Lenardo, M.J., 2002. Pleiotropic defects in lymphocyte activation caused by caspase-8 mutations lead to human immunodeficiency. Nature 419, 395–399. https://doi.org/10.1038/nature01063
Cometa, S., Zannella, C., Busto, F., De Filippis, A., Franci, G., Galdiero, M., De Giglio, E., 2022. Natural Formulations Based on Olea europaea L. Fruit Extract for the Topical Treatment of HSV-1 Infections. Molecules 27, 4273. https://doi.org/10.3390/molecules27134273
Crute, J.J., Lehman, I.R., 1989. Herpes simplex-1 DNA polymerase. J. Biol. Chem. 264, 19266–19270. https://doi.org/10.1016/S0021-9258(19)47296-7
Cursi, S., Rufini, A., Stagni, V., Condò, I., Matafora, V., Bachi, A., Bonifazi, A.P., Coppola, L., Superti-Furga, G., Testi, R., Barilà, D., 2006. Src kinase phosphorylates Caspase-8 on Tyr380: a novel mechanism of apoptosis suppression. EMBO J. 25, 1895–1905. https://doi.org/10.1038/sj.emboj.7601085
Dash, S.P., Gupta, S., Sarangi, P.P., 2024. Monocytes and macrophages: Origin, homing, differentiation, and functionality during inflammation. Heliyon 10, e29686. https://doi.org/10.1016/j.heliyon.2024.e29686
Davison, M.D., Rixon, F.J., Davison, A.J., 1992. Identification of Genes Encoding Two Capsid Proteins (VP24 and VP26) of Herpes Simplex Virus Type 1. J. Gen. Virol. 73, 2709–2713. https://doi.org/10.1099/0022-1317-73-10-2709
De Oliveira, A.P., Glauser, D.L., Laimbacher, A.S., Strasser, R., Schraner, E.M., Wild, P., Ziegler, U., Breakefield, X.O., Ackermann, M., Fraefel, C., 2008. Live Visualization of Herpes Simplex Virus Type 1 Compartment Dynamics. J. Virol. 82, 4974–4990. https://doi.org/10.1128/JVI.02431-07
DeBiasi, R.L., Kleinschmidt-DeMasters, B.K., Richardson-Burns, S., Tyler, K.L., 2002. Central nervous system apoptosis in human herpes simplex virus and cytomegalovirus encephalitis. J. Infect. Dis. 186, 1547–1557. https://doi.org/10.1086/345375
Delbridge, A.R.D., Grabow, S., Strasser, A., Vaux, D.L., 2016. Thirty years of BCL-2: translating cell death discoveries into novel cancer therapies. Nat. Rev. Cancer 16, 99–109. https://doi.org/10.1038/nrc.2015.17
Denes, C.E., Miranda-Saksena, M., Cunningham, A.L., Diefenbach, R.J., 2018. Cytoskeletons in the Closet—Subversion in Alphaherpesvirus Infections. Viruses 10, 79. https://doi.org/10.3390/v10020079
Desai, P., DeLuca, N.A., Person, S., 1998. Herpes Simplex Virus Type 1 VP26 Is Not Essential for Replication in Cell Culture but Influences Production of Infectious Virus in the Nervous System of Infected Mice. Virology 247, 115–124. https://doi.org/10.1006/viro.1998.9230
Desai, P.J., Schaffer, P.A., Minson, A.C., 1988. Excretion of Non-infectious Virus Particles Lacking Glycoprotein H by a Temperature-sensitive Mutant of Herpes Simplex Virus Type 1:

Evidence that gH Is Essential for Virion Infectivity. J. Gen. Virol. 69, 1147–1156. https://doi.org/10.1099/0022-1317-69-6-1147
Diwaker, D., Wilson, D.W., 2019. Microtubule-Dependent Trafficking of Alphaherpesviruses in the Nervous System: The Ins and Outs. Viruses 11, 1165. https://doi.org/10.3390/v11121165
Dufour, F., Bertrand, L., Pearson, A., Grandvaux, N., Langelier, Y., 2011a. The Ribonucleotide Reductase R1 Subunits of Herpes Simplex Virus 1 and 2 Protect Cells against Poly(I · C)-Induced Apoptosis. J. Virol. 85, 8689–8701. https://doi.org/10.1128/jvi.00362-11
Dufour, F., Sasseville, A.M.-J., Chabaud, S., Massie, B., Siegel, R.M., Langelier, Y., 2011b. The ribonucleotide reductase R1 subunits of herpes simplex virus types 1 and 2 protect cells against TNFα- and FasL-induced apoptosis by interacting with caspase-8. Apoptosis 16, 256–271. https://doi.org/10.1007/s10495-010-0560-2
Eidson, K.M., Hobbs, W.E., Manning, B.J., Carlson, P., DeLuca, N.A., 2002. Expression of Herpes Simplex Virus ICP0 Inhibits the Induction of Interferon-Stimulated Genes by Viral Infection. J. Virol. 76, 2180–2191. https://doi.org/10.1128/jvi.76.5.2180-2191.2002
EL-Aguel, A., Pennisi, R., Smeriglio, A., Kallel, I., Tamburello, M.P., D'Arrigo, M., Barreca, D., Gargouri, A., Trombetta, D., Mandalari, G., Sciortino, M.T., 2022. Punica granatum Peel and Leaf Extracts as Promising Strategies for HSV-1 Treatment. Viruses 14, 2639. https://doi.org/10.3390/v14122639
Elemam, N., Talaat, I., Maghazachi, A., 2022. CXCL10 Chemokine: A Critical Player in RNA and DNA Viral Infections. Viruses 14, 2445. https://doi.org/10.3390/v14112445
Elias, P., Lehman, I.R., 1988. Interaction of origin binding protein with an origin of replication of herpes simplex virus 1. Proc. Natl. Acad. Sci. U. S. A. 85, 2959–2963. https://doi.org/10.1073/pnas.85.9.2959
Elias, P., O'Donnell, M.E., Mocarski, E.S., Lehman, I.R., 1986. A DNA binding protein specific for an origin of replication of herpes simplex virus type 1. Proc. Natl. Acad. Sci. U. S. A. 83, 6322–6326. https://doi.org/10.1073/pnas.83.17.6322
Ellermann-Eriksen, S., 2005. Macrophages and cytokines in the early defence against herpes simplex virus. Virol. J. 2, 59. https://doi.org/10.1186/1743-422X-2-59
Elliott, G., Mouzakitis, G., O'Hare, P., 1995. VP16 interacts via its activation domain with VP22, a tegument protein of herpes simplex virus, and is relocated to a novel macromolecular assembly in coexpressing cells. J. Virol. 69, 7932–7941. https://doi.org/10.1128/jvi.69.12.7932-7941.1995
El-Toumy, S.A., Salib, J.Y., El-Kashak, W.A., Marty, C., Bedoux, G., Bourgougnon, N., 2018. Antiviral effect of polyphenol rich plant extracts on herpes simplex virus type 1. Food Sci. Hum. Wellness 7, 91–101. https://doi.org/10.1016/j.fshw.2018.01.001
Fan, Q., Kopp, S.J., Byskosh, N.C., Connolly, S.A., Longnecker, R., 2018. Natural Selection of Glycoprotein B Mutations That Rescue the Small-Plaque Phenotype of a Fusion-Impaired Herpes Simplex Virus Mutant. mBio 9, e01948-18. https://doi.org/10.1128/mBio.01948-18
Farnsworth, A., Wisner, T.W., Webb, M., Roller, R., Cohen, G., Eisenberg, R., Johnson, D.C., 2007. Herpes simplex virus glycoproteins gB and gH function in fusion between the virion envelope and the outer nuclear membrane. Proc. Natl. Acad. Sci. U. S. A. 104, 10187–10192. https://doi.org/10.1073/pnas.0703790104
Fatahzadeh, M., Schwartz, R.A., 2007. Human herpes simplex virus infections: Epidemiology, pathogenesis, symptomatology, diagnosis, and management. J. Am. Acad. Dermatol. 57, 737–763. https://doi.org/10.1016/j.jaad.2007.06.027
Feltham, R., Vince, J.E., Lawlor, K.E., 2017. Caspase-8: not so silently deadly. Clin. Transl. Immunol. 6, e124. https://doi.org/10.1038/cti.2016.83
Feng, S., Yang, Y., Mei, Y., Ma, L., Zhu, D., Hoti, N., Castanares, M., Wu, M., 2007. Cleavage of RIP3 inactivates its caspase-independent apoptosis pathway by removal of kinase domain. Cell. Signal. 19, 2056–2067. https://doi.org/10.1016/j.cellsig.2007.05.016
Feoktistova, M., Geserick, P., Kellert, B., Dimitrova, D.P., Langlais, C., Hupe, M., Cain, K., MacFarlane, M., Häcker, G., Leverkus, M., 2011. cIAPs Block Ripoptosome Formation, a RIP1/Caspase-8 Containing Intracellular Cell Death Complex Differentially Regulated by cFLIP Isoforms. Mol. Cell 43, 449–463. https://doi.org/10.1016/j.molcel.2011.06.011
Fianco, G., Cenci, C., Barilà, D., 2016. Caspase-8 expression and its Src-dependent phosphorylation on Tyr380 promote cancer cell neoplastic transformation and resistance to anoikis. Exp. Cell Res. 347, 114–122. https://doi.org/10.1016/j.yexcr.2016.07.013

Fianco, G., Contadini, C., Ferri, A., Cirotti, C., Stagni, V., Barilà, D., 2018. Caspase-8: A Novel Target to Overcome Resistance to Chemotherapy in Glioblastoma. Int. J. Mol. Sci. 19, 3798. https://doi.org/10.3390/ijms19123798

Fianco, G., Mongiardi, M.P., Levi, A., De Luca, T., Desideri, M., Trisciuoglio, D., Del Bufalo, D., Cinà, I., Di Benedetto, A., Mottolese, M., Gentile, A., Centonze, D., Ferrè, F., Barilà, D., 2017. Caspase-8 contributes to angiogenesis and chemotherapy resistance in glioblastoma. eLife 6, e22593. https://doi.org/10.7554/eLife.22593

Finlay, D., Vuori, K., 2007. Novel Noncatalytic Role for Caspase-8 in Promoting Src-Mediated Adhesion and Erk Signaling in Neuroblastoma Cells. Cancer Res. 67, 11704–11711. https://doi.org/10.1158/0008-5472.CAN-07-1906

Fisher, G.H., Rosenberg, F.J., Straus, S.E., Dale, J.K., Middelton, L.A., Lin, A.Y., Strober, W., Lenardo, M.J., Puck, J.M., 1995. Dominant interfering fas gene mutations impair apoptosis in a human autoimmune lymphoproliferative syndrome. Cell 81, 935–946. https://doi.org/10.1016/0092-8674(95)90013-6

Forrester, A., Farrell, H., Wilkinson, G., Kaye, J., Davis-Poynter, N., Minson, T., 1992. Construction and properties of a mutant of herpes simplex virus type 1 with glycoprotein H coding sequences deleted. J. Virol. 66, 341–348. https://doi.org/10.1128/jvi.66.1.341-348.1992

Fritsch, M., Günther, S.D., Schwarzer, R., Albert, M.-C., Schorn, F., Werthenbach, J.P., Schiffmann, L.M., Stair, N., Stocks, H., Seeger, J.M., Lamkanfi, M., Krönke, M., Pasparakis, M., Kashkar, H., 2019. Caspase-8 is the molecular switch for apoptosis, necroptosis and pyroptosis. Nature 575, 683–687. https://doi.org/10.1038/s41586-019-1770-6

Fuchs, W., Granzow, H., Klupp, B.G., Kopp, M., Mettenleiter, T.C., 2002. The UL48 Tegument Protein of Pseudorabies Virus Is Critical for Intracytoplasmic Assembly of Infectious Virions. J. Virol. 76, 6729–6742. https://doi.org/10.1128/JVI.76.13.6729-6742.2002

Fuentes-Prior, P., Salvesen, G.S., 2004. The protein structures that shape caspase activity, specificity, activation and inhibition. Biochem. J. 384, 201–232. https://doi.org/10.1042/BJ20041142

Fulda, S., Küfer, M.U., Meyer, E., van Valen, F., Dockhorn-Dworniczak, B., Debatin, K.-M., 2001. Sensitization for death receptor- or drug-induced apoptosis by re-expression of caspase-8 through demethylation or gene transfer. Oncogene 20, 5865–5877. https://doi.org/10.1038/sj.onc.1204750

Fuller, A.O., Santos, R.E., Spear, P.G., 1989. Neutralizing antibodies specific for glycoprotein H of herpes simplex virus permit viral attachment to cells but prevent penetration. J. Virol. 63, 3435–3443. https://doi.org/10.1128/jvi.63.8.3435-3443.1989

Furuya, N., Yu, J., Byfield, M., Pattingre, S., Levine, B., 2005. The Evolutionarily Conserved Domain of Beclin 1 is Required for Vps34 Binding, Autophagy, and Tumor Suppressor Function. Autophagy 1, 46–52. https://doi.org/10.4161/auto.1.1.1542

Gal-Ben-Ari, S., Barrera, I., Ehrlich, M., Rosenblum, K., 2019. PKR: A Kinase to Remember. Front. Mol. Neurosci. 11. https://doi.org/10.3389/fnmol.2018.00480

Gallo, M.L., Dorsky, D.I., Crumpacker, C.S., Parris, D.S., 1989. The essential 65-kilodalton DNA-binding protein of herpes simplex virus stimulates the virus-encoded DNA polymerase. J. Virol. 63, 5023–5029. https://doi.org/10.1128/jvi.63.12.5023-5029.1989

Galluzzi, L., Brenner, C., Morselli, E., Touat, Z., Kroemer, G., 2008. Viral control of mitochondrial apoptosis. PLoS Pathog. 4, e1000018. https://doi.org/10.1371/journal.ppat.1000018

Garcia-Perez, P., Xiao, J., Munekata, P.E.S., Lorenzo, J.M., Barba, F.J., Rajoka, M.S.R., Barros, L., Mascoloti Sprea, R., Amaral, J.S., Prieto, M.A., Simal-Gandara, J., 2021. Revalorization of Almond By-Products for the Design of Novel Functional Foods: An Updated Review. Foods 10, 1823. https://doi.org/10.3390/foods10081823

Garrido, I., Monagas, M., Gómez-Cordovés, C., Bartolomé, B., 2008. Polyphenols and Antioxidant Properties of Almond Skins: Influence of Industrial Processing. J. Food Sci. 73, C106–C115. https://doi.org/10.1111/j.1750-3841.2007.00637.x

Gianni, T., Cerretani, A., DuBois, R., Salvioli, S., Blystone, S.S., Rey, F., Campadelli-Fiume, G., 2010. Herpes Simplex Virus Glycoproteins H/L Bind to Cells Independently of αVβ3 Integrin and Inhibit Virus Entry, and Their Constitutive Expression Restricts Infection. J. Virol. 84, 4013–4025. https://doi.org/10.1128/jvi.02502-09

Gibson, W., Marcy, A.I., Comolli, J.C., Lee, J., 1990. Identification of precursor to cytomegalovirus capsid assembly protein and evidence that processing results in loss of its carboxy-terminal end. J. Virol. 64, 1241–1249. https://doi.org/10.1128/jvi.64.3.1241-1249.1990

Gillet, L., May, J.S., Colaco, S., Stevenson, P.G., 2007. Glycoprotein L Disruption Reveals Two Functional Forms of the Murine Gammaherpesvirus 68 Glycoprotein H. J. Virol. 81, 280–291. https://doi.org/10.1128/JVI.01616-06

Gonzalvez, F., Lawrence, D., Yang, B., Yee, S., Pitti, R., Marsters, S., Pham, V.C., Stephan, J.-P., Lill, J., Ashkenazi, A., 2012. TRAF2 Sets a Threshold for Extrinsic Apoptosis by Tagging Caspase-8 with a Ubiquitin Shutoff Timer. Mol. Cell 48, 888–899. https://doi.org/10.1016/j.molcel.2012.09.031

Gorbalenya, A.E., Koonin, E.V., Donchenko, A.P., Blinov, V.M., 1989. Two related superfamilies of putative helicases involved in replication, recombination, repair and expression of DNA and RNA genomes. Nucleic Acids Res. 17, 4713–4730. https://doi.org/10.1093/nar/17.12.4713

Gottlieb, J., Marcy, A.I., Coen, D.M., Challberg, M.D., 1990. The herpes simplex virus type 1 UL42 gene product: a subunit of DNA polymerase that functions to increase processivity. J. Virol. 64, 5976–5987. https://doi.org/10.1128/jvi.64.12.5976-5987.1990

Guo, H., Omoto, S., Harris, P.A., Finger, J.N., Bertin, J., Gough, P.J., Kaiser, W.J., Mocarski, E.S., 2015. Herpes Simplex Virus Suppresses Necroptosis in Human Cells. Cell Host Microbe 17, 243–251. https://doi.org/10.1016/j.chom.2015.01.003

Haarr, L., Skulstad, S., 1994. The herpes simplex virus type 1 particle: structure and molecular functions. APMIS 102, 321–346. https://doi.org/10.1111/j.1699-0463.1994.tb04882.x

Häcker, G., 2000. The morphology of apoptosis. Cell Tissue Res. 301, 5–17. https://doi.org/10.1007/s004410000193

Han, J.-H., Park, J., Kang, T.-B., Lee, K.-H., 2021. Regulation of Caspase-8 Activity at the Crossroads of Pro-Inflammation and Anti-Inflammation. Int. J. Mol. Sci. 22, 3318. https://doi.org/10.3390/ijms22073318

Hayden, M.S., Ghosh, S., 2011. NF-κB in immunobiology. Cell Res. 21, 223–244. https://doi.org/10.1038/cr.2011.13

He, B., Gross, M., Roizman, B., 1997. The γ134.5 protein of herpes simplex virus 1 complexes with protein phosphatase 1α to dephosphorylate the α subunit of the eukaryotic translation initiation factor 2 and preclude the shutoff of protein synthesis by double-stranded RNA-activated protein kinase. Proc. Natl. Acad. Sci. 94, 843–848. https://doi.org/10.1073/pnas.94.3.843

He, X., Lehman, I.R., 2001. An initial ATP-independent step in the unwinding of a herpes simplex virus type I origin of replication by a complex of the viral origin-binding protein and single-strand DNA-binding protein. Proc. Natl. Acad. Sci. 98, 3024–3028. https://doi.org/10.1073/pnas.061028298

Henderson, G., Peng, W., Jin, L., Perng, G.-C., Nesburn, A.B., Wechsler, S.L., Jones, C., 2002. Regulation of caspase 8- and caspase 9-induced apoptosis by the herpes simplex virus type 1 latency-associated transcript. J. Neurovirol. 8 Suppl 2, 103–111. https://doi.org/10.1080/13550280290101085

Henry, C.M., Martin, S.J., 2017. Caspase-8 Acts in a Non-enzymatic Role as a Scaffold for Assembly of a Pro-inflammatory "FADDosome" Complex upon TRAIL Stimulation. Mol. Cell 65, 715-729.e5. https://doi.org/10.1016/j.molcel.2017.01.022

Hernandez, T.R., Lehman, I.R., 1990. Functional interaction between the herpes simplex-1 DNA polymerase and UL42 protein. J. Biol. Chem. 265, 11227–11232. https://doi.org/10.1016/S0021-9258(19)38580-1

Hill, A.B., Barnett, B.C., McMichael, A.J., McGeoch, D.J., 1994. HLA class I molecules are not transported to the cell surface in cells infected with herpes simplex virus types 1 and 2. J. Immunol. Baltim. Md 1950 152, 2736–2741.

Himeji, D., Horiuchi, T., Tsukamoto, H., Hayashi, K., Watanabe, T., Harada, M., 2002. Characterization of caspase-8L: a novel isoform of caspase-8 that behaves as an inhibitor of the caspase cascade. Blood 99, 4070–4078. https://doi.org/10.1182/blood.V99.11.4070

Hoffmann, J.C., Pappa, A., Krammer, P.H., Lavrik, I.N., 2009. A New C-Terminal Cleavage Product of Procaspase-8, p30, Defines an Alternative Pathway of Procaspase-8 Activation. Mol. Cell. Biol. 29, 4431–4440. https://doi.org/10.1128/MCB.02261-07

Homa, F.L., Brown, J.C., 1997. Capsid assembly and DNA packaging in herpes simplex virus. Rev. Med. Virol. 7, 107–122. https://doi.org/10.1002/(sici)1099-1654(199707)7:2%253C107::aid-rmv191%253E3.0.co;2-m

Honess, R.W., 1975. Regulation of herpesvirus macromolecular synthesis: sequential transition of polypeptide synthesis requires functional viral polypeptides. Proc. Natl. Acad. Sci. U. S. A. 72, 1276–1280. https://doi.org/10.1073/pnas.72.4.1276

Honess, R.W., Roizman, B., 1974. Regulation of Herpesvirus Macromolecular Synthesis I. Cascade Regulation of the Synthesis of Three Groups of Viral Proteins 1. J. Virol. 14, 8–19. https://doi.org/10.1128/jvi.14.1.8-19.1974

Honess, R.W., Watson, D.H., 1976. Herpes Simplex Virus Resistance and Sensitivity to Phosphunoacetic Acid.

Hong, T., Bae, S.-M., Song, G., Lim, W., 2024. Guide for generating single-cell–derived knockout clones in mammalian cell lines using the CRISPR/Cas9 system. Mol. Cells 47, 100087. https://doi.org/10.1016/j.mocell.2024.100087

Hopkins-Donaldson, S., Ziegler, A., Kurtz, S., Bigosch, C., Kandioler, D., Ludwig, C., Zangemeister-Wittke, U., Stahel, R., 2003. Silencing of death receptor and caspase-8 expression in small cell lung carcinoma cell lines and tumors by DNA methylation. Cell Death Differ. 10, 356–364. https://doi.org/10.1038/sj.cdd.4401157

Hou, W., Han, J., Lu, C., Goldstein, L.A., Rabinowich, H., 2010. Autophagic degradation of active caspase-8: A crosstalk mechanism between autophagy and apoptosis. Autophagy 6, 891–900. https://doi.org/10.4161/auto.6.7.13038

Hu, W.-H., Johnson, H., Shu, H.-B., 2000. Activation of NF-κB by FADD, Casper, and Caspase-8 *. J. Biol. Chem. 275, 10838–10844. https://doi.org/10.1074/jbc.275.15.10838

Huang, S., Okamoto, K., Yu, C., Sinicrope, F.A., 2013. p62/Sequestosome-1 Up-regulation Promotes ABT-263-induced Caspase-8 Aggregation/Activation on the Autophagosome. J. Biol. Chem. 288, 33654–33666. https://doi.org/10.1074/jbc.M113.518134

Hughey, C.A., Janusziewicz, R., Minardi, C.S., Phung, J., Huffman, B.A., Reyes, L., Wilcox, B.E., Prakash, A., 2012. Distribution of almond polyphenols in blanch water and skins as a function of blanching time and temperature. Food Chem. 131, 1165–1173. https://doi.org/10.1016/j.foodchem.2011.09.093

Hung, P.-Y., Ho, B.-C., Lee, S.-Y., Chang, S.-Y., Kao, C.-L., Lee, S.-S., Lee, C.-N., 2015. Houttuynia cordata Targets the Beginning Stage of Herpes Simplex Virus Infection. PLOS ONE 10, e0115475. https://doi.org/10.1371/journal.pone.0115475

Hutchinson, L., Browne, H., Wargent, V., Davis-Poynter, N., Primorac, S., Goldsmith, K., Minson, A.C., Johnson, D.C., 1992. A novel herpes simplex virus glycoprotein, gL, forms a complex with glycoprotein H (gH) and affects normal folding and surface expression of gH. J. Virol. 66, 2240–2250. https://doi.org/10.1128/jvi.66.4.2240-2250.1992

Ingegneri, M., Smeriglio, A., Rando, R., Gervasi, T., Tamburello, M.P., Ginestra, G., La Camera, E., Pennisi, R., Sciortino, M.T., Mandalari, G., Trombetta, D., 2023. Composition and Biological Properties of Blanched Skin and Blanch Water Belonging to Three Sicilian Almond Cultivars. Nutrients 15, 1545. https://doi.org/10.3390/nu15061545

Irmler, M., Thome, M., Hahne, M., Schneider, P., Hofmann, K., Steiner, V., Bodmer, J.-L., Schröter, M., Burns, K., Mattmann, C., Rimoldi, D., French, L.E., Tschopp, J., 1997. Inhibition of death receptor signals by cellular FLIP. Nature 388, 190–195. https://doi.org/10.1038/40657

Iwai, K., Fujita, H., Sasaki, Y., 2014. Linear ubiquitin chains: NF-κB signalling, cell death and beyond. Nat. Rev. Mol. Cell Biol. 15, 503–508. https://doi.org/10.1038/nrm3836

Jacquel, A., Benikhlef, N., Paggetti, J., Lalaoui, N., Guery, L., Dufour, E.K., Ciudad, M., Racoeur, C., Micheau, O., Delva, L., Droin, N., Solary, E., 2009. Colony-stimulating factor-1–induced oscillations in phosphatidylinositol-3 kinase/AKT are required for caspase activation in monocytes undergoing differentiation into macrophages. Blood 114, 3633–3641. https://doi.org/10.1182/blood-2009-03-208843

Jacquel, A., Obba, S., Boyer, L., Dufies, M., Robert, G., Gounon, P., Lemichez, E., Luciano, F., Solary, E., Auberger, P., 2012a. Autophagy is required for CSF-1–induced macrophagic differentiation and acquisition of phagocytic functions. Blood 119, 4527–4531. https://doi.org/10.1182/blood-2011-11-392167

Jacquel, A., Obba, S., Solary, E., Auberger, P., 2012b. Proper macrophagic differentiation requires both autophagy and caspase activation. Autophagy 8, 1141–1143. https://doi.org/10.4161/auto.20367

Javouhey, E., Gibert, B., Arrigo, A.-P., Diaz, J.J., Diaz-Latoud, C., 2008. Protection against heat and staurosporine mediated apoptosis by the HSV-1 US11 protein. Virology 376, 31–41. https://doi.org/10.1016/j.virol.2008.02.031

Jerome, K.R., Fox, R., Chen, Z., Sears, A.E., Lee, H., Corey, L., 1999. Herpes Simplex Virus Inhibits Apoptosis through the Action of Two Genes, Us5 and Us3. J. Virol. 73, 8950–8957. https://doi.org/10.1128/jvi.73.11.8950-8957.1999

Jiang, M., Qi, L., Li, L., Wu, Y., Song, D., Li, Y., 2021. Caspase-8: A key protein of cross-talk signal way in " PANOPTOSIS " in cancer. Int. J. Cancer 149, 1408–1420. https://doi.org/10.1002/ijc.33698

Jiang, Y.-C., Feng, H., Lin, Y.-C., Guo, X.-R., 2016. New strategies against drug resistance to herpes simplex virus. Int. J. Oral Sci. 8, 1–6. https://doi.org/10.1038/ijos.2016.3

Jin, Z., Li, Y., Pitti, R., Lawrence, D., Pham, V.C., Lill, J.R., Ashkenazi, A., 2009. Cullin3-Based Polyubiquitination and p62-Dependent Aggregation of Caspase-8 Mediate Extrinsic Apoptosis Signaling. Cell 137, 721–735. https://doi.org/10.1016/j.cell.2009.03.015

Johnson, K.E., Song, B., Knipe, D.M., 2008. Role for herpes simplex virus 1 ICP27 in the inhibition of type I interferon signaling. Virology 374, 487–494. https://doi.org/10.1016/j.virol.2008.01.001

Kaiser, W.J., Upton, J.W., Long, A.B., Livingston-Rosanoff, D., Daley-Bauer, L.P., Hakem, R., Caspary, T., Mocarski, E.S., 2011. RIP3 mediates the embryonic lethality of caspase-8-deficient mice. Nature 471, 368–372. https://doi.org/10.1038/nature09857

Kalamvoki, M., Deschamps, T., 2016. Extracellular vesicles during Herpes Simplex Virus type 1 infection: an inquire. Virol. J. 13, 63. https://doi.org/10.1186/s12985-016-0518-2

Kallenberger, S.M., Beaudouin, J., Claus, J., Fischer, C., Sorger, P.K., Legewie, S., Eils, R., 2014. Intra- and Interdimeric Caspase-8 Self-Cleavage Controls Strength and Timing of CD95-Induced Apoptosis. Sci. Signal. 7. https://doi.org/10.1126/scisignal.2004738

Kang, T.-B., Ben-Moshe, T., Varfolomeev, E.E., Pewzner-Jung, Y., Yogev, N., Jurewicz, A., Waisman, A., Brenner, O., Haffner, R., Gustafsson, E., Ramakrishnan, P., Lapidot, T., Wallach, D., 2004. Caspase-8 Serves Both Apoptotic and Nonapoptotic Roles1. J. Immunol. 173, 2976–2984. https://doi.org/10.4049/jimmunol.173.5.2976

Kang, T.-B., Yang, S.-H., Toth, B., Kovalenko, A., Wallach, D., 2013. Caspase-8 Blocks Kinase RIPK3-Mediated Activation of the NLRP3 Inflammasome. Immunity 38, 27–40. https://doi.org/10.1016/j.immuni.2012.09.015

Kather, A., Raftery, M.J., Devi-Rao, G., Lippmann, J., Giese, T., Sandri-Goldin, R.M., Schönrich, G., 2010. Herpes Simplex Virus Type 1 (HSV-1)-Induced Apoptosis in Human Dendritic Cells as a Result of Downregulation of Cellular FLICE-Inhibitory Protein and Reduced Expression of HSV-1 Antiapoptotic Latency-Associated Transcript Sequences. J. Virol. 84, 1034–1046. https://doi.org/10.1128/JVI.01409-09

Keller, N., Ozmadenci, D., Ichim, G., Stupack, D., 2018. Caspase-8 function, and phosphorylation, in cell migration. Semin. Cell Dev. Biol. 82, 105–117. https://doi.org/10.1016/j.semcdb.2018.01.009

Kellogg, C., Kouznetsova, V.L., Tsigelny, I.F., 2021. Implications of viral infection in cancer development. Biochim. Biophys. Acta BBA - Rev. Cancer 1876, 188622. https://doi.org/10.1016/j.bbcan.2021.188622

Kennedy, N.J., Kataoka, T., Tschopp, J., Budd, R.C., 1999. Caspase Activation Is Required for T Cell Proliferation. J. Exp. Med. 190, 1891–1896. https://doi.org/10.1084/jem.190.12.1891

Kim, H.S., Lee, J.W., Soung, Y.H., Park, W.S., Kim, S.Y., Lee, J.H., Park, J.Y., Cho, Y.G., Kim, C.J., Jeong, S.W., Nam, S.W., Kim, S.H., Lee, J.Y., Yoo, N.J., Lee, S.H., 2003. Inactivating mutations of caspase-8 gene in colorectal carcinomas. Gastroenterology 125, 708–715. https://doi.org/10.1016/S0016-5085(03)01059-X

Kinzler, E.R., Compton, T., 2005. Characterization of Human Cytomegalovirus Glycoprotein-Induced Cell-Cell Fusion. J. Virol. 79, 7827–7837. https://doi.org/10.1128/JVI.79.12.7827-7837.2005

Knipe, D.M., Howley, P., 2013. Fields Virology, 6th ed.

Knopf, K.-W., 1979. Properties of Herpes Simplex Virus DNA Polymerase and Characterization of Its Associated Exonuclease Activity. Eur. J. Biochem. 98, 231–244. https://doi.org/10.1111/j.1432-1033.1979.tb13181.x

Koyama, A.H., Adachi, A., 1997. Induction of apoptosis by herpes simplex virus type 1. J. Gen. Virol. 78, 2909–2912. https://doi.org/10.1099/0022-1317-78-11-2909

Kramer, T., Enquist, L.W., 2013. Directional Spread of Alphaherpesviruses in the Nervous System. Viruses 5, 678–707. https://doi.org/10.3390/v5020678

Krueger, A., Schmitz, I., Baumann, S., Krammer, P.H., Kirchhoff, S., 2001. Cellular FLICE-inhibitory Protein Splice Variants Inhibit Different Steps of Caspase-8 Activation at the CD95 Death-inducing Signaling Complex. J. Biol. Chem. 276, 20633–20640. https://doi.org/10.1074/jbc.M101780200

Kutluay, S.B., Doroghazi, J., Roemer, M.E., Triezenberg, S.J., 2008. Curcumin inhibits herpes simplex virus immediate-early gene expression by a mechanism independent of p300/CBP histone acetyltransferase activity. Virology 373, 239–247. https://doi.org/10.1016/j.virol.2007.11.028

LaBoissière, S., O'Hare, P., 2000. Analysis of HCF, the Cellular Cofactor of VP16, in Herpes Simplex Virus-Infected Cells. J. Virol. 74, 99–109. https://doi.org/10.1128/jvi.74.1.99-109.2000

Lai, C., Wang, K., Zhao, Z., Zhang, L., Gu, H., Yang, P., Wang, X., 2017. C-C Motif Chemokine Ligand 2 (CCL2) Mediates Acute Lung Injury Induced by Lethal Influenza H7N9 Virus. Front. Microbiol. 8, 587. https://doi.org/10.3389/fmicb.2017.00587

Langland, J.O., Cameron, J.M., Heck, M.C., Jancovich, J.K., Jacobs, B.L., 2006. Inhibition of PKR by RNA and DNA viruses. Virus Res., Translational Control During Virus Infections 119, 100–110. https://doi.org/10.1016/j.virusres.2005.10.014

Lee, C.K., Knipe, D.M., 1985. An immunoassay for the study of DNA-binding activities of herpes simplex virus protein ICP8. J. Virol. 54, 731–738. https://doi.org/10.1128/jvi.54.3.731-738.1985

Lee, S.S.K., Lehman, I.R., 1999. The Interaction of Herpes Simplex Type 1 Virus Origin-binding Protein (UL9 Protein) with Box I, the High Affinity Element of the Viral Origin of DNA Replication *. J. Biol. Chem. 274, 18613–18617. https://doi.org/10.1074/jbc.274.26.18613

Lehman, I.R., Boehmer, P.E., 1999. Replication of Herpes Simplex Virus DNA *. J. Biol. Chem. 274, 28059–28062. https://doi.org/10.1074/jbc.274.40.28059

Levy, D.E., García-Sastre, A., 2001. The virus battles: IFN induction of the antiviral state and mechanisms of viral evasion. Cytokine Growth Factor Rev. 12, 143–156. https://doi.org/10.1016/S1359-6101(00)00027-7

Lin, R., Noyce, R.S., Collins, S.E., Everett, R.D., Mossman, K.L., 2004. The herpes simplex virus ICP0 RING finger domain inhibits IRF3- and IRF7-mediated activation of interferon-stimulated genes. J. Virol. 78, 1675–1684. https://doi.org/10.1128/jvi.78.4.1675-1684.2004

Liu, F.Y., Roizman, B., 1991. The herpes simplex virus 1 gene encoding a protease also contains within its coding domain the gene encoding the more abundant substrate. J. Virol. 65, 5149–5156. https://doi.org/10.1128/jvi.65.10.5149-5156.1991

Liu, T., Zhang, L., Joo, D., Sun, S.-C., 2017. NF-κB signaling in inflammation. Signal Transduct. Target. Ther. 2, 17023. https://doi.org/10.1038/sigtrans.2017.23

Locksley, R.M., Killeen, N., Lenardo, M.J., 2001. The TNF and TNF Receptor Superfamilies: Integrating Mammalian Biology. Cell 104, 487–501. https://doi.org/10.1016/S0092-8674(01)00237-9

Lussignol, M., Queval, C., Bernet-Camard, M.-F., Cotte-Laffitte, J., Beau, I., Codogno, P., Esclatine, A., 2013. The Herpes Simplex Virus 1 Us11 Protein Inhibits Autophagy through Its Interaction with the Protein Kinase PKR. J. Virol. 87, 859–871. https://doi.org/10.1128/jvi.01158-12

Makhov, A.M., Boehmer, P.E., Lehman, R.I., Griffith, J.D., 1996. Visualization of the Unwinding of Long DNA Chains by the Herpes Simplex Virus Type 1 UL9 Protein and ICP8. J. Mol. Biol. 258, 789–799. https://doi.org/10.1006/jmbi.1996.0287

Mandalari, G., Arcoraci, T., Martorana, M., Bisignano, C., Rizza, L., Bonina, F.P., Trombetta, D., Tomaino, A., 2013. Antioxidant and Photoprotective Effects of Blanch Water, a Byproduct of the Almond Processing Industry. Molecules 18, 12426–12440. https://doi.org/10.3390/molecules181012426

Mandalari, G., Bisignano, C., D'Arrigo, M., Ginestra, G., Arena, A., Tomaino, A., Wickham, M.S.J., 2010. Antimicrobial potential of polyphenols extracted from almond skins. Lett. Appl. Microbiol. 51, 83–89. https://doi.org/10.1111/j.1472-765X.2010.02862.x

Marino-Merlo, F., Klett, A., Papaianni, E., Drago, S.F.A., Macchi, B., Rincón, M.G., Andreola, F., Serafino, A., Grelli, S., Mastino, A., Borner, C., 2023. Caspase-8 is required for HSV-1-

induced apoptosis and promotes effective viral particle release via autophagy inhibition. Cell Death Differ. 30, 885–896. https://doi.org/10.1038/s41418-022-01084-y

Marino-Merlo, F., Papaianni, E., Medici, M.A., Macchi, B., Grelli, S., Mosca, C., Borner, C., Mastino, A., 2016. HSV-1-induced activation of NF-κB protects U937 monocytic cells against both virus replication and apoptosis. Cell Death Dis. 7, e2354–e2354. https://doi.org/10.1038/cddis.2016.250

Martinez-Martin, N., Viejo-Borbolla, A., Martín, R., Blanco, S., Benovic, J.L., Thelen, M., Alcamí, A., 2015. Herpes simplex virus enhances chemokine function through modulation of receptor trafficking and oligomerization. Nat. Commun. 6, 6163. https://doi.org/10.1038/ncomms7163

Mastino, A., Sciortino, M.T., Medici, M.A., Perri, D., Ammendolia, M.G., Grelli, S., Amici, C., Pernice, A., Guglielmino, S., 1997. Herpes simplex virus 2 causes apoptotic infection in monocytoid cells. Cell Death Differ. 4, 629–638. https://doi.org/10.1038/sj.cdd.4400289

Matsushima, K., Terashima, Y., Toda, E., Shand, F., Ueha, S., 2011. Chemokines in inflammatory and immune diseases. Inflamm. Regen. 31, 11–22. https://doi.org/10.2492/inflammregen.31.11

Matthess, Y., Raab, M., Sanhaji, M., Lavrik, I.N., Strebhardt, K., 2010. Cdk1/Cyclin B1 Controls Fas-Mediated Apoptosis by Regulating Caspase-8 Activity. Mol. Cell. Biol. 30, 5726–5740. https://doi.org/10.1128/MCB.00731-10

Mauri, D.N., Ebner, R., Montgomery, R.I., Kochel, K.D., Cheung, T.C., Yu, G.L., Ruben, S., Murphy, M., Eisenberg, R.J., Cohen, G.H., Spear, P.G., Ware, C.F., 1998. LIGHT, a new member of the TNF superfamily, and lymphotoxin alpha are ligands for herpesvirus entry mediator. Immunity 8, 21–30. https://doi.org/10.1016/s1074-7613(00)80455-0

McKimmie, C., Michlmayr, D., 2014. Role of CXCL10 in central nervous system inflammation. Int. J. Interferon Cytokine Mediat. Res. 1. https://doi.org/10.2147/IJICMR.S35953

McLauchlan, J., Addison, C., Craigie, M.C., Rixon, F.J., 1992. Noninfectious L-particles supply functions which can facilitate infection by HSV-1. Virology 190, 682–688. https://doi.org/10.1016/0042-6822(92)90906-6

McLean, T.I., Bachenheimer, S.L., 1999. Activation of cJUN N-Terminal Kinase by Herpes Simplex Virus Type 1 Enhances Viral Replication. J. Virol. 73, 8415–8426. https://doi.org/10.1128/jvi.73.10.8415-8426.1999

McNabb, D.S., Courtney, R.J., 1992. Identification and characterization of the herpes simplex virus type 1 virion protein encoded by the UL35 open reading frame. J. Virol. 66, 2653–2663. https://doi.org/10.1128/jvi.66.5.2653-2663.1992

McNamee, E.E., Taylor, T.J., Knipe, D.M., 2000. A Dominant-Negative Herpesvirus Protein Inhibits Intranuclear Targeting of Viral Proteins: Effects on DNA Replication and Late Gene Expression. J. Virol. 74, 10122–10131. https://doi.org/10.1128/jvi.74.21.10122-10131.2000

Medici, M.A., Sciortino, M.T., Perri, D., Amici, C., Avitabile, E., Ciotti, M., Balestrieri, E., De Smaele, E., Franzoso, G., Mastino, A., 2003. Protection by Herpes Simplex Virus Glycoprotein D against Fas-mediated Apoptosis. J. Biol. Chem. 278, 36059–36067. https://doi.org/10.1074/jbc.M306198200

Melchjorsen, J., Pedersen, F.S., Mogensen, S.C., Paludan, S.R., 2002. Herpes Simplex Virus Selectively Induces Expression of the CC Chemokine RANTES/CCL5 in Macrophages through a Mechanism Dependent on PKR and ICP0. J. Virol. 76, 2780–2788. https://doi.org/10.1128/JVI.76.6.2780-2788.2002

Melchjorsen, J., Rintahaka, J., Søby, S., Horan, K.A., Poltajainen, A., Østergaard, L., Paludan, S.R., Matikainen, S., 2010. Early Innate Recognition of Herpes Simplex Virus in Human Primary Macrophages Is Mediated via the MDA5/MAVS-Dependent and MDA5/MAVS/RNA Polymerase III-Independent Pathways. J. Virol. 84, 11350–11358. https://doi.org/10.1128/JVI.01106-10

Melchjorsen, J., Sirén, J., Julkunen, I., Paludan, S.R., Matikainen, S., 2006. Induction of cytokine expression by herpes simplex virus in human monocyte-derived macrophages and dendritic cells is dependent on virus replication and is counteracted by ICP27 targeting NF-κB and IRF-3. J. Gen. Virol. 87, 1099–1108. https://doi.org/10.1099/vir.0.81541-0

Micheau, O., Thome, M., Schneider, P., Holler, N., Tschopp, J., Nicholson, D.W., Briand, C., Grütter, M.G., 2002. The Long Form of FLIP Is an Activator of Caspase-8 at the Fas Death-

inducing Signaling Complex. J. Biol. Chem. 277, 45162–45171. https://doi.org/10.1074/jbc.M206882200
Micheau, O., Tschopp, J., 2003. Induction of TNF Receptor I-Mediated Apoptosis via Two Sequential Signaling Complexes. Cell 114, 181–190. https://doi.org/10.1016/S0092-8674(03)00521-X
Miles, D., Athmanathan, S., Thakur, A., Willcox, M., 2003. A novel apoptotic interaction between HSV-1 and human corneal epithelial cells. Curr. Eye Res. 26, 165–174. https://doi.org/10.1076/ceyr.26.3.165.14899
Miller, M.A., Karacay, B., Zhu, X., O'Dorisio, M.S., Sandler, A.D., 2006. Caspase 8L, a novel inhibitory isoform of caspase 8, is associated with undifferentiated neuroblastoma. Apoptosis 11, 15–24. https://doi.org/10.1007/s10495-005-3258-0
Mocarski, E.S., Upton, J.W., Kaiser, W.J., 2015. Viral infection and the evolution of caspase 8-regulated apoptotic and necrotic death pathways. Nat. Rev. Immunol. 12, 79–88. https://doi.org/10.1038/nri3131
Mohr, A., Zwacka, R.M., Jarmy, G., Büneker, C., Schrezenmeier, H., Döhner, K., Beltinger, C., Wiesneth, M., Debatin, K.-M., Stahnke, K., 2005. Caspase-8L expression protects CD34+ hematopoietic progenitor cells and leukemic cells from CD95-mediated apoptosis. Oncogene 24, 2421–2429. https://doi.org/10.1038/sj.onc.1208432
Montgomery, R.I., Warner, M.S., Lum, B.J., Spear, P.G., 1996. Herpes simplex virus-1 entry into cells mediated by a novel member of the TNF/NGF receptor family. Cell 87, 427–436. https://doi.org/10.1016/s0092-8674(00)81363-x
Morfin, F., Thouvenot, D., 2003. Herpes simplex virus resistance to antiviral drugs. J. Clin. Virol. 26, 29–37. https://doi.org/10.1016/S1386-6532(02)00263-9
Mossman, K.L., Sherburne, R., Lavery, C., Duncan, J., Smiley, J.R., 2000. Evidence that Herpes Simplex Virus VP16 Is Required for Viral Egress Downstream of the Initial Envelopment Event. J. Virol. 74, 6287–6299. https://doi.org/10.1128/jvi.74.14.6287-6299.2000
Mundschau, L.J., Faller, D.V., 1995. Platelet-derived Growth Factor Signal Transduction through the Interferon-inducible Kinase PKR: IMMEDIATE EARLY GENE INDUCTION (∗). J. Biol. Chem. 270, 3100–3106. https://doi.org/10.1074/jbc.270.7.3100
Munger, J., Chee, A.V., Roizman, B., 2001. The US3 Protein Kinase Blocks Apoptosis Induced by the d120 Mutant of Herpes Simplex Virus 1 at a Premitochondrial Stage. J. Virol. 75, 5491–5497. https://doi.org/10.1128/jvi.75.12.5491-5497.2001
Munger, J., Roizman, B., 2001. The US3 protein kinase of herpes simplex virus 1 mediates the posttranslational modification of BAD and prevents BAD-induced programmed cell death in the absence of other viral proteins. Proc. Natl. Acad. Sci. 98, 10410–10415. https://doi.org/10.1073/pnas.181344498
Musarra-Pizzo, M., Ginestra, G., Smeriglio, A., Pennisi, R., Sciortino, M.T., Mandalari, G., 2019. The Antimicrobial and Antiviral Activity of Polyphenols from Almond (Prunus dulcis L.) Skin. Nutrients 11, 2355. https://doi.org/10.3390/nu11102355
Musarra-Pizzo, M., Pennisi, R., Ben-Amor, I., Smeriglio, A., Mandalari, G., Sciortino, M.T., 2020. In Vitro Anti-HSV-1 Activity of Polyphenol-Rich Extracts and Pure Polyphenol Compounds Derived from Pistachios Kernels (Pistacia vera L.). Plants 9, 267. https://doi.org/10.3390/plants9020267
Musarra-Pizzo, M., Pennisi, R., Lombardo, D., Velletri, T., Sciortino, M.T., 2022. Direct cleavage of caspase-8 by herpes simplex virus 1 tegument protein US11. Sci. Rep. 12, 12317. https://doi.org/10.1038/s41598-022-15942-9
Newcomb, W.W., Juhas, R.M., Thomsen, D.R., Homa, F.L., Burch, A.D., Weller, S.K., Brown, J.C., 2001. The UL6 Gene Product Forms the Portal for Entry of DNA into the Herpes Simplex Virus Capsid. J. Virol. 75, 10923–10932. https://doi.org/10.1128/JVI.75.22.10923-10932.2001
Newcomb, W.W., Trus, B.L., Booy, F.P., Steven, A.C., Wall, J.S., Brown, J.C., 1993. Structure of the Herpes Simplex Virus Capsid Molecular Composition of the Pentons and the Triplexes. J. Mol. Biol. 232, 499–511. https://doi.org/10.1006/jmbi.1993.1406
Newton, K., Wickliffe, K.E., Maltzman, A., Dugger, D.L., Reja, R., Zhang, Y., Roose-Girma, M., Modrusan, Z., Sagolla, M.S., Webster, J.D., Dixit, V.M., 2019. Activity of caspase-8 determines plasticity between cell death pathways. Nature 575, 679–682. https://doi.org/10.1038/s41586-019-1752-8

Nguyen, M.L., Blaho, J.A., 2006. Apoptosis During Herpes Simplex Virus Infection, in: Advances in Virus Research. Academic Press, pp. 67–97. https://doi.org/10.1016/S0065-3527(06)69002-7

Nguyen, M.L., Kraft, R.M., Blaho, J.A., 2005. African green monkey kidney Vero cells require de novo protein synthesis for efficient herpes simplex virus 1-dependent apoptosis. Virology 336, 274–290. https://doi.org/10.1016/j.virol.2005.03.026

Nicoll, M.P., Hann, W., Shivkumar, M., Harman, L.E.R., Connor, V., Coleman, H.M., Proença, J.T., Efstathiou, S., 2016. The HSV-1 Latency-Associated Transcript Functions to Repress Latent Phase Lytic Gene Expression and Suppress Virus Reactivation from Latently Infected Neurons. PLOS Pathog. 12, e1005539. https://doi.org/10.1371/journal.ppat.1005539

Obba, S., Hizir, Z., Boyer, L., Selimoglu-Buet, D., Pfeifer, A., Michel, G., Hamouda, M.-A., Gonçalvès, D., Cerezo, M., Marchetti, S., Rocchi, S., Droin, N., Cluzeau, T., Robert, G., Luciano, F., Robaye, B., Foretz, M., Viollet, B., Legros, L., Solary, E., Auberger, P., Jacquel, A., 2015. The PRKAA1/AMPKα1 pathway triggers autophagy during CSF1-induced human monocyte differentiation and is a potential target in CMML. Autophagy 11, 1114–1129. https://doi.org/10.1080/15548627.2015.1034406

O'Donnell, M.E., Elias, P., Lehman, I.R., 1987. Processive replication of single-stranded DNA templates by the herpes simplex virus-induced DNA polymerase. J. Biol. Chem. 262, 4252–4259. https://doi.org/10.1016/S0021-9258(18)61340-7

O'Hare, P., Goding, C.R., 1988. Herpes simplex virus regulatory elements and the immunoglobulin octamer domain bind a common factor and are both targets for virion transactivation. Cell 52, 435–445. https://doi.org/10.1016/S0092-8674(88)80036-9

O'Hare, P., Goding, C.R., Haigh, A., 1988. Direct combinatorial interaction between a herpes simplex virus regulatory protein and a cellular octamer-binding factor mediates specific induction of virus immediate-early gene expression. EMBO J. 7, 4231–4238. https://doi.org/10.1002/j.1460-2075.1988.tb03320.x

Ojala, P.M., Sodeik, B., Ebersold, M.W., Kutay, U., Helenius, A., 2000. Herpes Simplex Virus Type 1 Entry into Host Cells: Reconstitution of Capsid Binding and Uncoating at the Nuclear Pore Complex In Vitro. Mol. Cell. Biol. 20, 4922–4931. https://doi.org/10.1128/MCB.20.13.4922-4931.2000

Olivo, P.D., Nelson, N.J., Challberg, M.D., 1988. Herpes simplex virus DNA replication: the UL9 gene encodes an origin-binding protein. Proc. Natl. Acad. Sci. U. S. A. 85, 5414–5418. https://doi.org/10.1073/pnas.85.15.5414

Omar, S.H., 2010. Oleuropein in Olive and its Pharmacological Effects. Sci. Pharm. 78, 133–154. https://doi.org/10.3797/scipharm.0912-18

Omerović, J., Lev, L., Longnecker, R., 2005. The Amino Terminus of Epstein-Barr Virus Glycoprotein gH Is Important for Fusion with Epithelial and B Cells. J. Virol. 79, 12408–12415. https://doi.org/10.1128/JVI.79.19.12408-12415.2005

Oral, O., Oz-Arslan, D., Itah, Z., Naghavi, A., Deveci, R., Karacali, S., Gozuacik, D., 2012. Cleavage of Atg3 protein by caspase-8 regulates autophagy during receptor-activated cell death. Apoptosis 17, 810–820. https://doi.org/10.1007/s10495-012-0735-0

Orning, P., Lien, E., 2021. Multiple roles of caspase-8 in cell death, inflammation, and innate immunity. J. Leukoc. Biol. 109, 121–141. https://doi.org/10.1002/JLB.3MR0420-305R

Palomino, D.C.T., Marti, L.C., 2015. Chemokines and immunity. Einstein São Paulo 13, 469–473. https://doi.org/10.1590/S1679-45082015RB3438

Pang, J., Vince, J.E., 2023. The role of caspase-8 in inflammatory signalling and pyroptotic cell death. Semin. Immunol. 70, 101832. https://doi.org/10.1016/j.smim.2023.101832

Parris, D.S., Cross, A., Haarr, L., Orr, A., Frame, M.C., Murphy, M., McGeoch, D.J., Marsden, H.S., 1988. Identification of the gene encoding the 65-kilodalton DNA-binding protein of herpes simplex virus type 1. J. Virol. 62, 818–825. https://doi.org/10.1128/jvi.62.3.818-825.1988

Pennisi, R., Ben Amor, I., Gargouri, B., Attia, H., Zaabi, R., Chira, A.B., Saoudi, M., Piperno, A., Trischitta, P., Tamburello, M.P., Sciortino, M.T., 2023. Analysis of Antioxidant and Antiviral Effects of Olive (Olea europaea L.) Leaf Extracts and Pure Compound Using Cancer Cell Model. Biomolecules 13, 238. https://doi.org/10.3390/biom13020238

Pennisi, R., Musarra-Pizzo, M., Velletri, T., Mazzaglia, A., Neri, G., Scala, A., Piperno, A., Sciortino, M.T., 2022. Cancer-Related Intracellular Signalling Pathways Activated by

DOXorubicin/Cyclodextrin-Graphene-Based Nanomaterials. Biomolecules 12, 63. https://doi.org/10.3390/biom12010063
Person, S., Laquerre, S., Desai, P., Hempel, J., 1993. Herpes simplex virus type 1 capsid protein, VP21, originates within the UL26 open reading frame. J. Gen. Virol. 74, 2269–2273. https://doi.org/10.1099/0022-1317-74-10-2269
Peters, G.A., Khoo, D., Mohr, I., Sen, G.C., 2002. Inhibition of PACT-Mediated Activation of PKR by the Herpes Simplex Virus Type 1 Us11 Protein. J. Virol. 76, 11054–11064. https://doi.org/10.1128/jvi.76.21.11054-11064.2002
Piret, J., Boivin, G., 2011. Resistance of herpes simplex viruses to nucleoside analogues: mechanisms, prevalence, and management. Antimicrob. Agents Chemother. 55, 459–472. https://doi.org/10.1128/AAC.00615-10
Pomeranz, L.E., Reynolds, A.E., Hengartner, C.J., 2005. Molecular Biology of Pseudorabies Virus: Impact on Neurovirology and Veterinary Medicine. Microbiol. Mol. Biol. Rev. 69, 462–500. https://doi.org/10.1128/MMBR.69.3.462-500.2005
Pontejo, S.M., Murphy, P.M., Pease, J.E., 2018. Chemokine Subversion by Human Herpesviruses. J. Innate Immun. 10, 465–478. https://doi.org/10.1159/000492161
Pop, C., Salvesen, G.S., 2009. Human Caspases: Activation, Specificity, and Regulation. J. Biol. Chem. 284, 21777–21781. https://doi.org/10.1074/jbc.R800084200
Poppers, J., Mulvey, M., Khoo, D., Mohr, I., 2000. Inhibition of PKR Activation by the Proline-Rich RNA Binding Domain of the Herpes Simplex Virus Type 1 Us11 Protein. J. Virol. 74, 11215–11221. https://doi.org/10.1128/jvi.74.23.11215-11221.2000
Prgomet, I., Gonçalves, B., Domínguez-Perles, R., Pascual-Seva, N., Barros, A.I.R.N.A., 2017. Valorization Challenges to Almond Residues: Phytochemical Composition and Functional Application. Molecules 22, 1774. https://doi.org/10.3390/molecules22101774
Quinn, J.P., McGeoch, D.J., 1985. DNA sequence of the region in the genome of herpes simplex virus type 1 containing the genes for DNA polymerase and the major DNA binding protein. Nucleic Acids Res. 13, 8143–8163. https://doi.org/10.1093/nar/13.22.8143
Raftery, M.J., Behrens, C.K., Müller, A., Krammer, P.H., Walczak, H., Schönrich, G., 1999. Herpes Simplex Virus Type 1 Infection of Activated Cytotoxic T Cells: Induction of Fratricide as a Mechanism of Viral Immune Evasion. J. Exp. Med. 190, 1103–1114. https://doi.org/10.1084/jem.190.8.1103
Rager-Zisman, B., Quan, P.C., Rosner, M., Moller, J.R., Bloom, B.R., 1987. Role of NK cells in protection of mice against herpes simplex virus-1 infection. J. Immunol. Baltim. Md 1950 138, 884–888.
Rahman, I., Biswas, S.K., Kirkham, P.A., 2006. Regulation of inflammation and redox signaling by dietary polyphenols. Biochem. Pharmacol., Special Issue: Cell Signalling, Transcription and Translation as Therapeutic Targets 72, 1439–1452. https://doi.org/10.1016/j.bcp.2006.07.004
Raza, S., Alvisi, G., Shahin, F., Husain, U., Rabbani, M., Yaqub, T., Anjum, A.A., Sheikh, A.A., Nawaz, M., Ali, M.A., 2018. Role of Rab GTPases in HSV-1 infection: Molecular understanding of viral maturation and egress. Microb. Pathog. 118, 146–153. https://doi.org/10.1016/j.micpath.2018.03.028
Reardon, J.E., 1989. Herpes simplex virus type 1 and human DNA polymerase interactions with 2′-deoxyguanosine 5′-triphosphate analogues. J. Biol. Chem. 264, 19039–19044. https://doi.org/10.1016/S0021-9258(19)47263-3
Rébé, C., Cathelin, S., Launay, S., Filomenko, R., Prévotat, L., L'Ollivier, C., Gyan, E., Micheau, O., Grant, S., Dubart-Kupperschmitt, A., Fontenay, M., Solary, E., 2006. Caspase-8 prevents sustained activation of NF-κB in monocytes undergoing macrophagic differentiation. Blood 109, 1442–1450. https://doi.org/10.1182/blood-2006-03-011585
Rice, S.A., Su, L.S., Knipe, D.M., 1989. Herpes simplex virus alpha protein ICP27 possesses separable positive and negative regulatory activities. J. Virol. 63, 3399–3407. https://doi.org/10.1128/jvi.63.8.3399-3407.1989
Rixon, F.J., Addison, C., McGregor, A., Macnab, S.J., Nicholson, P., Preston, V.G., Tatman, J.D., 1996. Multiple Interactions Control the Intracellular Localization of the Herpes Simplex Virus Type 1 Capsid Proteins. J. Gen. Virol. 77, 2251–2260. https://doi.org/10.1099/0022-1317-77-9-2251

Romani, A., Ieri, F., Urciuoli, S., Noce, A., Marrone, G., Nediani, C., Bernini, R., 2019. Health Effects of Phenolic Compounds Found in Extra-Virgin Olive Oil, By-Products, and Leaf of Olea europaea L. Nutrients 11, 1776. https://doi.org/10.3390/nu11081776

Roop, C., Hutchinson, L., Johnson, D.C., 1993. A mutant herpes simplex virus type 1 unable to express glycoprotein L cannot enter cells, and its particles lack glycoprotein H. J. Virol. 67, 2285–2297. https://doi.org/10.1128/jvi.67.4.2285-2297.1993

Ruyechan, W.T., 1983. The major herpes simplex virus DNA-binding protein holds single-stranded DNA in an extended configuration. J. Virol. 46, 661–666. https://doi.org/10.1128/jvi.46.2.661-666.1983

Ruyechan, W.T., Weir, A.C., 1984. Interaction with nucleic acids and stimulation of the viral DNA polymerase by the herpes simplex virus type 1 major DNA-binding protein. J. Virol. 52, 727–733. https://doi.org/10.1128/jvi.52.3.727-733.1984

Saad, A., Zhou, Z.H., Jakana, J., Chiu, W., Rixon, F.J., 1999. Roles of Triplex and Scaffolding Proteins in Herpes Simplex Virus Type 1 Capsid Formation Suggested by Structures of Recombinant Particles. J. Virol. 73, 6821–6830. https://doi.org/10.1128/jvi.73.8.6821-6830.1999

Safrin, S., Cherrington, J., Jaffe, H.S., 1999. Cidofovir. Review of current and potential clinical uses. Adv. Exp. Med. Biol. 458, 111–120.

Sakamaki, K., Inoue, T., Asano, M., Sudo, K., Kazama, H., Sakagami, J., Sakata, S., Ozaki, M., Nakamura, S., Toyokuni, S., Osumi, N., Iwakura, Y., Yonehara, S., 2002. Ex vivo whole-embryo culture of caspase-8-deficient embryos normalize their aberrant phenotypes in the developing neural tube and heart. Cell Death Differ. 9, 1196–1206. https://doi.org/10.1038/sj.cdd.4401090

Salmena, L., Lemmers, B., Hakem, A., Matysiak-Zablocki, E., Murakami, K., Au, P.Y.B., Berry, D.M., Tamblyn, L., Shehabeldin, A., Migon, E., Wakeham, A., Bouchard, D., Yeh, W.C., McGlade, J.C., Ohashi, P.S., Hakem, R., 2003. Essential role for caspase 8 in T-cell homeostasis and T-cell-mediated immunity. Genes Dev. 17, 883–895. https://doi.org/10.1101/gad.1063703

Samson, M., Edinger, A.L., Stordeur, P., Rucker, J., Verhasselt, V., Sharron, M., Govaerts, C., Mollereau, C., Vassart, G., Doms, R.W., Parmentier, M., 1998. ChemR23, a putative chemoattractant receptor, is expressed in monocyte-derived dendritic cells and macrophages and is a coreceptor for SIV and some primary HIV-1 strains. Eur. J. Immunol. 28, 1689–1700. https://doi.org/10.1002/(SICI)1521-4141(199805)28:05%253C1689::AID-IMMU1689%253E3.0.CO;2-I

Sànchez, R., Mohr, I., 2007. Inhibition of Cellular 2′-5′ Oligoadenylate Synthetase by the Herpes Simplex Virus Type 1 Us11 Protein. J. Virol. 81, 3455–3464. https://doi.org/10.1128/jvi.02520-06

Santoro, M.G., Rossi, A., Amici, C., 2003. NF-κB and virus infection: who controls whom. EMBO J. 22, 2552–2560. https://doi.org/10.1093/emboj/cdg267

Sarisky, R.T., Crosson, P., Cano, R., Quail, M.R., Nguyen, T.T., Wittrock, R.J., Bacon, T.H., Sacks, S.L., Caspers-Velu, L., Hodinka, R.L., Leary, J.J., 2002. Comparison of methods for identifying resistant herpes simplex virus and measuring antiviral susceptibility. J. Clin. Virol. 23, 191–200. https://doi.org/10.1016/S1386-6532(01)00221-9

Scaffidi, C., Medema, J.P., Krammer, P.H., Peter, M.E., 1997. FLICE Is Predominantly Expressed as Two Functionally Active Isoforms, Caspase-8/a and Caspase-8/b. J. Biol. Chem. 272, 26953–26958. https://doi.org/10.1074/jbc.272.43.26953

Schelhaas, M., Jansen, M., Haase, I., Knebel-Mörsdorf, D., 2003. Herpes simplex virus type 1 exhibits a tropism for basal entry in polarized epithelial cells. J. Gen. Virol. 84, 2473–2484. https://doi.org/10.1099/vir.0.19226-0

Schilling, R., Geserick, P., Leverkus, M., 2014. Characterization of the Ripoptosome and Its Components, in: Methods in Enzymology. Elsevier, pp. 83–102. https://doi.org/10.1016/B978-0-12-801430-1.00004-4

Sciortino, M.T., Medici, M.A., Marino-Merlo, F., Zaccaria, D., Giuffrè, M., Venuti, A., Grelli, S., Mastino, A., 2007. Signaling Pathway Used by HSV-1 to Induce NF-κB Activation: Possible Role of Herpes Virus Entry Receptor A. Ann. N. Y. Acad. Sci. 1096, 89–96. https://doi.org/10.1196/annals.1397.074

Sciortino, M.T., Parisi, T., Siracusano, G., Mastino, A., Taddeo, B., Roizman, B., 2013. The Virion Host Shutoff RNase Plays a Key Role in Blocking the Activation of Protein Kinase R in

Cells Infected with Herpes Simplex Virus 1. J. Virol. 87, 3271–3276. https://doi.org/10.1128/jvi.03049-12
Sedger, L.M., McDermott, M.F., 2014. TNF and TNF-receptors: From mediators of cell death and inflammation to therapeutic giants – past, present and future. Cytokine Growth Factor Rev. 25, 453–472. https://doi.org/10.1016/j.cytogfr.2014.07.016
Senturk, H., Yıldız, F., 2018. Protective effects of Olea Europaea L. (olive) leaf extract against oxidative stress injury generated with renal ischemia reperfusion. J. Anim. Plant Sci. 28, 1027–1033.
Shalini, S., Dorstyn, L., Dawar, S., Kumar, S., 2015. Old, new and emerging functions of caspases. Cell Death Differ. 22, 526–539. https://doi.org/10.1038/cdd.2014.216
Sharifi-Rad, M., Anil Kumar, N.V., Zucca, P., Varoni, E.M., Dini, L., Panzarini, E., Rajkovic, J., Tsouh Fokou, P.V., Azzini, E., Peluso, I., Prakash Mishra, A., Nigam, M., El Rayess, Y., Beyrouthy, M.E., Polito, L., Iriti, M., Martins, N., Martorell, M., Docea, A.O., Setzer, W.N., Calina, D., Cho, W.C., Sharifi-Rad, J., 2020. Lifestyle, Oxidative Stress, and Antioxidants: Back and Forth in the Pathophysiology of Chronic Diseases. Front. Physiol. 11. https://doi.org/10.3389/fphys.2020.00694
Shen, C., Pei, J., Guo, X., Zhou, L., Li, Q., Quan, J., 2018. Structural basis for dimerization of the death effector domain of the F122A mutant of Caspase-8. Sci. Rep. 8, 16723. https://doi.org/10.1038/s41598-018-35153-5
Simpson, D.S., Gabrielyan, A., Feltham, R., 2021. RIPK1 ubiquitination: Evidence, correlations and the undefined. Semin. Cell Dev. Biol., 1. Hormonal signalling in plant development by Tom Bennett2. RIP kinases in cell regulation by James Vince 109, 76–85. https://doi.org/10.1016/j.semcdb.2020.08.008
Sinha, S., Kundu, C.N., 2021. Cancer and COVID-19: Why are cancer patients more susceptible to COVID-19? Med. Oncol. 38, 101. https://doi.org/10.1007/s12032-021-01553-3
Siracusano, G., Venuti, A., Lombardo, D., Mastino, A., Esclatine, A., Sciortino, M.T., 2016. Early activation of MyD88-mediated autophagy sustains HSV-1 replication in human monocytic THP-1 cells. Sci. Rep. 6, 31302. https://doi.org/10.1038/srep31302
Smeriglio, A., Mandalari, G., Bisignano, C., Filocamo, A., Barreca, D., Bellocco, E., Trombetta, D., 2016. Polyphenolic content and biological properties of Avola almond (*Prunus dulcis* Mill. D.A. Webb) skin and its industrial byproducts. Ind. Crops Prod. 83, 283–293. https://doi.org/10.1016/j.indcrop.2015.11.089
Smibert, C.A., Popova, B., Xiao, P., Capone, J.P., Smiley, J.R., 1994. Herpes simplex virus VP16 forms a complex with the virion host shutoff protein vhs. J. Virol. 68, 2339–2346. https://doi.org/10.1128/jvi.68.4.2339-2346.1994
Smith, A.E., Helenius, A., 2004. How viruses enter animal cells. Science 304, 237–242. https://doi.org/10.1126/science.1094823
Smith, G., 2012. Herpesvirus Transport to the Nervous System and Back Again. Annu. Rev. Microbiol. 66, 10.1146/annurev-micro-092611–150051. https://doi.org/10.1146/annurev-micro-092611-150051
Smith, J.B., Herbert, J.J., Truong, N.R., Cunningham, A.L., 2022. Cytokines and chemokines: The vital role they play in herpes simplex virus mucosal immunology. Front. Immunol. 13, 936235. https://doi.org/10.3389/fimmu.2022.936235
Solier, S., Fontenay, M., Vainchenker, W., Droin, N., Solary, E., 2017. Non-apoptotic functions of caspases in myeloid cell differentiation. Cell Death Differ. 24, 1337–1347. https://doi.org/10.1038/cdd.2017.19
Sordet, O., Rébé, C., Plenchette, S., Zermati, Y., Hermine, O., Vainchenker, W., Garrido, C., Solary, E., Dubrez-Daloz, L., 2002. Specific involvement of caspases in the differentiation of monocytes into macrophages. Blood 100, 4446–4453. https://doi.org/10.1182/blood-2002-06-1778
Steiner, I., Kennedy, P.G., Pachner, A.R., 2007. The neurotropic herpes viruses: herpes simplex and varicella-zoster. Lancet Neurol. 6, 1015–1028. https://doi.org/10.1016/S1474-4422(07)70267-3
Strang, B.L., Stow, N.D., 2005. Circularization of the Herpes Simplex Virus Type 1 Genome upon Lytic Infection. J. Virol. 79, 12487–12494. https://doi.org/10.1128/jvi.79.19.12487-12494.2005
Stupack, D.G., 2013. Caspase-8 as a therapeutic target in cancer. Cancer Lett., Apoptosis Targeting Drugs in Cancer 332, 133–140. https://doi.org/10.1016/j.canlet.2010.07.022

Su, H., Bidère, N., Zheng, L., Cubre, A., Sakai, K., Dale, J., Salmena, L., Hakem, R., Straus, S., Lenardo, M., 2005. Requirement for Caspase-8 in NF-κB Activation by Antigen Receptor. Science 307, 1465–1468. https://doi.org/10.1126/science.1104765

Sun, L., Wang, H., Wang, Z., He, S., Chen, S., Liao, D., Wang, L., Yan, J., Liu, W., Lei, X., Wang, X., 2012. Mixed Lineage Kinase Domain-like Protein Mediates Necrosis Signaling Downstream of RIP3 Kinase. Cell 148, 213–227. https://doi.org/10.1016/j.cell.2011.11.031

Suzich, J.B., Cliffe, A.R., 2018. Strength in diversity: Understanding the pathways to herpes simplex virus reactivation. Virology 522, 81–91. https://doi.org/10.1016/j.virol.2018.07.011

Taddeo, B., Sciortino, M.T., Zhang, W., Roizman, B., 2007. Interaction of herpes simplex virus RNase with VP16 and VP22 is required for the accumulation of the protein but not for accumulation of mRNA. Proc. Natl. Acad. Sci. 104, 12163–12168. https://doi.org/10.1073/pnas.0705245104

Tanida, I., 2011. Autophagosome Formation and Molecular Mechanism of Autophagy. Antioxid. Redox Signal. 14, 2201–2214. https://doi.org/10.1089/ars.2010.3482

Taylor, T.J., Brockman, M.A., McNamee, E.E., Knipe, D.M., 2002. Herpes simplex virus. Front. Biosci. J. Virtual Libr. 7, d752-764. https://doi.org/10.2741/taylor

Teitz, T., Wei, T., Valentine, M.B., Vanin, E.F., Grenet, J., Valentine, V.A., Behm, F.G., Look, A.T., Lahti, J.M., Kidd, V.J., 2000. Caspase 8 is deleted or silenced preferentially in childhood neuroblastomas with amplification of MYCN. Nat. Med. 6, 529–535. https://doi.org/10.1038/75007

Tenev, T., Bianchi, K., Darding, M., Broemer, M., Langlais, C., Wallberg, F., Zachariou, A., Lopez, J., MacFarlane, M., Cain, K., Meier, P., 2011. The Ripoptosome, a Signaling Platform that Assembles in Response to Genotoxic Stress and Loss of IAPs. Mol. Cell 43, 432–448. https://doi.org/10.1016/j.molcel.2011.06.006

Thapa, M., Welner, R.S., Pelayo, R., Carr, D.J.J., 2008. CXCL9 and CXCL10 expression are critical for control of genital herpes simplex virus type 2 infection through mobilization of HSV-specific CTL and NK cells to the nervous system. J. Immunol. Baltim. Md 1950 180, 1098–1106. https://doi.org/10.4049/jimmunol.180.2.1098

Thornberry, N.A., 1998. Caspases: key mediators of apoptosis. Chem. Biol. 5, R97–R103. https://doi.org/10.1016/S1074-5521(98)90615-9

Tischer, B.K., Smith, G.A., Osterrieder, N., 2010. En Passant Mutagenesis: A Two Step Markerless Red Recombination System, in: Braman, J. (Ed.), In Vitro Mutagenesis Protocols, Methods in Molecular Biology. Humana Press, Totowa, NJ, pp. 421–430. https://doi.org/10.1007/978-1-60761-652-8_30

Toews, G.B., 2009. Macrophages, in: Barnes, P.J., Drazen, J.M., Rennard, S.I., Thomson, N.C. (Eds.), Asthma and COPD (Second Edition) Chapter 11. Academic Press, Oxford, pp. 133–143. https://doi.org/10.1016/B978-0-12-374001-4.00011-0

Torres, V.A., Mielgo, A., Barilà, D., Anderson, D.H., Stupack, D., 2008. Caspase 8 promotes peripheral localization and activation of Rab5. J. Biol. Chem. 283, 36280–36289. https://doi.org/10.1074/jbc.M805878200

Tsuchiya, Y., Nakabayashi, O., Nakano, H., 2015. FLIP the Switch: Regulation of Apoptosis and Necroptosis by cFLIP. Int. J. Mol. Sci. 16, 30321–30341. https://doi.org/10.3390/ijms161226232

Tummers, B., Green, D.R., 2017. Caspase-8: regulating life and death. Immunol. Rev. 277, 76–89. https://doi.org/10.1111/imr.12541

Tyler, K.L., 2004. Herpes simplex virus infections of the central nervous system: encephalitis and meningitis, including Mollaret's. Herpes J. IHMF 11 Suppl 2, 57A-64A.

Valerio, G.S., Lin, C.C., 2019. Ocular manifestations of herpes simplex virus. Curr. Opin. Ophthalmol. 30, 525–531. https://doi.org/10.1097/ICU.0000000000000618

van Diemen, F.R., Kruse, E.M., Hooykaas, M.J.G., Bruggeling, C.E., Schürch, A.C., van Ham, P.M., Imhof, S.M., Nijhuis, M., Wiertz, E.J.H.J., Lebbink, R.J., 2016. CRISPR/Cas9-Mediated Genome Editing of Herpesviruses Limits Productive and Latent Infections. PLoS Pathog. 12, e1005701. https://doi.org/10.1371/journal.ppat.1005701

Varfolomeev, E.E., Schuchmann, M., Luria, V., Chiannilkulchai, N., Beckmann, J.S., Mett, I.L., Rebrikov, D., Brodianski, V.M., Kemper, O.C., Kollet, O., Lapidot, T., Soffer, D., Sobe, T., Avraham, K.B., Goncharov, T., Holtmann, H., Lonai, P., Wallach, D., 1998. Targeted Disruption of the Mouse Caspase 8 Gene Ablates Cell Death Induction by the TNF

Receptors, Fas/Apo1, and DR3 and Is Lethal Prenatally. Immunity 9, 267–276. https://doi.org/10.1016/S1074-7613(00)80609-3
Venuti, A., Musarra-Pizzo, M., Pennisi, R., Tankov, S., Medici, M.A., Mastino, A., Rebane, A., Sciortino, M.T., 2019. HSV-1\EGFP stimulates miR-146a expression in a NF-κB-dependent manner in monocytic THP-1 cells. Sci. Rep. 9, 5157. https://doi.org/10.1038/s41598-019-41530-5
Verzosa, A.L., McGeever, L.A., Bhark, S.-J., Delgado, T., Salazar, N., Sanchez, E.L., 2021. Herpes Simplex Virus 1 Infection of Neuronal and Non-Neuronal Cells Elicits Specific Innate Immune Responses and Immune Evasion Mechanisms. Front. Immunol. 12, 644664. https://doi.org/10.3389/fimmu.2021.644664
Wagstaff, A.J., Bryson, H.M., 1994. Foscarnet. Drugs 48, 199–226. https://doi.org/10.2165/00003495-199448020-00007
Walker, J.E., Saraste, M., Runswick, M.J., Gay, N.J., 1982. Distantly related sequences in the alpha- and beta-subunits of ATP synthase, myosin, kinases and other ATP-requiring enzymes and a common nucleotide binding fold. EMBO J. 1, 945–951. https://doi.org/10.1002/j.1460-2075.1982.tb01276.x
Walsh, C.M., Wen, B.G., Chinnaiyan, A.M., O'Rourke, K., Dixit, V.M., Hedrick, S.M., 1998. A Role for FADD in T Cell Activation and Development. Immunity 8, 439–449. https://doi.org/10.1016/S1074-7613(00)80549-X
Wang, H., Borlongan, M., Kaufman, H.L., Le, U., Nauwynck, H.J., Rabkin, S.D., Saha, D., 2024. Cytokine-armed oncolytic herpes simplex viruses: a game-changer in cancer immunotherapy? J. Immunother. Cancer 12, e008025. https://doi.org/10.1136/jitc-2023-008025
Wang, Y., Karki, R., Mall, R., Sharma, B.R., Kalathur, R.C., Lee, S., Kancharana, B., So, M., Combs, K.L., Kanneganti, T.-D., 2022. Molecular mechanism of RIPK1 and caspase-8 in homeostatic type I interferon production and regulation. Cell Rep. 41, 111434. https://doi.org/10.1016/j.celrep.2022.111434
Wang, Y., Tjandra, N., 2013. Structural Insights of tBid, the Caspase-8-activated Bid, and Its BH3 Domain. J. Biol. Chem. 288, 35840–35851. https://doi.org/10.1074/jbc.M113.503680
Watanabe, T., Hiasa, Y., Tokumoto, Y., Hirooka, M., Abe, M., Ikeda, Y., Matsuura, B., Chung, R.T., Onji, M., 2013. Protein Kinase R Modulates c-Fos and c-Jun Signaling to Promote Proliferation of Hepatocellular Carcinoma with Hepatitis C Virus Infection. PLOS ONE 8, e67750. https://doi.org/10.1371/journal.pone.0067750
Weinheimer, S.P., Boyd, B.A., Durham, S.K., Resnick, J.L., O'Boyle, D.R., 1992. Deletion of the VP16 open reading frame of herpes simplex virus type 1. J. Virol. 66, 258–269. https://doi.org/10.1128/jvi.66.1.258-269.1992
Weinlich, R., Oberst, A., Beere, H.M., Green, D.R., 2017. Necroptosis in development, inflammation and disease. Nat. Rev. Mol. Cell Biol. 18, 127–136. https://doi.org/10.1038/nrm.2016.149
Weller, S.K., Coen, D.M., 2012. Herpes Simplex Viruses: Mechanisms of DNA Replication. Cold Spring Harb. Perspect. Biol. 4, a013011. https://doi.org/10.1101/cshperspect.a013011
Whitbeck, J.C., Peng, C., Lou, H., Xu, R., Willis, S.H., Ponce de Leon, M., Peng, T., Nicola, A.V., Montgomery, R.I., Warner, M.S., Soulika, A.M., Spruce, L.A., Moore, W.T., Lambris, J.D., Spear, P.G., Cohen, G.H., Eisenberg, R.J., 1997. Glycoprotein D of herpes simplex virus (HSV) binds directly to HVEM, a member of the tumor necrosis factor receptor superfamily and a mediator of HSV entry. J. Virol. 71, 6083–6093. https://doi.org/10.1128/JVI.71.8.6083-6093.1997
Whitley, R., 2006. New approaches to the therapy of HSV infections. Herpes J. IHMF 13, 53–55.
Wirawan, E., Vande Walle, L., Kersse, K., Cornelis, S., Claerhout, S., Vanoverberghe, I., Roelandt, R., De Rycke, R., Verspurten, J., Declercq, W., Agostinis, P., Vanden Berghe, T., Lippens, S., Vandenabeele, P., 2010. Caspase-mediated cleavage of Beclin-1 inactivates Beclin-1-induced autophagy and enhances apoptosis by promoting the release of proapoptotic factors from mitochondria. Cell Death Dis. 1, e18–e18. https://doi.org/10.1038/cddis.2009.16
Wormser, G.P., Rubin, D.H., 2002. Fundamental Virology, 4th Edition By David M. Knipe, Peter M. Howley, Diane E. Griffin, Robert A. Lamb, Malcolm A. Martin, Bernard Roizman, and Stephen E. Straus Philadelphia: Lippincott Williams & Wilkins, 2001. 1408 pp. $99.95 (cloth).Fields Virology, 4th Edition, Volumes I and II By David M. Knipe, Peter M. Howley, Diane E. Griffin, Robert A. Lamb, Malcolm A. Martin, Bernard Roizman, and

Stephen E. Straus Philadelphia: Lippincott Williams & Wilkins, 2001. 3280 pp. $339.00 (cloth). Clin. Infect. Dis. 34, 1029–1030. https://doi.org/10.1086/339330
Wu, J., Wilson, J., He, J., Xiang, L., Schur, P.H., Mountz, J.D., 1996. Fas ligand mutation in a patient with systemic lupus erythematosus and lymphoproliferative disease. J. Clin. Invest. 98, 1107–1113. https://doi.org/10.1172/JCI118892
Xie, P., Deng, Y., Huang, L., Zhang, C., 2022. Effect of olive leaf (Olea europaea L.) extract addition to broiler diets on the growth performance, breast meat quality, antioxidant capacity and caecal bacterial populations. Ital. J. Anim. Sci. 21, 1246–1258. https://doi.org/10.1080/1828051X.2022.2105265
Xing, J., Wang, S., Lin, R., Mossman, K.L., Zheng, C., 2012. Herpes Simplex Virus 1 Tegument Protein US11 Downmodulates the RLR Signaling Pathway via Direct Interaction with RIG-I and MDA-5. J. Virol. 86, 3528–3540. https://doi.org/10.1128/JVI.06713-11
Yeh, W.-C., Itie, A., Elia, A.J., Ng, M., Shu, H.-B., Wakeham, A., Mirtsos, C., Suzuki, N., Bonnard, M., Goeddel, D.V., Mak, T.W., 2000. Requirement for Casper (c-FLIP) in Regulation of Death Receptor–Induced Apoptosis and Embryonic Development. Immunity 12, 633–642. https://doi.org/10.1016/S1074-7613(00)80214-9
Yeh, W.-C., Pompa, J.L. de la, McCurrach, M.E., Shu, H.-B., Elia, A.J., Shahinian, A., Ng, M., Wakeham, A., Khoo, W., Mitchell, K., El-Deiry, W.S., Lowe, S.W., Goeddel, D.V., Mak, T.W., 1998. FADD: Essential for Embryo Development and Signaling from Some, But Not All, Inducers of Apoptosis. Science 279, 1954–1958. https://doi.org/10.1126/science.279.5358.1954
York, I.A., Roop, C., Andrews, D.W., Riddell, S.R., Graham, F.L., Johnson, D.C., 1994. A cytosolic herpes simplex virus protein inhibits antigen presentation to CD8+ T lymphocytes. Cell 77, 525–535. https://doi.org/10.1016/0092-8674(94)90215-1
Yoshimura, T., Oppenheim, J.J., 2011. Chemokine-like receptor 1 (CMKLR1) and chemokine (C–C motif) receptor-like 2 (CCRL2); Two multifunctional receptors with unusual properties. Exp. Cell Res. 317, 674–684. https://doi.org/10.1016/j.yexcr.2010.10.023
You, Y., Cheng, A.-C., Wang, M.-S., Jia, R.-Y., Sun, K.-F., Yang, Q., Wu, Y., Zhu, D., Chen, S., Liu, M.-F., Zhao, X.-X., Chen, X.-Y., 2017. The suppression of apoptosis by α-herpesvirus. Cell Death Dis. 8, e2749–e2749. https://doi.org/10.1038/cddis.2017.139
Young, M.M., Takahashi, Y., Khan, O., Park, S., Hori, T., Yun, J., Sharma, A.K., Amin, S., Hu, C.-D., Zhang, J., Kester, M., Wang, H.-G., 2012. Autophagosomal Membrane Serves as Platform for Intracellular Death-inducing Signaling Complex (iDISC)-mediated Caspase-8 Activation and Apoptosis. J. Biol. Chem. 287, 12455–12468. https://doi.org/10.1074/jbc.M111.309104
Yu, H., Sun, Y., Zhang, J., Zhang, W., Liu, W., Liu, P., Liu, K., Sun, J., Liang, H., Zhang, P., Wang, X., Liu, X., Xu, X., 2024. Influenza A virus infection activates caspase-8 to enhance innate antiviral immunity by cleaving CYLD and blocking TAK1 and RIG-I deubiquitination. Cell. Mol. Life Sci. 81, 355. https://doi.org/10.1007/s00018-024-05392-z
Yu, L., Alva, A., Su, H., Dutt, P., Freundt, E., Welsh, S., Baehrecke, E.H., Lenardo, M.J., 2004. Regulation of an *ATG7* - *beclin 1* Program of Autophagic Cell Death by Caspase-8. Science 304, 1500–1502. https://doi.org/10.1126/science.1096645
Zahra, K.F., Lefter, R., Ali, A., Abdellah, E.-C., Trus, C., Ciobica, A., Timofte, D., 2021. The Involvement of the Oxidative Stress Status in Cancer Pathology: A Double View on the Role of the Antioxidants. Oxid. Med. Cell. Longev. 2021, 9965916. https://doi.org/10.1155/2021/9965916
Zerboni, L., Che, X., Reichelt, M., Qiao, Y., Gu, H., Arvin, A., 2013. Herpes Simplex Virus 1 Tropism for Human Sensory Ganglion Neurons in the Severe Combined Immunodeficiency Mouse Model of Neuropathogenesis. J. Virol. 87, 2791–2802. https://doi.org/10.1128/JVI.01375-12
Zhang, C., Zhang, J., Xin, X., Zhu, S., Niu, E., Wu, Q., Li, T., Liu, D., 2022. Changes in Phytochemical Profiles and Biological Activity of Olive Leaves Treated by Two Drying Methods. Front. Nutr. 9. https://doi.org/10.3389/fnut.2022.854680
Zhang, Q., Lenardo, M.J., Baltimore, D., 2017. 30 Years of NF-κB: A Blossoming of Relevance to Human Pathobiology. Cell 168, 37–57. https://doi.org/10.1016/j.cell.2016.12.012
Zhang, W., Zhu, C., Liao, Y., Zhou, M., Xu, W., Zou, Z., 2024. Caspase-8 in inflammatory diseases: a potential therapeutic target. Cell. Mol. Biol. Lett. 29, 130. https://doi.org/10.1186/s11658-024-00646-x

Zhang, Y., Sirko, D.A., McKnight, J.L., 1991. Role of herpes simplex virus type 1 UL46 and UL47 in alpha TIF-mediated transcriptional induction: characterization of three viral deletion mutants. J. Virol. 65, 829–841. https://doi.org/10.1128/jvi.65.2.829-841.1991

Zhou, G., Avitabile, E., Campadelli-Fiume, G., Roizman, B., 2003. The Domains of Glycoprotein D Required To Block Apoptosis Induced by Herpes Simplex Virus 1 Are Largely Distinct from Those Involved in Cell-Cell Fusion and Binding to Nectin1. J. Virol. 77, 3759–3767. https://doi.org/10.1128/JVI.77.6.3759-3767.2003

Zhou, Z.H., Dougherty, M., Jakana, J., He, J., Rixon, F.J., Chiu, W., 2000. Seeing the Herpesvirus Capsid at 8.5 Å. Science 288, 877–880. https://doi.org/10.1126/science.288.5467.877

Zhou, Z.H., He, J., Jakana, J., Tatman, J., 1995. Assembly of VP26 in herpes simplex virus-1 inferred from structures of wild- type and recombinant capsids [WWW Document]. URL https://www.nature.com/articles/nsb1195-1026 (accessed 8.19.25).

Zhu, Q., Courtney, R.J., 1994. Chemical Cross-Linking of Virion Envelope and Tegument Proteins of Herpes Simplex Virus Type 1. Virology 204, 590–599. https://doi.org/10.1006/viro.1994.1573

Zou, H., Yang, R., Hao, J., Wang, J., Sun, C., Fesik, S.W., Wu, J.C., Tomaselli, K.J., Armstrong, R.C., 2003. Regulation of the Apaf-1/Caspase-9 Apoptosome by Caspase-3 and XIAP. J. Biol. Chem. 278, 8091–8098. https://doi.org/10.1074/jbc.M204783200

Acknowledgements

Firstly, I would like to thank my supervisor, Prof. Dr. Maria Teresa Sciortino, for giving me the opportunity to pursue my doctoral studies and for involving me in a challenging research project. I acknowledge her guidance and the role it played in shaping this doctoral experience. I would also like to thank my second supervisor, Prof. Dr. Rosamaria Pennisi, for her thoughtful suggestions and comments, which contributed to the development of this work.

I would like to thank Prof. Dr. Wolfram Brune for the generous opportunities and trust he offered me over the years, as well as for his availability and valuable advice during my research stay in his laboratory. I would also like to express my thanks to Dr. Eleonore Ostermann for her constant support and for the time she dedicated to discussing research questions and experimental approaches while working in the laboratory.

I would like to acknowledge Jan Knickmann for his expertise and assistance in the analysis of next-generation sequencing data, and Dr. Christian Conze and Dr. Felix Flomm for their suggestions and their time and effort during the experimental work.

Thanks to my colleagues from the Molecular Virology laboratory at the University of Messina, Federica and Marianna, for the pleasant time we spent together over this period. My sincere thanks go to Paola for the closeness and understanding that were fundamental at the beginning of this experience and that I will always remember.

I would like to thank all present and former members of the Virus-Host Interaction research group at the Leibniz-Institut für Virologie - Dongdong, Eleonore, Enrico, Ina, Irke, Jan, Laura, Laura-Marie, Luis, Maria, Michaela, Vincent - for welcoming me as one of their own, as well as for making me feel truly at home during my time there. Special thanks to Ana, Andrea, Giorgia, and Xuan, whose presence and support went far beyond the professional sphere. We shared laughter, meals, advice,

and many moments that made this time especially meaningful. This journey would not have been the same without them.

Finally, I wish to express my deepest gratitude to my mother, Paola, for her boundless love and unwavering encouragement throughout my life. I am sincerely grateful to all the people who, in different ways and at different times, have been by my side along the way: Rosetta, Paolo, Cinzia, Sabrina, Laura, Carmelo, Andrea, Alessia, Fabio, Francesca, Melanie, Vlad, Niklas, Sofia, Martina, Lorenzo, Lidia, Maria Lucia, Ignacio, Claudiu, and Philipp. My heartfelt thanks to Ivano for his support and love.